Distributed Optimal Power Flow in a DC Distribution System

Step towards smarter energy management

Sahil Karambelkar

Technische Universiteit Delft

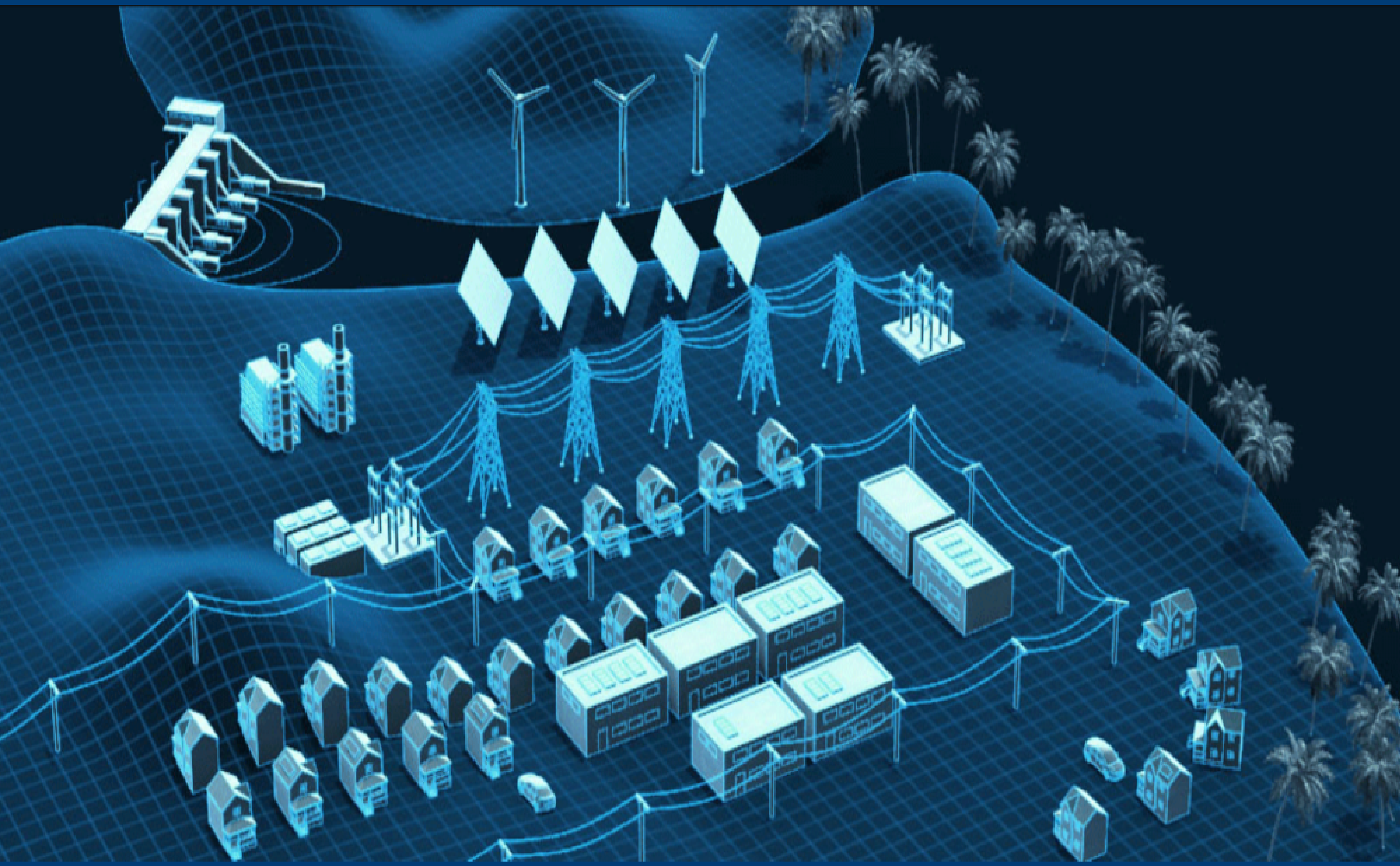

Delft University of Technology

Challenge the future

Distributed Optimal Power Flow in a DC Distribution System

Step towards smarter energy management

by

Sahil Karambelkar

in partial fulfillment of the requirements for the degree of

Master of Science
in Sustainable Energy Technology

at the Delft University of Technology,
to be defended publicly on Tuesday September 26, 2017 at 9:00 AM.

Supervisor:	Dr. Ir. Laura Ramirez Elizondo
Advisors:	Ir. Laurens Mackay
	Ir. Shantanu Chakraborty
Thesis committee:	Prof. Dr. Pavol Bauer
	Prof. Dr. Ir. Zofia Lukszo
	Dr. Ir. Marjan Popov

This thesis is confidential and cannot be made public until September 30, 2018.

Delft University of Technology

Preface

Preface...

Sahil Karambelkar
Delft, September 2017

Contents

List of Figures

LIST OF TABLES

List of Symbols

λ_m	Locational Marginal Price at node m
$\mathscr{L}$	Lagrange Function
$\mu_m^{\overline{P}}$	Dual variable for upper power limit at node m
$\mu_m^{\overline{U}}$	Dual variable for upper voltage limit at node m
$\mu_m^{\underline{P}}$	Dual variable for lower power limit at node m
$\mu_m^{\underline{U}}$	Dual variable for lower power limit at node m
$\mu_{m,n}$	Congestion multiplier for line connecting node m and n
$\overline{I}_{m,n}$	Maximum cable current capacity
$\overline{P}_m$	Maximum capacity of Generator at node m
$\overline{U}_m$	Maximum nodal voltage at node m
θ_m	Voltage phase angle at node m
$\underline{P}_m$	Minimum capacity of Generator at node m
$\underline{U}_m$	Minimum nodal voltage at node m
A_m	Quadratic cost co-efficient at node m
B_m	Linear cost co-efficient at node m
C_m	Fixed cost of generator at node m
$G_{m,n}$	Conductance of line connecting node m and node n
i_m^S	Nodal current at node m
p_m^S	Power of source S at node m
u_m	Nodal voltage at node m
$Y_{m,n}$	Admittance of line connecting node m and node n

List of Acronyms

- **OPF**: Optimal Power Flow
- **AC**: Alternating Current
- **DC**: Direct Current
- **ED**: Economic Dispatch
- **FC**: Fuel Cell
- **LVAC**: Low Voltage Alternating Current
- **LVDC**: Low Voltage Direct Current
- **PV**: Photo-Voltaic Systems
- **KKT**: Karesh Kuhn Tucker
- **LMP**: Locational Marginal Prices
- **DER**: Distributed Energy Resources

Abstract

Rise in distributed energy resources has prompted a shift in the way electricity market operators function. Traditionally, centralized optimization techniques are used by such operators to plan for economic dispatches of power to minimize the overall operational costs and increase system social welfare. Due to the dispersed nature of renewable energy sources as scattered nodes in a system, it can get difficult to accommodate them in a centralized optimization problem. Also, sharing of complete information for such nodes can create privacy issues. This motivates research in the field of distributed optimization techniques.

This thesis aims to develop a distributed optimization algorithm for a DC distribution system which would take into account network congestion and line losses and ultimately provide a more precise optimal solution. Based on past research for distributed optimization approaches for AC systems, the Consensus and Innovations approach was used to model an algorithm and provide nodal optimization for a DC system with minimal data exchange. The developed model was implemented on various DC network topologies like meshed grids, single line networks, T Shaped networks, etc. and a converged output of system variables was accomplished. The results were also compared with a centralized optimization approach to check for deviations. The decision variables for the developed approach were found to be well within the deviation range of 2 percent. The algorithm managed to provide distributed optimization within a DC system while minimizing power generator operational costs and cost associated with network losses.

1
Introduction

Energy demand and carbon emissions associated with this energy demand have been growing continually for the past 25 years [7]. In the past and even in current times, there have been talks about a potential trade-off between economic growth and climate change risk. Some experts argue that the world needs to accept the effect of economic growth on the environment for the next few decades in order for steady development. This means keeping the case of climate change as back-ended and focusing on growth instead of energy transition. In recent times, experts on the topic have proposed lateral growth keeping the climate change action as a strong parameter [8]. This motivates us to anticipate a world with energy transition and advancements in energy systems.

1.1. Shift to Distributed Energy Generation

Conventionally, power plants are thought to be energy generating sources of large centralized units. In recent years, the trend has shifted to decentralized generation units of lower capacity scale but located close to the point of consumption. This advancement helps the user tackle specific power requirements specially in areas affected by power shortages or outages [9]. In special cases of distributed energy generation, single buildings can be almost self-supporting in terms of electricity, heat, and cooling requirements. These distributed energy resources (DER) can comprise of several technologies, such as micro turbines, photovoltaic panels, small to medium wind turbines, fuel cells, diesel gensets, etc.

A distributed energy generation system would be most suited for countries which are vastly spread over larger areas with sparse population or the developing countries experiencing utility grid unreliability. This would take the burden off the large central generation units which in some cases cannot cope with the load requirements [10]. Distributed generation therefore proves to be reliable, efficient and an environmentally friendly option for growth with respect to sustainable development. Various research papers differentiate between decentralized and distributed energy generation in terms of integration of single units in a system [11]. For the sake of simplicity, we assume the term decentralized and distributed to entail the same meaning.

1.2. Importance of Microgrids in the Future

Jiayi et al. in his paper [12] on distributed energy resources and microgrids defines a microgrid as a concept which assumes a cluster of nodes and microsources operating as a single controllable system that provides energy (electricity and heat) to its local region. Lasseter et al. [13] introduces the potential benefits of a microgrid system such as, improvement of local power reliability, reduction in feeder losses, prevent local voltage fluctuations, increased efficiency by reusing waste heat (CHP) and provide uninterrupted power supply fluctuations.

A microgrid is basically required to operate in two different states: normal interconnected mode (grid connected) or islanded mode (off-grid connected). Many of the DER's used in a microgrid setup are not suitable for direct connections to the electrical network due to the variation in the characteristics of the energy produced. For such situations, power electronic devices are used such as converters (AC-DC, DC-DC, DC-AC). As per the trend followed in the past, microgrids are normally centrally controlled. With the growing consumption needs and possibilities of using DERs, the importance of distributed control has augmented.

Developing regions like India and Africa have specific areas which encounter electricity grid unreliability. The local government authorities in India claim the expense of grid extension to such areas is relatively high. Considering the region of India, some states like Jharkhand and Bihar face power deficits of upto 30% [14]. This means the supply is not meeting the demand and lacks by a significant margin of 30%. The local authority claims that in order to power such rural pockets with no grid connections, the grid should be extended to these low consumption loads. The cost of doing so outweighs the returns from the energy unit payments by the consumers, hence rendering the grid expansion as an uneconomical solution. A microgrid setup with distributed energy resources based on local availability and energy storage systems could help to solve the problem. The load demands would be better satisfied and the main grid will not be burdened. This would possibly help reduce carbon footprints and augment renewable energy generation as well. Other significant benefits are higher power quality, cost effectiveness and high reliability.

1.3. RISE OF DC SYSTEMS AND LVDC

Easy transformation capability into different levels for different applications made AC power the standard choice for commercial energy systems in the past. The long distance transmission ability and as stated by Justo et al. [1] it's inherent characteristic from the fossil energy driven rotating machines made AC power networks to become the primary choice. The AC loads have also predominantly dominated the markets. Increased concerns over global warming, outdated power systems in use, advancements in renewable energy technologies, higher energy consumption needs and increased DC loads indicate the need for alternative energy system networks.

Quick advancements in power electronics technology has potentially increased the use of DC loads [15]. This has resulted in DC microgrid systems being used in applications such as avionics, manufacturing industries, automotive and marine systems for power distribution [16]. Modern electronic loads such as computers and servers in data centers, banks and electronic factories, modern aircraft and International Space Station (ISS) have DC power requirements [17].

1.3.1. LVAC NETWORKS

The electricity generating units which have an AC power output are directly connected on the AC bus line and then to the main system with the help of power converters for stable coupling. Examples of such AC generating units are wind turbines, diesel generators, low-head hydro generation, biogas systems, tidal and wave turbines [1]. DC power producing units on the other hand require power inverters for DC-AC operation before being connected on the AC link [1]. The AC loads are directly connected while the DC loads need AC-DC power conversion before their connection on the AC link. An LVAC network illustration is presented in Figure 1.1.

1.3.2. LVDC NETWORKS

Looking into the future, a DC distribution system could become an alternative approach to supply future loads connected on a bus system and could be optimally controlled by an Energy Management System (EMS). Primary DERs used in microgrid setups like photovoltaic (PV) systems and fuel cells have a DC power output. They can be directly connected on the DC bus line. The use of string inverters or central inverters for PV panels could be deployed based on optimality calculations. The

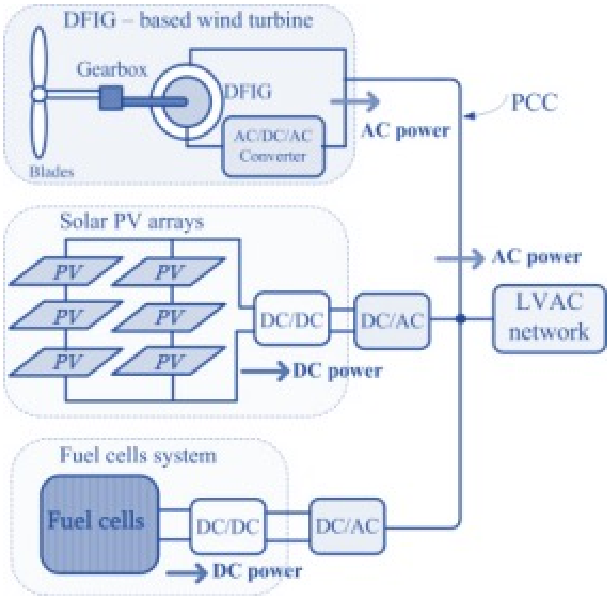

Figure 1.1: LVAC Network [1]

energy storage systems like batteries also work on DC input/output power. This makes interconnections on the LVDC network easier along with minimizing cost of extra power electronic components [18]. In the case of AC generating units like wind turbines and diesel gensets, a rectifier is used before connecting it on the DC link. This can be seen in Figure 1.2. The network avoids excessive conversion losses and can prove to be more economical in certain situations.

The LVDC system seems promising to improve the efficiency of delivering power to the distribution network and help in facilitating more connections of distributed renewable energy generation units [16]. Recent studies like [19] conclude that DC microgrids have appealing features in terms of simple structures, low system cost and an overall improvement in system efficiency as fewer power converters are used as compared to AC microgrids.

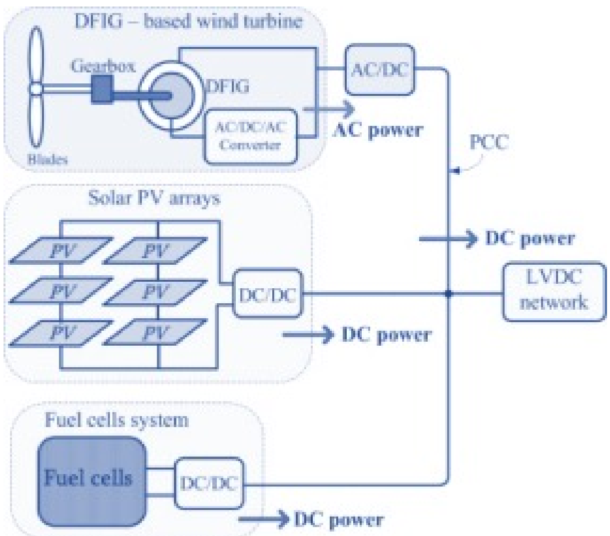

Figure 1.2: LVDC Network [1]

1.3.3. LOOKING INTO THE FUTURE

Knowledge in the DC microgrid segment is limited as of today, which fosters opportunities in further research of potential advancements. The benefits cited by many authors are normally based on pilot projects and small scale research setups. Various Dutch companies like Alliander and Rexel along with other European firms like Engie are investing in DC systems in projects such as the "The Green Village (TGV)" located in the city of Delft, The Netherlands. TGV aims to facilitate these innovative projects by providing a test bed for research and development. Setting up of a DC microgrid to cater to various stakeholders (PV generators, DC consumers and energy storage systems) is on the agenda. Interest shown by such stakeholders in the energy chain towards implementing DC systems portraits a bright future for researchers.

1.3.4. STANDARDIZATION OF LVDC SYSTEMS

Operations of DC microgrids requires standard protocols in terms of voltage standards and network configurations. This can be accomplished for a single building operating as a nanogrid or even a community powered through a microgrid. Such norms help in running the microgid in an efficient manner.

VOLTAGE STANDARDIZATION

To power DC loads, the typical voltages used in DC systems are generally 48 V, 24 V or 12 V [20]. Examples of such DC loads are LED lightining, loads connected to USB Type-C connectors and USB power delivery [21].

According to Mackay et al. [20], the future DC microgrid systems will be expected to have standardization of input voltage levels for generic devices to converge to a value in the range of 350 - 400 V. He states "These voltage levels are widely used in the dc links of ac power supplies today. Therefore, these voltage levels would allow easy implementation of dc ready devices" [22]. If for example, 350 V is chosen as a standard on the DC distribution bus within a microgrid, loads connected to the link can be powered with lower current magnitudes as compared to using 230 V as an input. This reduces transmission losses and improves overall efficiency of the distribution system. For bipolar microgrids, the larger loads connected between the positive and negative pole can have an input voltage of 700V. Refer Figure 1.3 for a layout of a typical LVDC system.

Becker et al. [23] analyzed that the 380 V standard matches the industry needs for consumer electronics in a more suitable fashion. This results in the cables used for distribution to be thinner and cheaper as the required current flow is reduced.

1.4. IMPORTANCE OF OPTIMIZATION IN FUTURE ENERGY SYSTEMS

Depleting fossil reserves and alarming global rise in greenhouse gas (GHG) emissions has prompted an energy transition towards a greener energy generation. Energy systems engineering provides a methodological and scientific framework for complex energy problems. Realistic integrated solutions can be obtained by holistic, systems based approach [24]. Decision making and structured planning for solving energy system problems requires optimization modeling strategies which could be used along with mixed integer linear programming (MILP) and mixed integer non-linear programming (MINLP) algorithms.

Planning of community scale renewable energy systems is an imperative problem at hand and consists of justifying the allocation patterns of energy resources and services, energy structure and economic development, formulation of energy policies and trade-offs with regards to energy consumption, analysis of interactions between economic costs, system reliability and supply - demand consensus [25]. Many authors claim to solve these objectives by applying linear programming and MILP techniques to obtain solutions that can provide desired energy resource/service allocation and capacity expansion plans with a minimized system cost, maximized system reliability and max-

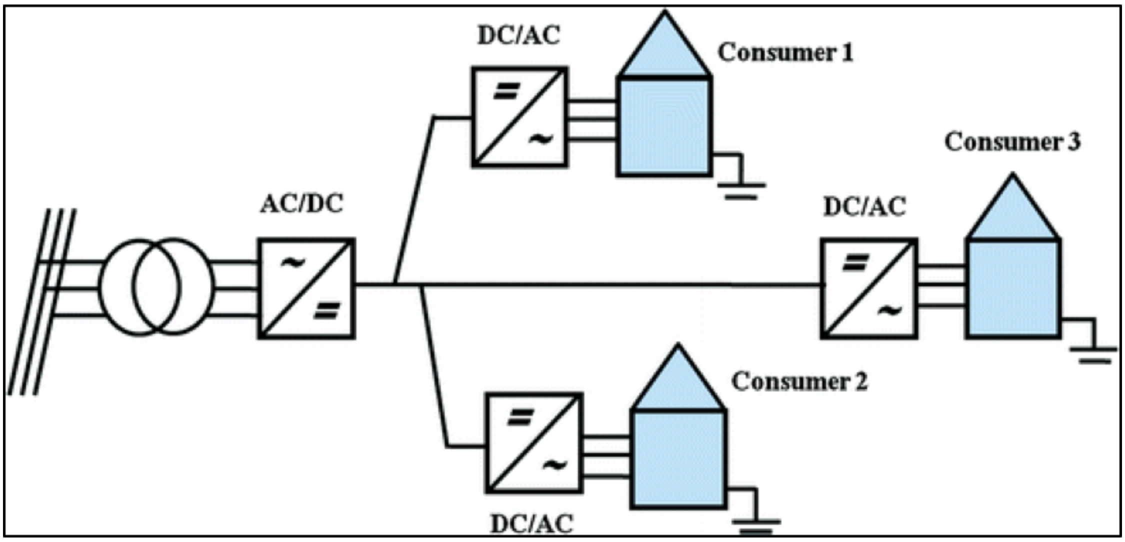

Figure 1.3: A typical LVDC system with nodal points [2]

imized energy security [26]. The importance of these new optimization techniques for short term energy planning is due to the uncertainties associated with renewable energy systems. In order to increase the penetration of these systems, minimizing operational costs and maximizing reliability is vital.

Moreover, the microgrid setups would consist of hybrid energy systems working together to power loads such as buildings, a community, manufacturing facility or office units. Vast portions of the developing regions like India still rely heavily on diesel generator based back-up power. This has negative effects due to two primary reasons: (a) The diesel gensets use fossil based fuel which has harmful carbon emissions which ultimately degrades the environment. (b) The diesel genset units have fixed power capacity ratings. For e.g, A 1 kVA capacity unit is available in the market with the next higher capacity of 10 kVA. If the consumption requirements fall in between the available capacity, there is increased cost and loss of efficiency. This results in suboptimality which is unnecessary.

Optimizing power flows from distributed energy generating units based on cost structures while meeting the system constraints with respect to generator capacity, distribution line restrictions, supply - demand consensus is the basic framework for an optimization problem. Numerous algorithms exist in literature which deal with optimizing frameworks for generic as well as case specific scenarios [27].

The Optimal Power Flow (OPF) technique has become standard practice with digital computers providing solutions to energy problems. These techniques have been implemented by several Independent System Operators (ISO) that use a centralized dispatch approach for alleviating transmission system congestion [28]. Distributed OPF is a relatively newer concept which has in recent times caught the attention of researchers due to increase in distributed energy resources. Earlier power plant planning operations required centralized control due to distance in location of generation and consumption units. Increase in deployment of LVDC systems prompts the use of distributed OPF to be incorporated to optimize the system power flows while reducing overall system operational costs. This makes OPF a feasible tool for solving distributed optimization problems. The OPF algorithms used in past papers like [29] are predominantly for AC networks involving active and reactive power. The set of equality and inequality constraints are formulated to suit the AC network topology. The reasons to dive into distributed control are plentiful based on how the energy generation systems are transitioning. The factors driving distributed optimization is that it is scalable, more robust towards communication failures and cyber-attacks, and can prove to be more resilient to power outages [1].

1.5. Objectives and Research Questions

1.5.1. Objective

Based on the motivation provided in the above section, the objective of this study is:

> *To develop a distributed optimization algorithm for a DC distribution system to account for congestion and line losses in the network while minimizing the overall system operational costs.*

1.5.2. Research Questions

The primary research question for this thesis is: **"How can distributed optimization be implemented in a DC distribution system to account for losses and congestion in the network?"** An initial start to answer the main research question is to find a suitable method to implement a distributed Optimal Power Flow algorithm in a DC distribution system. Literature review provides various methods to perform a fully distributed OPF. The different methods consider an AC distribution network and assume zero distribution line losses. Practical DC distribution systems will violate this assumption. A method is then chosen based on specific insights from literature review and further modified to be implemented in a DC microgrid set-up while considering distribution line losses.

Based on the primary research question, other set of sub-questions will also be answered. The sub-questions are as follows:

1. **"How can linear cost functions of power generators and zero marginal cost power generators be accounted for?"** The approximated DC OPF algorithm presented in literature can only be implemented for quadratic cost functions. Appropriate alterations and improvements need to be carried out to answer the above sub-question.

2. **"How can voltage limits be satisfied without the use of a slack bus?"** Insights from literature review state that voltage limits are not considered in the distributed optimization problems. In some cases if they are considered, in order to maintain voltage magnitudes of the system in a specific range, a slack bus is used. A slack bus is nothing but a reference bus [6]. This keeps the voltage of the system within the required range.

3. **"What are the effects of the distributed algorithm on meshed power grids?"** Optimization techniques for meshed grids can prove to be tricky. An effective functioning of the distributed optimization is the aim for the presented sub-question. The above sub-question will be answered once the modified distributed OPF is implemented for a meshed grid and MATLAB simulations are run to check for convergence.

1.6. THESIS FLOW CHART: METHODOLOGY ADOPTED

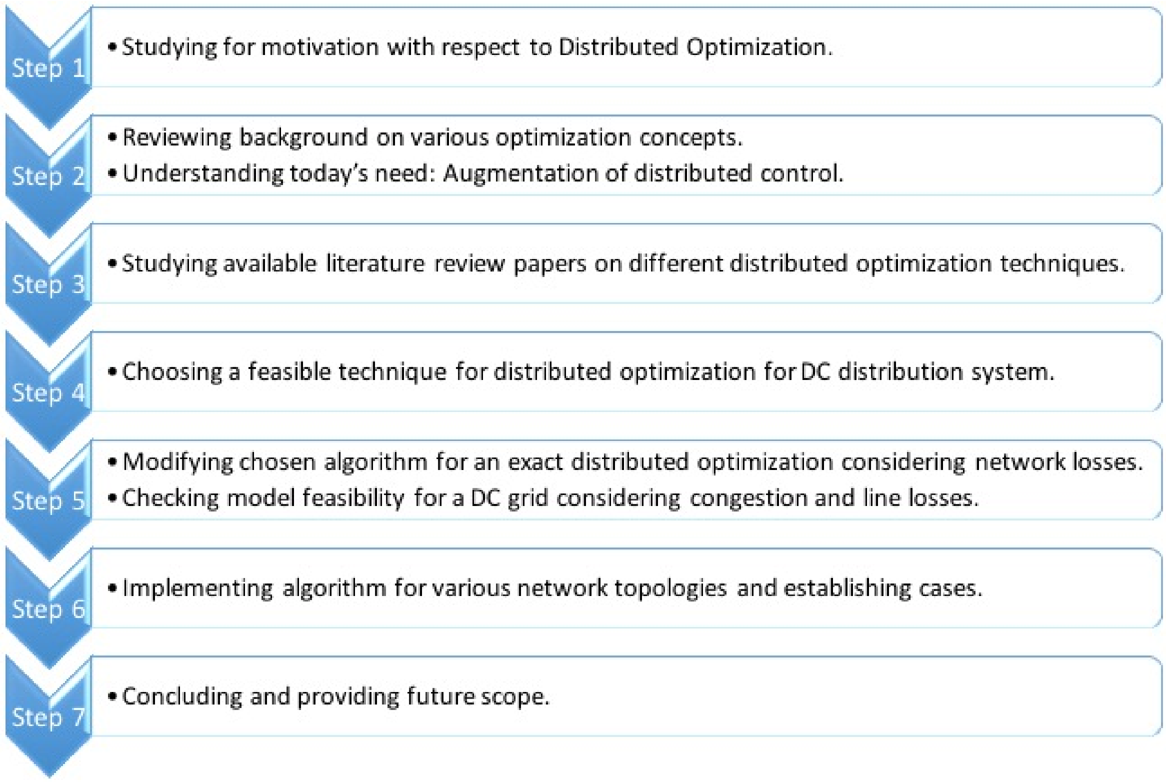

1.7. REPORT STRUCTURE

This section will provide an overview of the report structure and its content in brief.

Chapter 2 provides details on concepts primarily used in energy optimization techniques. Concepts such as Economic Dispatch, Locational Marginal Price and its use in Optimal Power Flow problems are explained. The chapter concludes with offering advantages of distributed optimization techniques over its centralized counterpart.

Chapter 3 presents various distributed Optimal Power Flow methods. Every method is explained and analyzed with respect to insights from literature review. After a comparative discussion, a method is chosen, which is a good fit to achieve the thesis objective.

Chapter 4 presents a detailed description of the chosen distributed Optimal Power Flow method. The method is minutely broken down to understand its procedure and mechanism for an AC network. Finally an analysis on the model is presented stating the required modifications to achieve the thesis objective.

Chapter 5 is the heart of the thesis. Initially, a distributed algorithm is presented based on modifications from Chapter 4. This model assumes no losses in the DC network. Furthermore, a distributed optimization model which accounts for congestion and line losses in a DC distribution system is presented. This aims to answer the main research question of the thesis. This is followed by a simple case study to better understand the functioning of the model.

Chapter 6 presents various cases of network topologies to test the convergence of the distributed algorithm. The cases considered aim to present practical DC networks.

Chapter 7 provides a conclusion followed by opportunities for future work.

2

Background on Optimization of Energy Systems

This chapter dives into details of certain optimization concepts which play a pivotal role in the modelling of the distributed Optimal Power Flow algorithm. Sound understanding of optimization formulations, its equations and the solution from these equations is required for a deeper interpretation of the concept. Below sections will deal with Economic Dispatch for power systems with quadratic and linear cost functions. The procedure depends on the type of constraints: whether equality or non-equality constraints. The application of this to Optimal Power Flow (OPF) problems is briefed upon. Based on the implementation of OPF to power grids, comprehending what the solution has to offer is also vital. The importance and role of Locational Marginal Prices (LMP) is therefore studied. Finally, the benefits of using distributed OPF over a centralized OPF is investigated.

2.1. Economic Dispatch and OPF

The Economic Load Dispatch problem is part of OPF and is defined as the scheduling of power generating units to provide energy to load demands, while minimizing the total operational costs of the power system and satisfying all the system constraints [30] [31]. "The schedule of generation for the various generators in the system to satisfy the minimum operating cost condition for a particular load is termed as generation scheduling" as stated by Mishra et al [30].

The OPF problem consists of an objective function which is basically a cost function which is dependent on power generated by the generators [31] [32]. It is generally measured in terms of Currency/hour. For this study we consider the unit to be EUR/hr. The cost function normally considered in literature is of quadratic nature. The quadratic cost functions are considered for generators such as gas turbines and diesel generators which can be used in an LVDC network [33]. Some distributed energy sources like the Fuel Cell (FC) system have operational costs associated with the usage of fuel to generate electricity. As stated by Simoes et al. [34], FC systems have a linear cost function based on the power it generates. When it comes to renewable energy systems like photovoltaic (PV) systems and small wind turbines, the operational cost is negligible as these systems do not require any fuel to produce electricity. They are associated with maintenance costs which can be neglected. Therefore, these systems have zero marginal costs. Marginal cost is basically the first derivative of the cost function with respect to the power generated and is measured in terms of EUR/kWh [35]. For zero cost functions like the PV system and wind turbines, the associated marginal cost is also zero. For FC systems which have a linear cost function, the marginal cost is fixed and equal to the cost co-efficient. For quadratic cost functions, the marginal cost is dependent on the power produced. Hence, for such systems, more the power produced, higher is the marginal cost.

$$C(P_{G1}) = A_1 P_{G1}^2 + B_1 P_{G1} + C_1 \tag{2.1}$$
$$C(P_{G2}) = B_2 P_{G2} + C_2 \tag{2.2}$$
$$C(P_{G3}) = 0 \tag{2.3}$$

where, P_{G1}, P_{G2} and P_{G3} represent power generated from different generators. Equation (2.1) is the cost function for a gas turbine or diesel generator. Equation (2.2) is for a FC system or other systems with a linear cost function. Equation 2.3 is for renewable energy systems like PV or wind turbines with nearly zero operational costs. The cost co-efficients like A_1, B_1, C_1, B_2 and C_2 are constants and depend on generator properties. A higher cost co-efficient signifies an expensive generator and vice-versa.

The marginal cost is then calculated by taking the first derivative of these functions with respect to the power generated P_G [35].

$$MC(P_{G1}) = A_1 P_{G1} + B_1 \tag{2.4}$$
$$MC(P_{G2}) = B_2 \tag{2.5}$$
$$MC(P_{G3}) = 0 \tag{2.6}$$

where, MC represents the marginal cost (also called as incremental cost) [35] of the generator.

The ED problem also consists of equality and inequality constraints depending on the type of problem. Practical scenarios have ED problems having both the type of constraints [31]. Equality constraint is generally an equation for the supply-demand consensus. Inequality constraints for example can be equations with power flow limits, or voltage limits, or power generation capacity limits, etc.

2.1.1. KARESH KUHN TUCKER (KKT) TECHNIQUE

Consider a simple optimization problem with a main objective function and a set of constraints.

$$\text{minimize} f(x) \tag{2.7}$$

Subject to:

$$h_i(x) = 0 \qquad \forall i \in N \tag{2.8}$$
$$g_j(x) \le G_{\max} \qquad \forall j \in M \tag{2.9}$$
$$g_j(x) \ge G_{\min} \qquad \forall j \in M \tag{2.10}$$

where, $f(x)$ is a function which is dependent on a variable x. The objective is to minimize this function. $h_i(x)$ is a set of N equality constraints and $g_j(x)$ is a set of M inequality constraints. The boundary limits for the inequality equations are $G_{\max}$ and $G_{\min}$. To solve such an optimization problem with inequality constraints, Karesh Kuhn Tucker (KKT) technique can be implemented [35]. To reach at an optimal solution of the optimization problem, KKT conditions for optimality are required to be solved. A Lagrange function is first formulated for the optimization problem and further the set of KKT conditions are solved. The Lagrange function for the problem formulation is:

$$\mathscr{L}(x) = f(x) + \lambda_i(h_i(x)) + \mu_{j\max}(g_j(x) - G_{\max}) + \mu_{j\min}(-g_j(x) + G_{\min}) \tag{2.11}$$

The set of necessary KKT conditions for a minimum of a function $f(x)$ is based on the Lagrangian function given by Equation (2.11). The KKT conditions are stated below.

The necessary KKT conditions for optimality are:

$$\frac{\partial \mathscr{L}(x)}{\partial x} = 0 \tag{2.12}$$

$$\frac{\partial \mathscr{L}(x)}{\partial \lambda_i} = 0 \tag{2.13}$$

The feasibility KKT conditions are:

$$h_i(x) = 0 \qquad \forall i \in N \tag{2.14}$$

$$g_j(x) \le G_{\max} \qquad \forall j \in M \tag{2.15}$$

$$g_j(x) \ge G_{\min} \qquad \forall j \in M \tag{2.16}$$

The complementary slackness conditions are:

$$\mu_{j\max}(g_j(x) - G_{max}) = 0 \tag{2.17}$$

$$\mu_{j\min}(-g_j(x) + G_{min}) = 0 \tag{2.18}$$

The positivity conditions are:

$$\mu_{j\max}, \mu_{j\min} \ge 0 \tag{2.19}$$

where, λ_i, $\mu_{j\max}$ and $\mu_{j\min}$ are dual variables of the problem. The number of dual variables are equal to the number of constraints present in the problem formulation [35]. These dual variables provide significant details on the system properties.For e.g. λ_i is equal to the marginal cost of the generator for an uncongested network. It is also termed as Locational Marginal Price (LMP). Details on this will follow in the immediate section.

All the above KKT conditions given by Equations (2.12) - (2.19) have to be satisfied and solved to derive an optimal solution of the given OPF problem.

2.2. SIGNIFICANCE OF LOCATIONAL MARGINAL PRICES

In distribution and transmission networks, congestion management is carried out to ensure supply and demand consensus at the least cost of operation. To manage the congestion constraints in a network, LMP is utilized [36–38]. LMP is defined as the lowest cost required to provide the next increment of demand at a node by obeying the network constraints. It is also termed as *Spot Prices* or *Nodal Prices* [39]. Traditionally, LMP are used to manage congestion in transmission lines using the Direct Current approximated Optimal Power Flow (DC OPF) approach, see Chapter 4. In an OPF problem, the LMP values at each node in the network are directly obtained as dual variables of the nodal power balance constraint. This is denoted by λ_i in the Lagrange function given by Equation (2.11). For convex problems, the KKT conditions specified above hold true and provide correct LMP values [40].

Nodal prices incorporate the cost of the energy source and the distribution constraints. For a lossless network with no distribution constraints, the nodal price is the same for all the connected nodes. If line losses and line limits are accounted , the LMP values differ at the nodes [38]. When congestion is present, there will be atleast one source which is marginal while the rest will be operating at either their minimum or maximum output. Furthermore, the LMP for such marginal source units is equal to the marginal cost of the power generator [40].

LMP are traditionally composed of three main parts: the energy term, loss term and the congestion term [40]. The energy term is same for all nodes present in the network, and depends on the reference node. The loss term reflects the marginal losses. It is a cost associated with providing extra power required to compensate for the line losses in the distribution or transmission cables. Finally, the congestion term represents the cost associated with congestion in the network connecting the particular node. This term is achieved through the dual variables of the OPF problem. More on this will be seen in the coming chapters. Thus, LMP reflects a fair price in a transmission system for a buyer and seller of energy.

2.3. CENTRALIZED AND DISTRIBUTED OPF

Centralized computation has traditionally been the primary tool for application of optimization algorithms used in electric power systems. In particular, Independent System Operators (ISO's) seek a minimum cost generated economic dispatch for large scale transmission systems by solving an Optimal Power Flow problem [41]. This OPF problem helps to minimize the overall system cost, subject to engineering limits and physical constraints owing to power flow equations. The ISO further gathers all necessary data and performs a central computation to solve the OPF problem [41].

With the ever increasing penetration of distributed renewable energy resources, the centralized optimization approach which is most prevalent in current power systems will potentially be ameliorated with distributed optimization algorithms. Rather than having a central database with complete system information on parameters and performing a centralized calculation, distributed optimization techniques are computed by multiple agents within the system that obtain data through interlinked communication with a limited set of neighbors [5]. Depending on the specifics of the distributed algorithm and application requirement, the agents can represent a single node or a group of nodes forming a region in a power grid.

Distributed optimization has numerous potential advantages over its centralized counterpart. Once the computing agents have been decided in the power system, the agents exchange only limited amounts of information with a subset of other agents. This provides benefits in terms of cybersecurity and data privacy while also reducing costs of unnecessary communication infrastructure [41, 42]. Another advantage of distributed OPF is it's robustness with respect to failure of individual agents which ultimately provides resilience during power outages. Finally, as stated by Molzahn et al. [41], "distributed optimization algorithms have the potential to be computationally superior to centralized algorithms, both in terms of solution speed and the maximum problem size that can be addressed".

These prospective benefits of distributed optimization prompts a detailed research for distributed algorithms applied to DC systems at the power distribution level. This establishes a base for the motivation behind the study.

3

Distributed Optimal Power Flow

In this chapter, various methods present in literature for distributed Optimal Power Flow implementation are looked upon. The rise in the use of distributed energy resources like photovoltaic systems, small to medium capacity wind turbines, small hydro plants, fuel cell systems, battery energy storage, plug-in vehicles with vehicle-to-grid capabilities, etc. makes distributed optimization advantageous over the traditional centralized approach [41]. The various methods of distributed OPF are presented and analyzed for suitability in a DC distribution system.The chosen method is elaborated in the last section for further modeling in a LVDC network. The goal is to enable a fully distributed solution of the Exact DC OPF i.e. formulation of generation settings which minimize the overall operational costs while ensuring a supply - demand consensus and obeying all the network constraints like line congestion and network power losses.

3.1. Rise of Distributed Optimization

In the past, research on traditional power systems primarily focused on the core of the system which consisted of huge amount of generation, via high voltage transmission, to the substations. The monitoring and control of these core activities involving planning and optimization were done by a single entity like an Independent System Operator (ISO) [43]. With the rise in integration of renewable energy and energy storage systems, self-healing ability and demand side management, the focus is shifted to the consumer end which consists of local distribution networks. This new concept of integration and modeling is termed as smart grid [44]. As mentioned in the previous chapter, the OPF can be implemented in such smart grids as it aims to minimize the generation costs of local generators subject to demand constraints and the network physical constraints. These network constraints comprise of power generation limits, power flow in connecting line limits, nodal voltage limits, etc.

In the distributed energy infrastructure, different entities take the control responsibility of different parts of the system. Although these are independent entities, the decision made by these control entities affect the decision of other entities as they are physically connected by a transmission or distribution line. This suggests that the entities need to link and collaborate with each other to achieve effective and reliable operation of the distribution grid. Hence, the conventional centralized algorithms and energy management solutions may no longer completely justify the role of controlling and operating such a distributed energy system [5].

3.2. Methods to solve distributed OPF

The OPF algorithm is an essential energy management function in electric power systems as stated by Kargarian et. al [5]. An extensive amount of research has been done on OPF solution methods to yield minimum costs in centralized power systems for a single control entity [31]. In order to accommodate multiple control entities which are interconnected, the OPF solution methods have to be modified and adjusted. This is achieved using the various distributed OPF algorithms. Set of advantages of the distributed approach over the traditional centralized approach is presented in Chapter 2, Section 2.3.

In general, papers about distributed OPF problems in smart grids available in literature have a similar procedure of operational algorithm. Firstly, an OPF is formulated for each control entity with respect to exchange of information between neighbouring entities. Then, iterative distributed algorithms are developed and implemented to arrive at a reliable and optimal operation of the distribution grid [5].

The distributed OPF algorithms have multiple control entities, with each entity responsible for its own physical region. This physical region can comprise of multiple buses connected by transmission or distribution lines or a single bus. This study deal with LVDC distribution system, hence the network is void of transmission lines. To coordinate the OPF solutions of the entities, seven decomposition coordination algorithms have been studied in the past. These include: Analytical Target Cascading (ATC), Alternative Direction Multiplier Method (ADMM) with Proximal Message Passing (PMP), Dual Decomposition, Auxilliary Problem Principle (APP), Optimality Condition Decomposition (OCD), Consensus + Innovations (C+I) and Gradient Dynamics [5, 41, 45]. The below subsections cover the key features of each algorithm and its solution method for an approximated DC OPF problem. Most papers have these algorithms applied to an AC distribution system.

Though the list of methods to solve a distributed OPF problem have a similar procedure, the framework of the methods vary. Dual Decomposition, ADMM with PMP, ATC and APP use augmented Lagrangian in their decomposition functions. OCD, C+I and gradient dynamics on the other hand solve the Karush–Kuhn–Tucker (KKT) conditions in a decentralized fashion [5]. For the sake of simplicity, the seven methods are categorized under the mentioned two frameworks of achieving an optimal solution. The categorization is mentioned in Table 3.1.

Table 3.1: Methods to Solve Distributed Optimal Power Flow Problems

Augmented Lagrangian Decomposition Based Methods	**Decentralized Solution of KKT Based Methods**
Dual Decomposition	Optimality Condition Decomposition (OCD)
Alternating Direction Multiplier Method (ADMM) with Proximal Message Passing (PMP)	Consensus + Innovation (C+I)
Analytical Target Cascading (ATC)	Gradient Dynamics
Auxiliary Problem Principle (APP	

3.2.1. EXACT DC OPTIMAL POWER FLOW FORMULATION

The objective of the distributed OPF problem is to determine the generation dispatch that yields the lowest cost to meet the load demands while all the system network and generation constraints are satisfied. The papers presented in the past like [5, 6, 46, 47] have used DC approximation for the OPF problem. These DC approximations are basically linear approximations which are discussed in Chapter 4.

The mentioned approximations need appropriate modifications for implementation in practical DC distribution systems. This is covered in detail in Chapter 5. Before, the various distributed OPF methods are explained and analyzed, it is important to keep in mind the objective of the study. The study formulates an Exact DC distributed OPF problem. This basically entails an OPF problem with congestion and line losses as part of the formulation. Keeping the set of equations in mind, various techniques can be examined for suitability. The cost function considered is of a quadratic nature but can be appropriately modified to accommodate linear cost equations as well. Network and generation constraints are considered as inequality constraints. The consensus for supplying generated power to the loads is presented as an equality constraint.

Objective

$$\min \sum_{m \in \mathcal{N}} \sum_{s \in \mathcal{S}} A_m (p_m^S)^2 + B_m p_m^S + C_m \tag{3.1}$$

$$\min \sum_{m \in \mathcal{N}} \sum_{s \in \mathcal{S}} A_m (i_m^S)^2 u_m^2 + B_m i_m^S u_m + C_m \tag{3.2}$$

Subject to

$$\sum i_m^S = \sum G_{m,n}(u_m - u_n) \qquad \forall (m,n) \in \mathcal{N} \tag{3.3}$$

$$-\overline{I}_{m,n} \leq G_{m,n}(u_m - u_n) \leq \overline{I}_{m,n} \qquad \forall (m,n) \in \mathcal{N} \tag{3.4}$$

$$\underline{P}_m^S \leq p_m^S \leq \overline{P}_m^S \qquad \forall s \in \mathcal{S} \tag{3.5}$$

$$\underline{P}_m^S \leq i_m^S u_m \leq \overline{P}_m^S \qquad \forall s \in \mathcal{S} \tag{3.6}$$

$$\underline{U}_m \leq u_m \leq \overline{U}_m \qquad \forall m \in \mathcal{N} \tag{3.7}$$

The cost function in the objective comprises of a quadratic equation as a function of generator power (p_m^S) which is split in terms of current at the nodes (i_m^S) and nodal voltage (u_m). This is done to individually optimize the voltage and current values for the distribution system. Equation (3.3) is an equality constraint to match the generated power to the power requirement. Equation (3.4) denotes the current line constraint for a transmission network. The inequality suggests the current holding capacity of the line. Equation (3.5) is broken down to (3.6) to denote the maximum and minimum power generator capacity. Lastly, Equation (3.7) denotes the allowable voltage values maintained in the grid.

These set of equations are formulated specially for this thesis. They are based on equations provided by past papers such as [46]. However, these papers do not consider an exact approach of optimization, hence overlook certain equations like (3.2) and (3.7) in their problem formulation.

Kargarian et al. [5] in their survey of distributed OPF, mention OPF formulations for a multi-region power system. In such a system, the regions are interconnected through tie-lines and the formulations are linked together. There are two general ways of reformulating the multi-region OPF for individual regions. The first one uses coupling variables where different regions may contain similar variables but the set of constraints are separated. The other one employs coupling constraints, where different regions may contain constraints with variables from two or more regions but the set of decision variables are separated. This study will not get into the details of multi-region power systems as the formulations which will be used are strictly based on Equations (3.1) - (3.7).

The seven methods to solve distributed OPF mentioned above have a broad conceptual similarity such that each approach considers distributed agents that exchange information of variables among one another and perform local computations to solve the system optimization problem [41]. However, contrast in the structuring in terms of information shared and algorithm used leads to differences in practical performances and computation times. To study such differences, the seven methods are investigated based on literature review.

3.2.2. DUAL DECOMPOSITION

Lagrangian functions for some specific optimization problems have a separable structure that can be capitalized using dual decomposition techniques [48].

Consider a general optimization problem of the form:

$$\min \sum_{m \in \mathcal{N}} f_m(x_m) \tag{3.8}$$

$$\sum_{m \in \mathcal{N}} A_m x_m = b \tag{3.9}$$

where, m is an instantaneous node or bus for $\mathcal{N}$ number of buses. The objective is a function of variable x_m and is subject to an equality constraint. A_m denotes the co-efficient and b denotes the associated vector. The Lagrangian for Equations (3.8) - (3.9) is:

$$\mathcal{L}(x, y) = \sum_{m \in \mathcal{N}} [f_m(x_m) + y(A_m x_m - b)] \tag{3.10}$$

where, y denotes the dual variable. The dual decomposition method uses an iterative method called "dual ascent" to solve the above formulation [41]. The iteration update for the decision variable and the dual variable is:

$$x_m(l+1) = \arg\min_{x_m} \mathcal{L}(x_m, y(l+1)) \tag{3.11}$$

$$y(l+1) = y(l) + \alpha(l)[\sum_{m \in \mathcal{N}} A_m x_m(l+1) - b] \tag{3.12}$$

where, 'l' is the iteration counter as the decision variable x_m and the dual variable y stabilizes to give an optimal value. $\alpha(l) > 0$ is the specified step size at iteration count 'l'. It can be seen that the update in Equation (3.11) is performed independently which enables a distributed fashion of implementation. However, the dual variable update shown in Equation (3.12) requires a central coordinator. The drawback of the dual decomposition technique is that the convergence is not guaranteed even for convex problems. The technique is dependent on the step sizes and problem characteristics.

3.2.3. ALTERNATING DIRECTION MULTIPLIER METHOD (ADMM) WITH PROXIMAL MESSAGE PASSING (PMP)

The Alternating Direction Method of Multipliers (ADMM) is a relatively well known and researched method in comparison to other distributed OPF algorithms. This technique is most commonly used for the solution of convex optimization problems in a distributed fashion specifically in large scale applications such as OPF and unit commitment in utility power grids [49]. ADMM is based on a decomposition coordination process, in which the large scale problem formulation is broken down to smaller sub-problems such that the solution procedure for the sub-problems is coordinated and the overall system reaches optimality [50, 51]. Hence, using solely ADMM in a distributed manner requires a central coordinator. To break it down, ADMM minimizes the augmented Lagrangian using a single Gauss-Seidel pass instead of the usual joint optimization.

To implement the ADMM technique, we initially derive the augmented Lagrangian function of the given optimization problem. Then, the augmented Lagrangian function is decomposed and the corresponding functions are minimized over sequential Gauss-Seidel iterations. At every iteration, in the beginning, each sub-problem which is the decomposed Lagrangian function is only minimized with respect to the set of decision variables (primal variables) based on which it is decomposed. Later, the dual variables are updated using the updated primal variables. This iteration loop continues until the convergence criteria is satisfied [5].

A network of two regions is connected through a tie line which essentially is a connecting bus. The ADMM method introduces copies of the coupling variables for each region in order to decouple the coupling constraints, while ensuring that the copies of coupling constraints are in agreement using consistency constraints. The components of the coupling set of variables are updated in a distributed manner. When we consider the case of this paper, exact distributed OPF for DC systems is a requirement. The nodal power balance equation is a coupling constraint as it involves the voltage values at the nodes of physically connected adjacent buses. Now, in order to decouple the power balance equation over the tie-lines, every node or region holds a copy of the voltage magnitude associated with it's neighbour in that region [3]. This concept of introducing copies of shared variables facilitates an autonomous approach for each sub-problem. Hence, each sub-problem is assigned to a region. However, as mentioned earlier, a coordinating agent has to ensure the sub-problem variables are reaching consensus over the course of the iterations.

Consider an optimization problem as stated below:

Objective Function

$$\min_{x,z} f(x) + g(z) \tag{3.13}$$

Subject To

$$Ax + Bz = c \tag{3.14}$$

where, x and z are the decision variables presented as functions in the objective function. c is the specified vector and A and B are co-efficients in the constraint equation. The augmented Lagrangian of the above formulation is [41]:

$$\mathcal{L}_p = f(x) + g(z) + y(Ax + Bz - c) + \frac{\rho}{2}||Ax + Bz - c||_2^2 \tag{3.15}$$

where, $\rho > 0$ is a specified penalty parameter and $||.||_2$ is the two norm for absolute value. It is visible in Equation (3.15) that it is the Lagrangian function of equation 3.13 and 3.14 with an added weighted squared norm of the constraint residual. The algorithm for ADMM runs iterations to minimize the augmented Lagrangian function by performing the following updates for the decision variables and dual variables:

$$x(l+1) = \arg\min_{x} \mathcal{L}_p(x, z(l), y(l)) \tag{3.16}$$

$$z(l+1) = \arg\min_{z} \mathcal{L}_p(x(l+1), z, y(l)) \tag{3.17}$$

$$y(l+1) = y(l) + \rho(Ax(l+1) + Bz(l+1) - c) \tag{3.18}$$

where, 'l' is the iteration counter and the updates are clearly the function of their previous iterative value and the iterative value of shared decision variables and dual variables. y is the dual variable. The updates for x and z are independent and hence can be performed in a distributed manner.

For this algorithm, if the functions of the primal variables are convex, it is guaranteed to converge to a solution. The rate of convergence is dependant on the value of ρ chosen and strategies have been developed in the past to have a parameter adaptive approach [49]. If the ADMM algorithm is applied to non-convex functions, the solution is not guaranteed to converge.

For optimization problems having inequality constraints, the ADMM algorithm needs a slight modification. The objective function is reformulated to accommodate the inequality constraints using an indicator function. The study will not get into details of the reformulated algorithm.

Based on the mentioned algorithm for ADMM, it is evident that a central coordinator is required to manage the updates of the dual variable shown in Equation (3.18). However, using a modification in the form of Proximal Message Passing (PMP) eliminates the need of the central controller and results in a fully decentralized algorithm [41]. Once the PMP algorithm is used, each iteration of each agent evaluates a "prox" function.

$$\mathrm{prox}_{f,\rho}(v) = \underset{x}{\arg\min}(f(x) + \rho/2||x - v||_2^2) \tag{3.19}$$

The vector x in Equation (3.19) contains local copies of both the decision variables (x and z) and the dual variable y. The vector v contains the average of the values in x for all the neighbouring buses. ρ is a tuning parameter [52]. The PMP minimizes each Gauss-Seidel pass which results in evaluating the prox functions with respect to the particular decision variable vector partition. Hence, using ADMM based PMP is a complete decentralized solution and highly scalable with respect to number of nodes or regions in a network. The PMP algorithm has also been applied to security constrained OPF problems as presented by Chakrabarti et. al [53]. The PMP applied in power grids have fabricated agents. The estimated values of power flows and voltage angles (for AC networks) or absolute voltage values (for DC networks) at each node at a particular iteration, termed as "messages" are then exchanged between connected nodes. The stopping criteria for the iterations is that the differences between these messages is minimum while the overall operation costs of the system over a given time is optimized.

Evaluating the prox function given in Equation (3.19) gives us a set of decision variable updates for the agents, such that they are closest to the previous iterative update as well as satisfy the constraints like power mismatch and angle mismatch. The cost function is minimized as well. The update equations as stated by Kargarian et. al [5] are as follows:

Proximal Plan Update

$$p_j^{l+1} = \mathrm{prox}_{f,\rho}(p_j^l - \overline{p}_j^l - u_j^l) \tag{3.20}$$

Scaled Price Update

$$u_N^{l+1} = u_n^l + \overline{p}_N^{l+1} \tag{3.21}$$

where, $p, \overline{p}, u, l, \rho, j and N$ are respectively the power, average power, power nodal price, iteration count, tuning parameter, agent subscript and node number.

3.2.4. ANALYTICAL TARGET CASCADING (ATC)

Analytical Target Cascading is a mutli-level, hierarchical optimization method for energy system design [54]. ATC basically formalizes the process of propagating top-level targets on all levels of hierarchy. The single top level element in the hierarchy represents the overall system while the lower levels represent the sub-problems of the parent element.The elements present in these various levels of hierarchy are coupled through target and response variables. The targets are set by the parent elements of the other elements they are coupled to, while the response is given by the lower elements on the closeness to reach the set target [3].

For each element an optimization problem is formulated. The formulation aims to find local variables, responses by elements to its parent, targets for its sub-problems and eventually minimizing an inconsistency weighted penalty function while meeting local design constraints [55]. Variable allocation structure is presented in Figure 3.1. Every element is free to use one or more analysis models to determine responses. These responses are then iteratively re-balanced until the higher level elements by changing targets and designs to achieve higher consistency. Sub-problems are not independent and hence require a coordination strategy to define a sequence in which the sub-problems are solved, and targets and responses are communicated. Generally distributed optimization techniques using decomposition theories incur higher computational costs as compared to all-in-one (AIO) strategy. Past research papers talk about numerical experiments which point out to two prime issues which increase computational effort to arrive at an optimal solution [56–58]. Large weights are needed for accurate sub-problem solutions and higher number of iterations are required in the coordination strategy that solves the optimization problem. Both these issues arise in the relaxation technique used to decompose and transform the original design problem. In an ideal solution, the targets and responses have to be equal, while the consistency constraints force them to match. However, for feasibility of sub-problems these consistency constraints have to be relaxed causing mismatch within the target and response values. These inconsistencies are further minimized using quadratic penalty functions [3].

Using quadratic penalty function requires large weights to find accurate solutions [59]. The large weights cause computational difficulties and problems in processing [56, 58]. Another issue with the quadratic penalty function is that it is inseparable, leading to sub-problems being dependent and requiring central coordination. To address this dependency, a coordination strategy has to be deployed which uses an iterative process of solving sub-problems and exchanging information on targets and responses. The use of such coordination strategies heavily augments the computation costs for achieving higher accuracy [3].

To overcome the weight issue and the relaxation faults, several authors like Lassiter et al. and Michalek and Papalambros [58, 60] have come up with alternative relaxation methods and nested solution algorithms to tackle the issue. Augmented Lagrangian relaxation techniques have been used along with the ATC problem to save computational costs and achieve accurate optimal results.

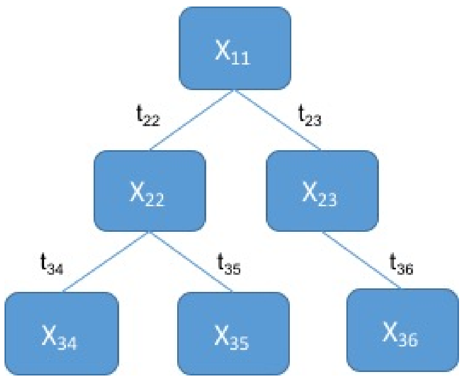

Figure 3.1: Variable allocation in Analytical Target Cascading [3]

3.2.5. AUXILIARY PROBLEM PRINCIPLE (APP)

Auxiliary Problem Principle was introduced early on in the decomposition theories for distributed optimal power flow solutions. The solution of an optimization problem is found by solving a sequence of auxiliary problems [5]. Research papers like [4, 45, 61–63] incorporate APP to enable a decentralized OPF implementation in a large scale power system application.

First, the power grid is broken down into several regions based on geography and network connectivity. Further, dummy buses are added in all tie-lines that connect that region with its neighbouring regions. A set of decision variables like voltage magnitude and current flows for DC distribution systems at these dummy buses are assigned to each region. For AC distribution systems, the variables will account for voltage magnitude and phase angle, active and reactive power. An example of the distributed implementation is presented in figure 3.2. A local OPF is formulated at every region and an iterative algorithm is deployed to arrive at an optimal operating point of the entire grid. The convergence criteria for the APP algorithm is that the corresponding variables at the dummy buses need to be equal or very very close to equal once the algorithm converges [5].

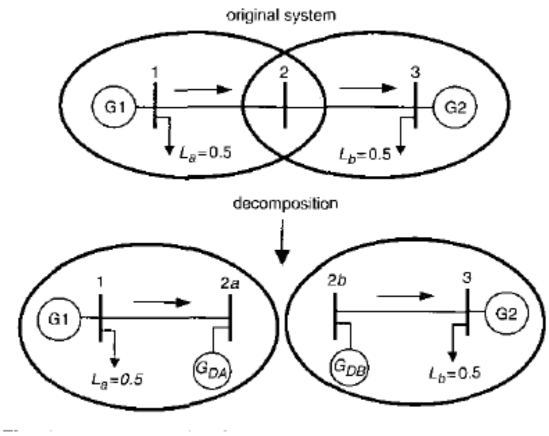

Figure 3.2: Example of distributed implementation of APP [4]

The APP principally decomposes an optimization problem with coupling variables into sub-problems. The coupling variables are further duplicated and one of the duplicated copies is assigned to each of the decomposed problem that are coupled by the coupling variables. As discussed above, for convergence of the two corresponding duplicated variables to match, a consistency constraint is imposed on the sub-problems. Similar to the ATC method, we relax the consistency constraints by an Augmented Lagrangian approach. Then, as stated by Cohen et al. [64], for the APP approach, the cross-terms in the augmented Lagrangian are linearized. The sub-problems then exchange values of the duplicated variables at the end of every iteration to finally determine the optimal operating point of the original optimization problem. For a particular iteration, a sub-problem needs to know the values of the coupling variables determined by other sub-problems in the earlier iteration. This leads to a process of parallel computation.

As a rule stated by Kargarian et al. [5], if the objective function of each sub-problem is convex and differentiable, the APP algorithm converges to an optimal solution regardless of the starting point. This means that the global optimum is reached. APP can also be used for non-convex optimization problems. If the solution to such problems yields a converged result, the necessary conditions of overall optimality are satisfied [64].

Consider a generic optimization problem given in Equation (3.13). The objective function is a function of two decision variables x and z. The problem is subject to a set of constraints which are functions of x and z independently or in a single equation. Figure 3.2 shows the decomposition carried out by the APP method to incorporate dummy variables for the two broken regions a and b. The dummy variables are y_a and y_b. Here, y can be interpreted as power flow passing through the border bus. It should not be misinterpreted as a dual variable which was considered for another approach mentioned before.

The update equations according to the APP algorithm are stated below [4].

Step 1: Solve OPF for region 'a'

$$x^{l+1} = \frac{\beta(L_a - y_a^l) + \gamma({y^l}_a - y_b^l) + \lambda^l}{1+\beta} \tag{3.22}$$

$$y_a^{l+1} = L_a - x^{l+1} \tag{3.23}$$

Step 2: Solve OPF for region 'b'

$$z^{l+1} = \frac{\beta(L_b - y_b^l) + \gamma(y^l{}_a - y_b^l) + \lambda^l}{2+\beta} \tag{3.24}$$

$$y_b^{l+1} = L_b - z^{l+1} \tag{3.25}$$

Step 3: Update λ

$$\lambda^{l+1} = \lambda^l + \alpha(y^l{}_a + y_b^l) \tag{3.26}$$

where, l is the iteration counter and L_a and L_b represent the power loads at the two regions. λ is the dual variable which is generally the cost to maintain the consistency constraint. α, β and γ are positive constants. The iterations for this approach run in a parallel computation fashion.

3.2.6. OPTIMALITY CONDITION DECOMPOSITION (OCD)

The Optimality Condition Decomposition method for solving distributed optimal power flow problems is basically an extension of the Lagrangian relaxation method. Various authors state its supremacy in terms of improved convergence properties over Lagrangian Relaxation and Augmented Lagrangian methods [65–68]. The approach is an iterative algorithm which solves the optimization problem for each region for every iteration in an independent fashion. Variables which appear in a specific region for a specific sub-problem and are under the responsibility of another area take values obtained in previous iterations [5].

As it is evident from the approach, the OCD method is suitable for solving optimization problems involving coupling constraints. In this method, the first-order optimality constraints associated with the overall problem are decomposed and solved by breaking it into sub-problems. At every iteration, the primal and dual variables are updated by solving the optimality conditions using a Newton-Raphson step. The updated variables associated with the boundary nodes between neighbouring regions are exchanged among the sub-problems.

The sub-problems which form a sub-system only interact with their connected counterparts which makes the approach distributed and not requiring a central coordinator. An illustration of the OCD technique is shown in Figure 3.3. The solid lines connecting sub-systems are the tie-lines while the dotted lines denote the communication link for exchange of information. The OCD framework is also capable of running in a centralized fashion where the central coordinator can act as a relay node between other sub-systems to deliver information.

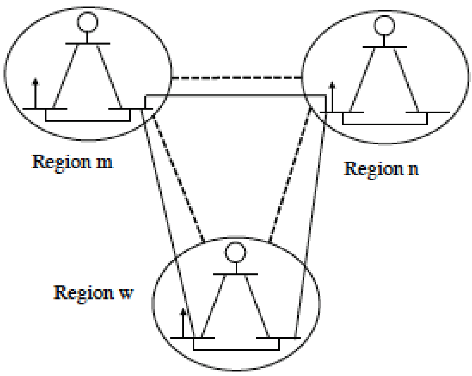

Figure 3.3: Distributed structure of an OCD implementation [5]

The formulated OPF is solved by first deriving its associated KKT conditions and further applying the Newton-Raphson method. The update equations for the primal and dual variables are calculated using the Jacobian of the KKT conditions [69].

The convergence speed of the OCD technique can be enhanced by computing linear sensitivities for the dual variables (like the 'λ') passed to each sub-problem [68].

3.2.7. CONSENSUS + INNOVATION (C+I)

The Consensus + Innovations approach is the most recent methodology presented [46, 47] to solve distributed optimal power flow problems. It is similar to the OCD technique as both perform a distributed solution of the KKT conditions. The difference lies in assigning the variables. In the OCD technique, each variable is assigned to a certain sub-problem, while the C+I technique uses an iterative approach that allows all the variables in a sub-problem to vary. Another advantage of the C+I technique over the OCD technique is that it is applicable at any level of partitioning. This means an individual agent can represent a single bus or even a large network of buses [41].

Authors such as Binetti et al., Zhang et al. and Yang et al. [70–73] have proposed distributed solutions for economic dispatch problems by enforcing an agreement on the marginal cost. A consensus based algorithm was used which followed an iterative procedure. The drawback of the consensus based algorithm is that it is applicable for power systems without line constraints i.e. it assumes that a network line at any point is never congested. However, if you consider line constraints as part of the optimal power flow model, the marginal costs at the two nodes connected by a congested line will be unequal. A situation like this cannot be handled by the sole consensus based method. To handle line constraints and to formulate a more exact solution for the OPF problem, Mohammadi et al. suggested an innovation based approach [6] [46]. The method focuses on solving the first order optimality conditions using iterative updates. It thus reduces the overall optimization problem to a coupled system of equation updates. The innovation updates consist of the optimality conditions which involve local information. Hence, the C+I technique for an uncongested network becomes a mere consensus based technique. Every node exchanges information only with its connected nodes in the power network.

The C+I technique in principle is different from the decomposition theory methods presented before. It directly solves the first order optimality conditions of the OPF problem, while the decomposition theory methods decompose the optimization problem into sub-problems and then solves the OPF for each sub-problem.

The convergence speeds of the C+I technique can be augmented by adding additional communication links between non-physically connected nodes. This speeds up the information spread over the network, thus leading to improved convergence rate [74]. Also, using asynchronous updates will help to reduce computation time and improve convergence rate [75].

3.2.8. GRADIENT DYNAMICS

The Gradient Dynamics technique goes way back in 1958 when it was proposed by Arrow et al. [76]. After the increase in distributed energy generation, this method was given recent treatment by Feijer et al. and Wang et al. [77, 78]. This approach is also based on embedding the KKT conditions, but in a dynamic system. The equilibria of this dynamic system reflects the KKT points for the original OPF problem.

Ma et al. [79] incorporates certain technical conditions and formulates an OPF problem which ensures that only the optima of the OPF problem are locally stable while the other KKT points remain unstable [80]. Hence, the OPF problem is solved using the dynamic system. The technique inherits the decomposibilty method within a power network as each bus serves as a computing agent which exchanges information with its neighbors.

The Gradient Dynamics method lacks enough preceding research for further applications in DC distributed systems. It's method to derive a solution for the decision variables is rather unresolved in the past literature. As compared to the other KKT based distributed techniques like the OCD and C+I, the Gradient Dynamics approach does not present update equations for all of the primal and dual variables.

3.3. COMPARATIVE ANALYSIS

With the growing penetration of distributed energy sources and focus on demand response, it is evident that distributed control of the many agents is essential to optimally coordinate within the system. In the above sections, seven distributed methods to achieve an OPF solution were presented. Four of these distributed algorithms were based on augmented Lagrangian relaxation, namely Dual Decomposition, ATC, ADMM with PMP and APP. OCD and C+I solved the KKT conditions in a distributed fashion. Some methods like the ADMM required a central controller, but when merged with the PMP technique followed a fully distributed process. Other methods like Dual Decomposition and Gradient Dynamics have minimal research papers.

The various sub-problems solve their own optimization problem and share information with other entities for a parallel computation. For ATC and ADMM with PMP, each iteration exchanges only the voltage angles and/or magnitudes of border buses. This definitely reduces the amount of data exchange per iteration, but as the sub-problems increase the complexity increases causing escalation of computational effort. As mentioned by Kargarian et al. [5], the ATC and ADMM is well suited for area-based OPF rather than nodal OPF. The motive of this study is to have a distributed OPF implemented within a DC microgrid. This would need an algorithm suited for nodal OPF. ATC is a model based hierarchical optimization method for multi-level system design. Each level of ATC may contain several sub-problems, thus increasing working complexity. It is more suited for multi-level management of power systems with multiple voltage or management levels. A major drawback of ATC is the requirement of a central controller as opposed to ADMM which perform in a fully distributed fashion using the PMP technique. The use of this central controller can potentially increase the system vulnerability, for instance against a cyber-attack or data manipulation [5].

The APP functions in a similar fashion as compared to the ADMM and ATC methods. An added step taken by APP is the linearization of the augmented Lagrangian function. The shared variables in APP is also the voltage phase angles and/or magnitudes at the border buses. The iterative equations in APP use variable values calculated in the previous iteration. This makes the APP a fully distributed OPF method. As seen in the Section 3.2.5, APP deploys set of dummy variables for each sub-region. Each dummy variable signifies the coupling constraint for the neighbouring areas. With increase in shared variables, the complexity of the system can increase causing higher computational time. This again indicates that APP is more efficient to solve area-based OPF rather than a nodal OPF problem.

OCD solves the KKT function and can perform effectively for non-convex optimization problems as well. Kargarian et al. [5] states its superiority in terms of better convergence properties as compared to Lagrangian Relaxation and Augmented Lagrangian methods. Each iteration in the OCD algorithm uses only a single Newton-Raphson step to carry out updates instead of solving the entire sub-problem, thus reducing computational costs. But, as compared to C+I, OCD does not find the exact solutions to the KKT conditions. Also, every sub-problem in the OCD technique is optimized separately. C+I is therefore a more polished version of OCD with a non-complex working algorithm. A vital difference between the OCD and C+I technique is the level of distributedness offered by the algorithm. C+I can be implemented at the nodal level as well as regional level of a power system. The method offers flexibility in terms of selecting size and number of regions. However, the OCD method is only suitable to solve OPF problems at the regional level due to violation of its convergence criterion when the number of sub-problems are substantial [5]. The C+I approach, solves a single optimization procedure for the system by solving the KKT conditions as a whole.

C+I is distinctly suitable for nodal level distributed OPF problems and hence studied in detail for this thesis. It solves the KKT conditions directly without solving any optimization problems during the course of its iterations. Also, the update functions are linear combination of the KKT conditions.

Using linear functions like these can potentially improve convergence speed. Application of C+I technique to non-convex problems has not been researched until now and needs further studies.

It is to be noted that the above analysis is based on literature survey and on understanding the different procedures of every method. No models or simulations have been developed to compare the output and convergence properties of these approaches.

4
Consensus and Innovations Approach: Approximated DC Optimal Power Flow for AC Distribution System

Past research papers like [6, 46, 47] have tackled the distributed OPF problem using the Consensus and Innovations approach. These papers have used DC approximations as linear approximations while solving the OPF problem. These approximations assume the line resistances to be negligible, hence assuming the distribution network to be lossless. The DC approximated OPF is implemented for AC network systems. This chapter discusses the details of the DC approximations, the mathematical formulations for the DC OPF problem and the update equations for the system variables. However, appropriate modifications have to be incorporated to model similar equations in a DC distribution network which is discussed in Chapter 5. Lastly, typical distribution networks cannot be assumed to be lossless, thus motivating a need for appropriate modifications to the DC OPF problem at hand. This is briefed upon in the last section. Details on the modifications are shown in Chapter 5.

4.1. Consensus and Innovations Approach

The C+I technique poses as an interesting method for applications in distributed OPF problems. Mohammadi et al. [46] in his paper presents an algorithm for an approximated DC OPF model for an AC system with line congestion. The model does not account for losses in the AC distribution line. Also, the solution of update equations presented in [47] are for an approximated DC OPF system. The prevalent AC networks in the transmission and distribution networks made it feasible to use AC OPF models in the past. However, in recent times with the growing trend towards DC distribution systems, the OPF models have to be modified to include the DC set of variables. The following chapter in this study will present a detailed set of equations and updates for a distributed OPF applied for an AC distribution system. The set of constraints will encompass the line limits and losses in the distribution lines while resulting in the optimized cost function value, along with primal and dual variables.

4.1.1. Approximated DC OPF Approach

The DC approximation is the most common linear approximation step and is based on certain set of assumptions [41]:

1. Reactive power flows can be neglected.

2. The network lines are lossless and the shunt elements can be neglected.

3. The voltage magnitudes at all the buses are approximately equal i.e. the magnitude of the voltage is approximately 1 p.u. (It is a relative voltage value as compared to an absolute value in normal scenarios)

4. Angle differences between connected buses are small such that $sin(\theta_m - \theta_n) = \theta_m - \theta_n$

Mohammadi et al. applies the above assumptions in his paper to present a C+I algorithm which enables a distributed solution of the approximated DC Optimal Power Flow problem [46]. The objective is to minimize the generation cost while fully supplying load demands and ensuring the set of constraints are satisfied. The set of equality constraint comprises of the supply demand consensus. The inequality constraints comprise of power generation limits for the generators and line limits on the distribution lines.

The approximated DC OPF is based on obtaining a solution to the first order optimality conditions of the formulated DC OPF problem in a fully distributed fashion. These optimality conditions include constraints which constitute a coupling of the Lagrange multipliers associated with the supply demand consensus, generation limits and line flow limits at neighbouring buses and distribution lines in the microgrid. The updates of the local variables and Lagrange multipliers contain terms which takes into account the coupling of the optimality conditions. The added specialty is the update for the Lagrange multiplier which contains an innovation terms which ensures supply-demand balance. The information which is exchanged between nodes is limited to the updates of the bus angle and the local Lagrange multipliers. Hence, there is no need to exchange information about the generation settings or the cost parameters associated at every node during the iterative process. The model also assumes the resistances of the distribution lines to be negligible.

4.1.2. MATHEMATICAL FORMULATION OF THE APPROXIMATED DC OPF

The formulated DC OPF takes into account a quadratic cost function but can also be modeled for a linear cost function. The objective is to meet demands at the least operating cost of power generators such that all the constraints are met.

Mathematically the approximated DC OPF is formulated as follows:

Objective

$$\min \sum_{m\in\mathcal{N}} \sum_{s\in\mathcal{S}} A_m (p_m^{\mathrm{S}})^2 + B_m p_m^{\mathrm{S}} + C_m \tag{4.1}$$

Subject to

$$\sum p_m^{\mathrm{S}} = \sum Y_{m,n}(\theta_m - \theta_n) \qquad \forall (m,n) \in \mathcal{N} \tag{4.2}$$

$$-\overline{P}_{m,n} \le Y_{m,n}(\theta_m - \theta_n) \le \overline{P}_{m,n} \qquad \forall (m,n) \in \mathcal{N} \tag{4.3}$$

$$\underline{P}_m^{\mathrm{S}} \le p_m^{\mathrm{S}} \le \overline{P}_m^{\mathrm{S}} \qquad \forall s \in \mathcal{S} \tag{4.4}$$

The quadratic cost function is a function of the power flow from the generators. It is given by Equation (4.1). But, as the approximations consider the voltage at every bus to be equal to 1 p.u., the cost function becomes eventually a function of the current flow from the generators. The objective is then to have an optimal current flow through the power generators. The cost parameters- A_m, B_m

and C_m represent the cost co-efficients associated with the quadratic, linear and fixed power generated terms. A_m and B_m provide cost parameter values for the operational costs of the generators as the objective function then varies with the amount of power generated. C_m on the other hand is a fixed cost which is incurred for the system and it's associated term is independent of the power produced by the generators. $'m'$ signifies a particular node in the microgrid and belongs to a set $\mathcal{N}$ which represents the total number of nodes in the system. Similarly, s signifies a particular power generator at node m and belongs to a set $\mathcal{S}$ which represents the total number of generators at a given node m. p_m^S represents the flow of power either from a generator or into a load at a particular node $'m'$. The sign notation used in this study is positive for power generators and negative for power consuming devices. Hence, if a node consists of a power generator, the power flow from the generator is p_m^S. If a node consists of a power consuming device, the power flow into this load is $-p_m^S$.

The equality constraint consists of the supply-demand balance given in Equation (4.2). As stated in the above paragraph, p_m^S represents the current flow from the generators due to the assumption made for the voltage magnitudes at the nodes. $Y_{m,n}$ represents the admittance of the line connecting node m and node n. The admittance for a distribution line is constant for every iteration. The phase angles at the nodes m and n are represented by θ_m and θ_n. The model here takes into account an AC network and thus works with admittance and phase angles. It eventually simplifies and AC OPF to an approximated DC OPF for an AC network. Later chapter will transform these set of equations which would be suitable for a DC distribution system.

The inequality constraints are given by Equations (4.3) and (4.4). Equation (4.3) signifies the current line limit for cables in the microgrid. Equation (4.4) is a constraint on the power generation capacities of the generators.

$\overline{P}_m^S$ and $\underline{P}_m^S$ are the upper and lower limits of the power generator at node m. $\overline{P}_{m,n}$ denotes the power flow limit for the distribution line connecting node m to node n in the network. The lower limit for the power flow constraint is specified as negative of the maximum limit to account for reverse flow sign convention.

The Lagrange function of the optimization problem given by Equations (4.1) - (4.4) is given by:

4.1.3. LAGRANGIAN FUNCTION OF THE DC OPF

$$\begin{aligned}
\mathcal{L} =& (\sum_{m\in\mathcal{N}}\sum_{s\in\mathcal{S}} A_m(p_m^S)^2 + B_m p_m^S + C_m) \\
&+ (\sum \lambda_m(\sum Y_{m,n}(\theta_m-\theta_n) - \sum p_m^S)) \\
&+ (\sum \mu_{m,n}(Y_{m,n}(\theta_m-\theta_n) - \overline{P}_{m,n})) \\
&+ (\sum \mu_{n,m}(-Y_{m,n}(\theta_m-\theta_n) - \overline{P}_{m,n})) \\
&+ (\sum \mu_m^{\overline{P}}(p_m^S - \overline{P}_m^S)) \\
&+ (\sum \mu_m^{\underline{P}}(-p_m^S + \underline{P}_m^S))
\end{aligned} \tag{4.5}$$

It is to be noted that for an optimization problem with equality and inequality constraints, the number of dual variables are equal to the total number of constraints. For the above formulation, λ_m, $\mu_{m,n}$, $\mu_{n,m}$, $\mu_m^{\overline{P}}$ and $\mu_m^{\underline{P}}$ are the dual variables. All of these dual variables are termed as Lagrange multipliers. For more details on this topic, kindly refer to Chapter 2.

The optimization problem as seen has been linear approximated. As stated by Molzahn [41], the C+I technique is guaranteed to converge to the DC OPF solution, which means the problem at hand is convex. Convex problems form a strong duality between the objective function and the constraints [81]. The dual variables of such a convex problem can be used to interpret Locational Marginal Prices (LMP) at the different nodes in the network. LMP in general is the marginal cost of supplying the next increment of energy at a particular location (node for our case). LMP are most commonly expressed in terms of power (EUR/W) and reflect the congestion and line losses in the network [82–86]. λ_m denotes the LMP for the different nodes but is expressed in terms of current (EUR/A).

4.1.4. First Order Optimality Conditions

$$\frac{\partial L}{\partial p_m^{\mathrm{S}}} = \sum_{s\in\mathcal{S}} 2A_m p_m^{\mathrm{S}} + B_m \\ -\lambda_m + \mu_m^{\overline{P}} - \mu_m^{\underline{P}} = 0 \tag{4.6}$$

$$\frac{\partial L}{\partial \theta_m} = \lambda_m \sum Y_{m,n} - \sum \lambda_n Y_{m,n} \\ + \sum Y_{m,n}(\mu_{m,n} - \mu_{n,m}) = 0 \tag{4.7}$$

$$\frac{\partial L}{\partial \lambda_m} = -\sum p_m^{\mathrm{S}} + \sum Y_{m,n}(\theta_m - \theta_n) = 0 \tag{4.8}$$

$$\frac{\partial L}{\partial \mu_{m,n}} = \sum Y_{m,n}(\theta_m - \theta_n) - \overline{P}_{m,n} \le 0 \tag{4.9}$$

$$\frac{\partial L}{\partial \mu_{n,m}} = -\sum Y_{m,n}(\theta_m - \theta_n) - \overline{P}_{m,n} \le 0 \tag{4.10}$$

$$\frac{\partial L}{\partial \mu_m^{\overline{P}}} = p_m^{\mathrm{S}} - \overline{P}_m^{\mathrm{S}} \le 0 \tag{4.11}$$

$$\frac{\partial L}{\partial \mu_m^{\underline{P}}} = -p_m^{\mathrm{S}} + \underline{P}_m^{\mathrm{S}} \le 0 \tag{4.12}$$

Complementary Slackness Conditions

$$\mu_{m,n}(\overline{P}_{m,n} - \sum Y_{m,n}(\theta_m - \theta_n)) = 0 \tag{4.13}$$

$$\mu_{n,m}(-\overline{P}_{m,n} + \sum Y_{m,n}(\theta_m - \theta_n)) = 0 \tag{4.14}$$

$$\mu_m^{\overline{P}}(\overline{P}_m^{\mathrm{S}} - p_m^{\mathrm{S}}) = 0 \tag{4.15}$$

$$\mu_m^{\underline{P}}(p_m^{\mathrm{S}} - \underline{P}_m^{\mathrm{S}}) = 0 \tag{4.16}$$

Positivity Conditions

$$\mu_{m,n}, \mu_{n,m}, \mu_m^{\overline{P}}, \mu_m^{\underline{P}} \ge 0 \tag{4.17}$$

Equations (4.6) - (4.12) are the first order optimality conditions for the DC OPF problem. The complementary slackness conditions mentioned in Equations (4.13) - (4.16) form a part of the necessary conditions for the Lagrange function. Equation (4.17) consists of the Lagrange multipliers and enforces positivity constraints on them. Together these equations form the necessary conditions for the Lagrange function mentioned in Equation (4.5). In order to arrive at an optimal solution for the DC OPF problem these set of constrained equations need to be solved [6].

The first order optimality conditions are derived by taking the first derivative of every system variable with respect to the Lagrange function and equating it to zero. For the set of inequality constraints, the first order derivative is then appropriately less than or greater than zero. The $\sum$ corresponds to the derivatives for all the nodes in the system and for all the generators at the node.

Complementary slackness conditions are based on virtue of logic. The Lagrange multipliers associated with the inequality constraints are only triggered when the associated variable either equals or exceeds the constrained boundary limit. As long as the variable is within the specified constrained boundary limits, the associated Lagrange multiplier maintains a value of zero. As soon as the variable crosses the constrained limit, the Lagrange multipliers act in a way to pull the variable value back in the boundary limits. This will be seen in the following sections on iterative system updates. Thus, the complementary slackness conditions state that either the Lagrange multiplier at a particular time period is zero and the variable is within limits or the variable reaches the extreme boundary limits rendering the difference term to be zero. For e.g. consider Equation (4.15). At a particular time period, when the power derived from the generator p^S_m is less than the upper constrained limit $\overline{P^S_m}$, the associated Lagrange multiplier $\mu^{\overline{P}}_m$ maintains a value of zero. At any instant when p^S_m reaches the maximum value of $\overline{P^S_m}$, the Lagrange multiplier $\mu^{\overline{P}}_m$ is triggered and invokes a positive value. But, the multiplied product of $\mu^{\overline{P}}_m$ and the difference between $\overline{P^S_m}$ and p^S_m at any point in time is always zero.

4.1.5. DISTRIBUTED APPROACH WITH ITERATIVE UPDATES

This section presents a distributed iterative approach to solve the mentioned first order constrained equation system. Every node exchanges limited information with its connected counterpart during the course of iterations. The variables which are exchanged between connected nodes are the θ_m and λ_m values.

As proposed by Mohammadi et al. [6], each node 'm' updates the variables λ_m, θ_m and p^S_m which are associated with that particular node and the $\mu_{m,n}$ which represent the constraints on the power flows from node m to node n. The iteration counter is denoted by 'l'. The iterates can be denoted by a standard- $x_m(l)$ and it includes all the variables associated with the node m at iteration count l, i.e. $x_m(l) = [\lambda_m(l), \theta_m(l), \mu_{m,n}(l), p^S_m(l)]$.

The local updates run through iterations in a general format given below:

$$x_m(l+1) = \mathbb{P}[x_m(l) + T g_m(x_n(l))] \tag{4.18}$$

where, $g_m(.)$ represents the first order optimality constraints related to node m. 'T' denotes the set of tuning parameters used for updates of different primal and dual variables. Moreover, $\mathscr{P}$ is a projection operator which projects the values of x_m onto its determined feasible space. As seen in Equation (4.18), the function $g_m(x_n(l))$ depends on the iterative values of $x_n(l)$ of the connected nodes in the physical neighbourhood of m.

VARIABLE ITERATIVE UPDATES

The updates as proposed by Mohammadi et al. [46] are based on purpose of intuition. The optimality conditions are linked with specific variable updates to achieve convergence for all the system variables. The linking of the first order optimality conditions with a particular variable update is dependent on the coupling variables associated with the condition equations. These updates as mentioned above, run in a parallel fashion.

The Lagrange multiplier λ_m which denotes the LMP values at different nodes is updated as follows:

$$\begin{aligned}
\lambda_m(l+1) &= \lambda_m(l) - \lambda_1\left(\frac{\partial L}{\partial \theta_m}\right) + \lambda_2\left(\frac{\partial L}{\partial \lambda_m}\right) && (4.19)\\
&= \lambda_m(l) - \lambda_1[\lambda_m(l)\sum Y_{m,n} - \sum \lambda_n(l) Y_{m,n} && (4.20)\\
&\quad + \sum Y_{m,n}(\mu_{m,n}(l) - \mu_{n,m}(l))]\\
&\quad + \lambda_2[-\sum P^S_m(l) + \sum Y_{m,n}(\theta_m(l) - \theta_n(l))]
\end{aligned}$$

where, λ_1 and λ_2 denote the tuning parameters and are positive constants, and l is the iteration counter. Here, as per Equation (4.18), the first term is the previous update value of λ_m, the second term corresponds to the optimality condition given by Equation (4.7) which reflects the coupling between the LMP values of node m and node n. The third term represents an added "Innovation Term" as stated by Mohammadi et al. [6]. It constitutes the power balance for demand and supply given by Equation (4.8).

The Equation (4.20) makes intuitive sense. If you consider the innovation term, the power balance has to be satisfied for the $\lambda_m(l+1)$ value to stabilize to a solution. If the generation of power is higher as compared to the load requirement, which means $\sum P_m^S(l)$ is positive and exceeds the power flow in the line to the connecting node, it leads to a reduction in $\lambda_m(l+1)$. As seen ahead, this reduction in $\lambda_m(l+1)$ reduces the power generation value which then restores the supply demand balance. Moreover, if no line constraints are present on the line connecting node m and node n, the $\mu's$ associated with the line are equal to zero, which results in the LMP values at the two nodes to be in agreement.

Once the LMP (λ_m) is updated, the generator power flow is updated as follows:

$$p_m^S(l+1) = \mathbb{P}[p_m^S(l) - \frac{1}{2A_m}\frac{\partial L}{\partial p_m^s}] \tag{4.21}$$

$$= \mathbb{P}[\frac{\lambda_m(l) - B_m}{2A_m}] \tag{4.22}$$

where, $\mathbb{P}$ is an operator which restricts the value determined by Equation (4.22) between the minimum and maximum capacity of the generator specified by constraint Equation (4.4). This means, if $p_m^S(l+1)$ exceeds the upper limit of power generation $\overline{P}_m^S$, it is set to the upper limit value. Similar logic applies for the lower limits. Thus, the Lagrange multipliers $\mu_m^{\overline{P}}$ and $\mu_m^{\underline{P}}$ are ignored which also perform the same task of maintaining power values between constrained boundaries. Here, the power update is linked to the optimality condition given by Equation (4.6).

The bus voltage phase angles are updated as follows:

$$\theta_m(l+1) = \theta_m(l) - \theta_1\frac{\partial L}{\partial \lambda_m} \tag{4.23}$$

$$= \theta_m(l) - \theta_1[-\sum p_m^S(l) + \sum Y_{m,n}(\theta_m(l) - \theta_n(l))] \tag{4.24}$$

where, θ_1 is a tuning parameter. The optimality condition linked to this update is the power balance equation given by Equation (4.8). This again is an intuitive connection. Consider a point where the demand exceeds the generation output, causing the value of $\sum P_m^S(l)$ to be negative and lower than the required power flow in the line connecting the adjacent node. This ultimately reduces $\theta_m(l+1)$ causing the power output from other generators to augment, thus moving towards θ_m stability.

The Lagrange multipliers associated with the inequality constraint of the line limit are updated as given below.

$$\mu_{m,n}(l+1) = \mathbb{P}[\mu_{m,n}(l) + \mu_1\frac{\partial L}{\partial \mu_{m,n}}] \tag{4.25}$$

$$= \mathbb{P}[\mu_{m,n}(l) + \mu_1[Y_{m,n}(\theta_m(l) - \theta_n(l)) - \overline{P}_{m,n}]] \tag{4.26}$$

$$\mu_{n,m}(l+1) = \mathbb{P}[\mu_{n,m}(l) + \mu_1\frac{\partial L}{\partial \mu_{n,m}}] \tag{4.27}$$

$$= \mathbb{P}[\mu_{n,m}(l) + \mu_1[-Y_{n,m}(\theta_m(l) - \theta_n(l)) - \overline{P}_{m,n}]] \tag{4.28}$$

Here, μ_1 is a positive tuning parameter. The first order optimality conditions used to link the above updates (4.25) and (4.27) are taken from Equations (4.9) and (4.10) respectively. The projection operator $\mathbb{P}$ ensures that the values of the Lagrange multiplier updates are always positive and helps in setting their values equal to zero if the updates in Equation (4.26) and (4.28) yield negative values. Consider a point in time where the line flow $P_{m,n} = Y_{m,n}(\theta_m(l) - \theta_n(l)$ is lower than the upper limit of the constraint on the line $\overline{P}_{m,n}$. At this point, the update of Equation (4.26) yields a negative value causing $\mu_{m,n}$ to decrease with a minimum value bounded to zero due to the projection operator. If the line flow crosses the upper limit, $\mu_{m,n}$ increases signifying the constraint is not met. The system then iterates to get the power flow within the boundary limits.

As seen from all the variable update equations, they are defined based on the variables from the previous iteration. This allows a parallel computation of the system variable updates. When all these updates are simulated in series, i.e. for e.g. you have updated λ_m which are used then to update p_m^S, Kar et al. [47] states the number of iterations until convergence reduces but overall computation time increases.

The tuning parameter values for all the updates are extremely sensitive and decide the convergence criteria for the DC OPF algorithm. They decide on the fate of the OPF problem converging or not. Mohammadi et al. decided on certain values of tuning parameters based on empirical research [6]. The values of these tuning parameters are given in Table 4.1. These tuning parameters are case specific and need to be tuned for every case it is implemented in. Due to their sensitive nature, the tuning parameters are difficult to achieve through empirical analysis. Regression analysis, by using the Least Square method for goodness of fit could be a potential solution to tune the parameters. This particular study is outside the scope of this thesis and can be a potential future scope for other researchers.

Table 4.1: Tuning Parameter Values [6]

Tuning Parameter	Value
λ_1	0.0056
λ_2	0.1485
θ_1	0.005
μ_1	0.008

4.2. APPROXIMATED DC OPF MODEL ANALYSIS

The approximated DC OPF solution presented incorporates the Consensus + Innovations approach to attain an optimal solution. The system model is designed for specific network properties. However, there are some interpretations of this model regarding alternative modifications for incorporating practical DC microgrid scenarios.

The approximated DC OPF algorithm interpretations are as follows:

- The algorithm is valid only when the cost function is quadratic. As seen in Equation (4.1), the objective function is of quadratic nature. However, in the power generation update given by Equation (4.21), the quadratic co-efficient A_m is in the denominator. For a linear cost function, the value of this co-efficient will be zero. This will cause the power generation update to give an indefinite value. Hence, the update of the power generation needs to be modified to account for linear cost functions. The following Chapter 5 will give a detailed version of the modified model.

- The current algorithm is for an AC network system. DC approximations are only applied to make a linear approximation. The model needs modification to account for DC distribution systems. The admittance $Y_{m,n}$ has to be replaced by conductance $G_{m,n}$. The difference in phase angles at buses for a AC distribution system causes the power flows in the line. For a DC distribution system, the same power flows in the line are caused due to differences in voltage magnitudes at the buses. Hence, in the modified algorithm θ_m needs to be replaced by voltage magnitude u_m.

- Finally, the approximated DC OPF assumes the network is free of losses due to the assumption of negligible line resistance. Applying these assumptions in a DC distribution network yields a solution which is not an exact optimal solution to a DC OPF problem. Typical distribution networks violate these assumptions, which motivates the development of accurate modifications to account for an exact optimized solution. The losses are incorporated in the algorithm and the modified model is shown in Chapter 5 with examples.

5

Distributed Optimal Power Flow for a DC Distribution System

This chapter presents an adaptation of the approximated DC OPF method applied alongside the Consensus and Innovations Approach. As seen in the previous chapter, the linear approximations are valid for an AC system assuming a lossless network of power distribution. These approximations will be modified to suit a DC distribution system. The first section will consider a lossless DC microgrid and present the modeled algorithm accordingly. Keeping in mind the practicality of actual DC networks, the algorithm is refashioned to consider losses in the DC network. Lastly, a three node case will follow which will be implemented with the refashioned model.

5.1. Lossless Distributed OPF for DC Microgrids (Non-Exact)

The set of equations mentioned in Chapter 4 are valid for a lossless AC distribution system. The driving force for power flow in an AC distribution system is based on difference in voltage phase angles. For the DC counterpart, this driving force is based on difference in voltage magnitudes across distribution lines. Hence, the θ_m values which denote the voltage phase angle at node m have to be replaced by voltage magnitude u_m.

As seen in Chapter 1, the voltage band which is maintained in typical DC networks is in the range of 350 to 380 V. The DC OPF model considered for this study, will also have to adhere to the allowable voltage limit. However, as witnessed in the assumptions of approximated DC OPF method, the voltage magnitudes are relative values and assumed to be approximately 1 p.u. ([6]. Hence, for the lossless model, the constraint on voltage magnitudes can be overlooked in the formulation. This constraint on voltage will have to be considered for a DC OPF model consisting of lines losses in the network.

5.1.1. Mathematical Formulation of DC OPF for a Lossless DC Network

The mathematical formulation of the lossless DC OPF for a DC distribution system is as follows:

Objective

$$\min \sum_{m\in\mathcal{N}} \sum_{s\in\mathcal{S}} A_m (p_m^{\mathrm{S}})^2 + B_m p_m^{\mathrm{S}} + C_m \tag{5.1}$$

Subject to

$$\sum p^{\mathrm{S}}_{m} = \sum G_{m,n}(u_m - u_n) \qquad \forall (m,n) \in \mathcal{N} \tag{5.2}$$
$$-\overline{P}_{m,n} \leq G_{m,n}(u_m - u_n) \leq \overline{P}_{m,n} \qquad \forall (m,n) \in \mathcal{N} \tag{5.3}$$
$$\underline{P}^{\mathrm{S}}_{m} \leq p^{\mathrm{S}}_{m} \leq \overline{P}^{\mathrm{S}}_{m} \qquad \forall s \in \mathcal{S} \tag{5.4}$$

The given cost function is again of quadratic type. This can be used in a DC microgrid if the generators comprise of gas turbines or diesel generators or other similar devices. The cost function given by Equation (5.1) can be altered to suit linear cost function based generators as well. For that, the quadratic cost co-efficient A_m has to be given a value of zero .

The equality constraint given by Equation (5.2) denotes the power balance. Since, the network consists of DC elements, the admittance is replaced by conductance for a distribution line connecting node m to node n and is denoted by $G_{m,n}$. Conductance is nothing but the inverse of the resistance in the cable. As the voltage magnitudes are relative and equal to 1 p.u., the power from the generator $\sum p^{\mathrm{S}}_{m}$ is basically the current from the generator minus the current fed into a load (if present) at the given node m. The R.H.S of Equation 5.2 therefore represents the current flow in the line connecting node m to node n. The inequality constraints are given by Equation (5.3) and (5.4), and denote the constraint on current flow in the line and power generation in the generator respectively. In many practical distribution systems, cables are not capable of handling current flows above a certain capacity limit. When the current flow crosses such limits, the line is in a state of congestion. To consider congestion in distribution lines, Equation (5.3) is exercised.

5.1.2. LAGRANGE FUNCTION FOR THE FORMULATION

The Lagrange function for the Equations (5.1) - (5.4) is given as:

$$\begin{aligned}
\mathcal{L} =& \Big(\sum_{m\in\mathcal{N}}\sum_{s\in\mathcal{S}} A_m(p^{\mathrm{S}}_{m})^2 + B_m p^{\mathrm{S}}_{m} + C_m\Big) \\
&+ \Big(\sum \lambda_m \big(\sum G_{m,n}(u_m - u_n) - \sum p^{\mathrm{S}}_{m}\big)\Big) \\
&+ \Big(\sum \mu_{m,n}\big(G_{m,n}(u_m - u_n) - \overline{P}_{m,n}\big)\Big) \\
&+ \Big(\sum \mu_{n,m}\big(-G_{m,n}(u_m - u_n) - \overline{P}_{m,n}\big)\Big) \\
&+ \Big(\sum \mu^{\overline{P}}_{m}\big(p^{\mathrm{S}}_{m} - \overline{P}^{\mathrm{S}}_{m}\big)\Big) \\
&+ \Big(\sum \mu^{\underline{P}}_{m}\big(-p^{\mathrm{S}}_{m} + \underline{P}^{\mathrm{S}}_{m}\big)\Big)
\end{aligned} \tag{5.5}$$

The dual variables which are considered in the Lagrange function given by Equation (5.5) are λ_m, $\mu_{m,n}$, $\mu_{n,m}$, $\mu^{\overline{P}}_{m}$ and $\mu^{\underline{P}}_{m}$. As stated earlier, the number of dual variables for an optimization problem is equal to the number of constraints in the problem. We have four inequality constraints presented by Equation (5.3) and (5.4) and one equality constraint.

The DC OPF problem is a convex problem, as mentioned by Mohammadi et al. and hence provides a strong duality between the objective function and set of constraints [6] [46]. As stated by Mackay et al. [81] the dual variable of convex problems can be used to interpret the LMP associated at the nodes. The dual variable used in the model here is λ_m which provides details on LMP. Since the λ_m is associated with an equality constraint specifying current flow balance, the unit used is EUR/A. If the voltage magnitude at node m is multiplied to this value of λ_m, you will achieve the power LMP in units of EUR/W.

The inequality constraints are associated with dual variables in the Lagrange function which denote the slackness in the system. These dual variables basically help in maintaining the constrained boundary limits as they are triggered every time a constraint is violated.

To understand how the Lagrange function is formed for OPF problems, kindly refer to Chapter 2. A detailed methodology is presented to understand OPF formulations.

5.1.3. FIRST ORDER OPTIMALITY CONDITIONS

The DC OPF problem for a lossless DC network has inequality constraints associated to line flow limits and power generator capacity limits. When an OPF problem contains inequality constraints, the KKT conditions have to satisfied and fulfilled to achieve an optimal solution to the problem. Hence, the problem at hand needs to satisfy the KKT based first order optimality conditions, the complementary slackness conditions and positivity conditions of the dual variables.

The KKT based first order optimality conditions are as follows:

$$\begin{aligned}
\frac{\partial L}{\partial p_m^{\mathrm{S}}} &= \sum_{s\in\mathscr{S}} 2A_m p_m^{\mathrm{S}} + B_m \\
&\quad - \lambda_m + \mu_m^{\overline{P}} - \mu_m^{\underline{P}} = 0 && (5.6)\\
\frac{\partial L}{\partial u_m} &= \lambda_m \sum G_{m,n} - \sum \lambda_n G_{m,n} \\
&\quad + \sum G_{m,n}(\mu_{m,n} - \mu_{n,m}) = 0 && (5.7)\\
\frac{\partial L}{\partial \lambda_m} &= -\sum p_m^{\mathrm{S}} + \sum G_{m,n}(u_m - u_n) = 0 && (5.8)\\
\frac{\partial L}{\partial \mu_{m,n}} &= \sum G_{m,n}(u_m - u_n) - \overline{P}_{m,n} \le 0 && (5.9)\\
\frac{\partial L}{\partial \mu_{n,m}} &= -\sum G_{m,n}(u_m - u_n) - \overline{P}_{m,n} \le 0 && (5.10)\\
\frac{\partial L}{\partial \mu_m^{\overline{P}}} &= p_m^{\mathrm{S}} - \overline{P}_m^{\mathrm{S}} \le 0 && (5.11)\\
\frac{\partial L}{\partial \mu_m^{\underline{P}}} &= -p_m^{\mathrm{S}} + \underline{P}_m^{\mathrm{S}} \le 0 && (5.12)
\end{aligned}$$

COMPLEMENTARY SLACKNESS CONDITIONS

The complementary slackness conditions are as follows:

$$\begin{aligned}
\mu_{m,n}(\overline{P}_{m,n} - \sum G_{m,n}(u_m - u_n)) &= 0 && (5.13)\\
\mu_{n,m}(-\overline{P}_{m,n} + \sum G_{m,n}(u_m - u_n)) &= 0 && (5.14)\\
\mu_m^{\overline{P}}(\overline{P}_m^{\mathrm{S}} - p_m^{\mathrm{S}}) &= 0 && (5.15)\\
\mu_m^{\underline{P}}(p_m^{\mathrm{S}} - \underline{P}_m^{\mathrm{S}}) &= 0 && (5.16)
\end{aligned}$$

POSITIVITY CONDITIONS

The positivity conditions on the dual variables are as follows:

$$\mu_{m,n}, \mu_{n,m}, \mu_m^{\overline{P}}, \mu_m^{\underline{P}} \ge 0 \tag{5.17}$$

The KKT based first order optimality conditions are the first derivative of the Lagrange function with respect to the primal and dual variables which are less than or equal to zero. The primal variables are the decision variables of the OPF problem which are the power generates from the generators p_m^{S} and the voltage magnitudes u_m at the nodes.

Equations (5.6) - (5.12) are the first order optimality conditions for the DC OPF problem. The complementary slackness conditions mentioned in Equations (5.13) - (5.16) form a part of the necessary conditions for the Lagrange function. Equation (5.17) consists of Lagrange multipliers and enforces positivity constraints on them. Together these equations form the necessary conditions for the Lagrange function mentioned in Equation (4.5). In order to arrive at an optimal solution for the DC OPF problem, these set of constrained equations need to be solved [6].

Complementary slackness conditions are based on virtue of logic. The Lagrange multipliers associated with the inequality constraints are only triggered when the associated variable either equals or exceeds the constrained boundary limit. As long as the variable is within the specified constrained boundary limits, the associated Lagrange multiplier maintains a value of zero. As soon as the variable crosses the constrained limit, the Lagrange multipliers act in a way to pull the variable value back in the boundary limits. This will be seen in the following sections on iterative system updates. Thus, the complementary slackness conditions state that either the Lagrange multiplier at a particular time period is zero and the variable is within limits or the variable reaches the extreme boundary limits rendering the difference term to be zero. For e.g. consider Equation (5.15). At a particular time period, when the power derived from the generator p_m^S is less than the upper constrained limit $\overline{P_m^S}$, the associated Lagrange multiplier $\mu_m^{\overline{P}}$ maintains a value of zero. At any instant when p_m^S reaches the maximum value of $\overline{P_m^S}$, the Lagrange multiplier $\mu_m^{\overline{P}}$ is triggered and invokes a positive value. But, the multiplied product of $\mu_m^{\overline{P}}$ and the difference between $\overline{P_m^S}$ and p_m^S at any point in time is always zero.

5.1.4. ITERATIVE UPDATES FOR THE LOSSLESS DC OPF MODEL

The first order optimality conditions considered above are used in the variable iterative process of the primal and dual variables. A link connecting specific optimality condition equations with the variable update is presented. This connecting link is the backbone of the Consensus and Innovations approach. For details on iterations of a general variable update and its link to values from previous iterations refer to Chapter 4, Section 4.1.5.

The updates as proposed by Mohammadi et al. [6] are intuition based and run in a parallel fashion.

The Lagrange multiplier λ_m which as mentioned above, denotes the current flow LMP values (EUR/A) follows the iterative update as follows:

$$\lambda_m(l+1) = \lambda_m(l) - \lambda_1\left(\frac{\partial L}{\partial u_m}\right) + \lambda_2\left(\frac{\partial L}{\partial \lambda_m}\right) \tag{5.18}$$

$$\begin{aligned} &= \lambda_m(l) - \lambda_1[\lambda_m(l)\sum G_{m,n} - \sum \lambda_n(l) G_{m,n} \\ &+ \sum G_{m,n}(\mu_{m,n}(l) - \mu_{n,m}(l))] \\ &+ \lambda_2[-\sum P_m^{\mathrm{S}}(l) + \sum G_{m,n}(u_m(l) - u_n(l))] \end{aligned} \tag{5.19}$$

where, λ_1 and λ_2 denote the tuning parameters and are positive constants and l is the iteration counter. Here, as per Equation (5.18), the first term is the previous update value of λ_m, the second term corresponds to the optimiality condition given by Equation (5.7) which reflects the coupling between the LMP values of node m and node n. The third term represents an added "Innovation Term" as stated by Mohammadi et al. [6]. It constitutes the power balance for demand and supply given by Equation (5.8).

Equation (5.19) makes intuitive sense. If you consider the innovation term, the power balance has to be satisfied for the $\lambda_m(l+1)$ value to stabilize to a solution. If the generation of power is higher as compared to the load requirement, which means $\sum P_m^{\mathrm{S}}(l)$ is positive and exceeds the power flow in the line to the connecting node, it leads to a reduction in $\lambda_m(l+1)$. As seen ahead, this reduction in $\lambda_m(l+1)$ reduces the power generation value which then restores the supply demand balance. Moreover, if no line constraints are present on the line connecting node m and node n, the $\mu's$ associated with the line are equal to zero, which results in the LMP values at the two nodes to be in agreement.

The stabilized λ_m values will provide the LMP at the different nodes present in the DC network. A high LMP value denotes higher cost to supply power to that particular node. The use of LMP values will be seen in the simple three node case study later.

Once the LMP (λ_m) is updated, the generator power flow is updated as follows:

$$p_m^S(l+1) = \mathbb{P}[p_m^S(l) - I_1 \frac{\partial L}{\partial p_m^s}] \tag{5.20}$$

$$= \mathbb{P}[p_m^S(l) - I_1(\sum_{s\in\mathscr{S}} 2A_m p_m^S + B_m - \lambda_m)] \tag{5.21}$$

where, I_1 is a tuning parameter which has been added to replace the earlier term provided by Mohammadi et al. in his paper [6] on approximated DC OPF. The term used by Mohammadi et al. had the quadratic cost co-efficient (A_m) in the denominator. This made applications of linear cost functions difficult to be implemented in the algorithm. To understand the equation, kindly refer to Chapter 4, Equation 4.21. Replacing that term with a tuning parameter I_1 allows updates of linear cost functions of generators and helps in achieving convergence. This is an added value research to the study. The value of this tuning parameter is again found by empirical research which can be seen in the case studies presented later.

The optimality condition linked to the power update is with respect to the power generation which makes intuitive sense. The projection operator $\mathbb{P}[.]$ is applied which restricts the power updates from violating the constrained boundary limits. This means, if $p_m^S(l+1)$ exceeds the upper limit of power generation $\overline{P}_m^S$, it is set to the upper limit value and similarly for the lower limits. Thus, the Lagrange multipliers $\mu_m^{\overline{P}}$ and $\mu_m^{\underline{P}}$ are ignored which also perform the same task of maintaining power values between constrained boundaries.

The nodal voltage magnitudes form a part of the decision variables and are updated as follows:

$$u_m(l+1) = u_m(l) - U_1 \frac{\partial L}{\partial \lambda_m} \tag{5.22}$$

$$= u_m(l) - U_1[-\sum p_m^S(l) + \sum G_{m,n}(u_m(l) - u_n(l))] \tag{5.23}$$

As seen in the above iterative update, the voltage magnitude at iteration $l+1$ is dependent on the voltage magnitude of the previous iteration l. This is true for all the variable updates in the Consensus and Innovations Approach. The optimalty condition linked to this update is the power balance equation given by Equation (5.8). The imbalance in the demand supply balance will either increase or decrease the voltage magnitude. Excess supply of power will increase the voltage magnitude, thus reducing the power generated from other generators in the system and restoring the power balance. Hence, the linkage of optimality condition makes intuitive sense.

The Lagrange multipliers associated with the inequality constraint of the line limit is updated as well.

$$\mu_{m,n}(l+1) = \mathbb{P}[\mu_{m,n}(l) + \mu_1 \frac{\partial L}{\partial \mu_{m,n}}] \tag{5.24}$$

$$= \mathbb{P}[\mu_{m,n}(l) + \mu_1[G_{m,n}(u_m(l) - u_n(l)) - \overline{P}_{m,n}]] \tag{5.25}$$

$$\mu_{n,m}(l+1) = \mathbb{P}[\mu_{n,m}(l) + \mu_1 \frac{\partial L}{\partial \mu_{n,m}}] \tag{5.26}$$

$$= \mathbb{P}[\mu_{n,m}(l) + \mu_1[-G_{n,m}(u_m(l) - u_n(l)) - \overline{P}_{m,n}]] \tag{5.27}$$

Here, μ_1 is a positive tuning parameter. The first order optimality conditions used to link the above updates (5.24) and (5.26) are taken from Equations (5.9) and (5.10) respectively. The projection operator $\mathbb{P}$ ensures that the values of the Lagrange multiplier updates are positive always and helps in setting their values equal to zero if the equation updates in Equations (5.25) and (5.27) yield negative values. Consider a point in time where the line flow $P_{m,n} = Y_{m,n}(\theta_m(l) - \theta_n(l)$ is lower than the upper limit of the constraint on the line $\overline{P}_{m,n}$. At this point, the update of Equation (5.25) yields a negative value causing $\mu_{m,n}$ to decrease with a minimum value bounded to zero due to the projection operator. If the line flow crosses the upper limit, $\mu_{m,n}$ increases signifying the constraint is not met. The system then iterates to get the power flow within the boundary limits.

The tuning parameter values for all the updates are extremely sensitive and play a major role in deciding weather an OPF problem will converge or remain unstable. The values of tuning parameters for this study are decided by carrying out empirical research in the MATLAB simulations of the given algorithm for specific case studies. The tuning parameters have to be in sync with the overall method as every parameter is varied from its previous iteration based on the value of the tuning parameter.

5.2. EXACT DISTRIBUTED OPF FOR A DC MICROGRID

Lossless DC networks have been studied and a DC OPF algorithm for the same has been presented in the previous section. Any DC distribution grid in practice will experience power loss in distribution lines due to resistance in cables. This will demand higher power being extracted from generators to compensate for the distribution power losses. To build a distributed algorithm for such a pragmatic DC distribution system, the lossless DC OPF code presented in Section 5.1 has to be greatly modified. The distributed algorithm with losses is termed as Exact DC OPF. Moreover, the Exact DC OPF algorithm is a single time period approach to perform a distributed optimization.

The DC OPF algorithm for a lossless DC network considered a single decision variable (p_m^S) in the cost function. If the code needs to account for distribution losses, the power term needs to be split into a product of current extracted (i_m^S) and the nodal voltage magnitude (u_m). Since, the objective function minimizes the overall operational costs of the system by minimizing the power extracted from the generators, it will also minimize the power losses in the distribution line. For losses to be minimum in a line, the nodal voltage magnitudes should be as high as possible, rendering the current flow in the line to be minimum. The power losses is proportional to the square of the current flow in the line. This can be proved mathematically.

Consider a network, where power flows between two nodes- m and n. The conductance of the line connecting the nodes is $G_{m,n}$. The nodal voltage magnitudes at the two nodes is u_m and u_n respectively. Now the difference between the power at node m and the power at node n will represent the losses in the line. Therefore the power loss P_{loss} is:

$$\begin{aligned} P_{loss} &= \text{Power at node m} - \text{Power at node n} && (5.28)\\ &= u_m[G_{m,n}(u_m - u_n)] - u_n[G_{m,n}(u_m - u_n)] && (5.29)\\ &= G_{m,n}(u_m - u_n)^2 && (5.30)\end{aligned}$$

Thus, higher the current flow in the line, higher is the cable losses. The loss in the line is dependent on the voltage magnitude. In a DC system consisting of several nodes bound by a voltage range of 325 - 375 V, the voltage magnitude of atleast one of the nodes should be 375 V to have minimum distribution losses. This will further minimize current flows as power transferred remains the same, thus ultimately reducing losses. This makes it evident for the objective function in the OPF formulation to have two decision variables representing nodal current and voltage magnitudes.

5.2.1. MATHEMATICAL FORMULATION OF EXACT DC OPF FOR A DC NETWORK WITH LOSSES

The mathematical formulation of the Exact DC OPF for a DC distribution system is as follows:

Objective

$$\min \sum_{m\in\mathcal{N}} \sum_{s\in\mathcal{S}} A_m (p_m^S)^2 + B_m p_m^S + C_m \tag{5.31}$$

$$\min \sum_{m\in\mathcal{N}} \sum_{s\in\mathcal{S}} A_m (i_m^S)^2 u_m^2 + B_m i_m^S u_m + C_m \tag{5.32}$$

Subject to

$$\sum i_m^S = \sum G_{m,n}(u_m - u_n) \qquad \forall (m,n) \in \mathcal{N} \tag{5.33}$$

$$-\overline{I}_{m,n} \le G_{m,n}(u_m - u_n) \le \overline{I}_{m,n} \qquad \forall (m,n) \in \mathcal{N} \tag{5.34}$$

$$\underline{P}_m^S \le p_m^S \le \overline{P}_m^S \qquad \forall s \in \mathcal{S} \tag{5.35}$$

$$\underline{P}_m^S \le i_m^S u_m \le \overline{P}_m^S \qquad \forall s \in \mathcal{S} \tag{5.36}$$

$$\underline{U}_m \le u_m \le \overline{U}_m \qquad \forall m \in \mathcal{N} \tag{5.37}$$

The objective function used for the algorithm to consider losses is given by Equation (5.32). The decision variables are i_m^S which denotes the current generated by source S at given node m, and u_m which denotes the nodal voltage magnitude at node m. The source S can denote a power generator or a fixed load device. The sign convention is same as before: positive for generators and negative for loads. S belongs to the set of $\mathcal{S}$ which represents the total number of sources at given node m. Moreover, m belongs to the set of $\mathcal{N}$, which denotes the total number of nodes in the DC microgrid.

The equality constraint given by Equation (5.33), represents the current flow balance. The LHS term denotes the nodal current flow, while the RHS term denotes the current flow in the line connecting the node. If voltage magnitude (u_m) is multiplied on both sides in Equation (5.33), a power balance is formed. Since, u_m is the common term, the equality constraint leads to a current flow balance.

Equation (5.34) represents the constraint on line flow. Any distribution cable is specified by a current flow capacity and not a power flow capacity [81]. The lower capacity bound is the negative of the higher capacity bound on the basis of reverse current flow properties, i.e. a current flowing from A to B is negative of the current flowing from B to A.

Equations (5.35) and (5.36) denote the same constraint on the power produced by the generator. Upper and lower bounds are specified by $\bar{\cdot}$ and $\underline{\cdot}$ respectively. Equation (5.37) is an added inequality constraint and represents the operational voltage range in the DC network. As discussed in Chapter 1, it is important to maintain allowable voltage values in a DC system which helps to increase the overall system efficiency.

The set of equations which are used for the Exact DC OPF formulation are Equations (5.32), (5.33), (5.34), (5.36) and (5.37).

5.2.2. LAGRANGE FUNCTION FOR THE FORMULATION

The Lagrange function for the Exact DC OPF formulation is as follows:

$$
\begin{aligned}
\mathscr{L} = & \Big(\sum_{m \in \mathcal{N}} \sum_{s \in \mathscr{S}} A_m (i_m^{\mathrm{S}})^2 u_m^2 + B_m i_m^{\mathrm{S}} u_m + C_m \Big) \\
& + \Big(\sum \lambda_m \big(\sum G_{m,n}(u_m - u_n) - \sum i_m^{\mathrm{S}} \big) \Big) \\
& + \Big(\sum \mu_{m,n} \big(G_{m,n}(u_m - u_n) - \overline{I}_{m,n} \big) \Big) \\
& + \Big(\sum \mu_{n,m} \big(-G_{m,n}(u_m - u_n) - \overline{I}_{m,n} \big) \Big) \\
& + \Big(\sum \mu_m^{\overline{P}} \big(i_m^{\mathrm{S}} u_m - \overline{P}_m^{\mathrm{S}} \big) \\
& + \sum \mu_m^{\underline{P}} \big(-i_m^{\mathrm{S}} u_m + \underline{P}_m^{\mathrm{S}} \big) \Big) \\
& + \Big(\sum \mu_m^{\overline{U}} \big(u_m - \overline{U}_m \big) \\
& + \Big(\sum \mu_m^{\underline{U}} \big(-u_m + \underline{U}_m \big)
\end{aligned}
\tag{5.38}
$$

λ_m is the current flow LMP and is associated with the current flow balance in the network. Apart from the four dual variables considered before, an added two dual variables for the voltage constraint are taken into account. They are denoted by $\mu_m^{\overline{U}}$ and $\mu_m^{\underline{U}}$. These added dual variables help to maintain the voltage magnitudes within the desired bound limits.

5.2.3. FIRST ORDER OPTIMALITY CONDITIONS

The KKT conditions which need to be solved and satisfied based on Equation (5.38) are mentioned below:

$$
\begin{aligned}
\frac{\partial L}{\partial i_m^{\mathrm{S}}} = & \sum_{s \in \mathscr{S}} 2 A_m u_m^2 i_m^{\mathrm{S}} + B_m u_m \\
& - \lambda_m + u_m (\mu_m^{\overline{P}} - \mu_m^{\underline{P}}) = 0
\end{aligned}
\tag{5.39}
$$

$$
\begin{aligned}
\frac{\partial L}{\partial u_m} = & \sum_{s \in \mathscr{S}} 2 A_m (i_m^{\mathrm{S}})^2 u_m + B_m i_m^{\mathrm{S}} \\
& + \lambda_m \sum G_{m,n} - \sum \lambda_n G_{m,n} \\
& + \sum G_{m,n} (\mu_{m,n} - \mu_{n,m}) \\
& + i_m^{\mathrm{S}} (\mu_m^{\overline{P}} - \mu_m^{\underline{P}}) \\
& + \mu_m^{\overline{U}} - \mu_m^{\underline{U}} = 0
\end{aligned}
\tag{5.40}
$$

$$
\frac{\partial L}{\partial \lambda_m} = - \sum i_m^{\mathrm{S}} + \sum G_{m,n} (u_m - u_n) = 0 \tag{5.41}
$$

$$
\frac{\partial L}{\partial \mu_{m,n}} = \sum G_{m,n} (u_m - u_n) - \overline{I}_{m,n} \leq 0 \tag{5.42}
$$

$$
\frac{\partial L}{\partial \mu_{n,m}} = - \sum G_{m,n} (u_m - u_n) - \overline{I}_{m,n} \leq 0 \tag{5.43}
$$

$$
\frac{\partial L}{\partial \mu_m^{\overline{P}}} = i_m^{\mathrm{S}} u_m - \overline{P}_m^{\mathrm{S}} \leq 0 \tag{5.44}
$$

$$
\frac{\partial L}{\partial \mu_m^{\underline{P}}} = - i_m^{\mathrm{S}} u_m + \underline{P}_m^{\mathrm{S}} \leq 0 \tag{5.45}
$$

$$
\frac{\partial L}{\partial \mu_m^{\overline{U}}} = u_m - \overline{U}_m \leq 0 \tag{5.46}
$$

$$
\frac{\partial L}{\partial \mu_m^{\underline{U}}} = - u_m + \underline{U}_m \leq 0 \tag{5.47}
$$

COMPLEMENTARY SLACKNESS CONDITIONS

$$\mu_{m,n}(\overline{I}_{m,n} - \sum G_{m,n}(u_m - u_n)) = 0 \tag{5.48}$$
$$\mu_{n,m}(-\overline{I}_{m,n} + \sum G_{m,n}(u_m - u_n)) = 0 \tag{5.49}$$
$$\mu^{\overline{P}}_m(\overline{P}^{\mathrm{S}}_m - i^{\mathrm{S}}_m u_m) = 0 \tag{5.50}$$
$$\mu^{\underline{P}}_m(i^{\mathrm{S}}_m u_m - \underline{P}^{\mathrm{S}}_m) = 0 \tag{5.51}$$
$$\mu^{\overline{U}}_m(\overline{U}_m - u_m) = 0 \tag{5.52}$$
$$\mu^{\underline{U}}_m(u_m - \underline{U}_m) = 0 \tag{5.53}$$

POSITIVITY CONDITIONS

$$\mu_{m,n}, \mu_{n,m}, \mu^{\overline{P}}_m, \mu^{\underline{P}}_m, \mu^{\overline{U}}_m, \mu^{\underline{U}}_m \geq 0 \tag{5.54}$$

The first derivative of the Lagrange function is taken with respect to all the system variables. The complementary slackness conditions are also necessary conditions and are given by Equations (5.48) - (5.53). Finally, all the dual variables are positive bound. Consider a particular pair of dual variables, say for e.g. $\mu_{m,n}$ and $\mu_{n,m}$. In the problem simulation, either one of them will have a positive value while the other will attain a value of zero. This is also true for the other set of dual variable pairs. It is logically true as a distribution line can be congested in only one direction.

5.2.4. ITERATIVE UPDATES FOR THE EXACT DC OPF MODEL

The Exact DC OPF model follows the iterative updates similar to the updates presented in the Lossless DC OPF model but with modifications in the equation set-up.

MODELING FOR LMP UPDATES

$$\lambda_m(l+1) = \lambda_m(l) - \lambda_1(\frac{\partial L}{\partial u_m}) + \lambda_2(\frac{\partial L}{\partial \lambda_m}) \tag{5.55}$$
$$\begin{aligned} &= \lambda_m(l) - \lambda_1[\sum_{s\in\mathcal{S}} 2A_m(i^{\mathrm{S}}_m(l))^2 u_m(l) + B_m i^{\mathrm{S}}_m(l) \\ &+ \lambda_m(l)\sum G_{m,n} - \sum \lambda_n(l) G_{m,n} \\ &+ \sum G_{m,n}(\mu_{m,n}(l) - \mu_{n,m}(l)) \\ &+ i^{\mathrm{S}}_m(l)(\mu^{\overline{P}}_m(l) - \mu^{\underline{P}}_m(l)) \\ &+ \mu^{\overline{U}}_m(l) - \mu^{\underline{U}}_m(l)] \\ &+ \lambda_2[-\sum i^{\mathrm{S}}_m(l) + \sum G_{m,n}(u_m(l) - u_n(l))] \end{aligned} \tag{5.56}$$

The LMP updates, denoted by λ_m for a particular node m follow the same intuitive mechanism stated before. The linkage of the optimality condition and an additional innovation term help in faster convergence of the LMP values.

MODELING FOR GENERATOR CURRENT UPDATES

$$i^{\mathrm{S}}_m(l+1) = i^{\mathrm{S}}_m(l) - I_1\frac{\partial L}{\partial i^{\mathrm{S}}_m} \tag{5.57}$$
$$\begin{aligned} &= i^{\mathrm{S}}_m(l) - I_1[\sum_{s\in\mathcal{S}} 2A_m u^2_m(l) i^{\mathrm{S}}_m(l) \\ &+ B_m u_m(l) - \lambda_m(l) + u_m(l)(\mu^{\overline{P}}_m(l) - \mu^{\underline{P}}_m(l))] \end{aligned} \tag{5.58}$$

The updates for the generator current follow a similar pattern as the power update considered in Lossless DC OPF. The power there represented the current as the voltage magnitudes where assumed to be 1 p.u. The projection operator has not been used as the dual variables have been included in the update equation. They perform the same task of maintaining the variable within the constrained boundary. The tuning parameter used is I_1 which is a positive constant.

MODELING FOR NODAL VOLTAGE UPDATES

$$u_m(l+1) = u_m(l) - U_1 \frac{\partial L}{\partial \lambda_m} \tag{5.59}$$

$$= u_m(l) - U_1[-\sum i_m^{\mathrm{S}}(l) + \sum G_{m,n}(u_m(l) - u_n(l))] \tag{5.60}$$

The nodal voltage update is highly sensitive to the values of the line conductance as seen in Equation (5.60). A high value of line conductance will result in convergence issues as the tuning parameters have to be tuned accordingly. A higher conductance value will require a lower value of tuning parameter U_1. This is done to achieve a well balanced and stabilized convergence of the update. Generally, for larger transmission lines, the conductance is relatively low. This allows the tuning parameters to take slightly larger values. The values of the tuning parameter have to be appropriated found out. For this study, it is done through empirical analysis.

MODELING FOR DUAL VARIABLES: LINE CONGESTION UPDATES

$$\mu_{m,n}(l+1) = \mathbb{P}[\mu_{m,n}(l) + \mu_1 \frac{\partial L}{\partial \mu_{m,n}}] \tag{5.61}$$

$$= \mathbb{P}[\mu_{m,n}(l) + \mu_1[G_{m,n}(u_m(l) - u_n(l)) - \overline{I}_{m,n}]] \tag{5.62}$$

$$\mu_{n,m}(l+1) = \mathbb{P}[\mu_{n,m}(l) + \mu_1 \frac{\partial L}{\partial \mu_{n,m}}] \tag{5.63}$$

$$= \mathbb{P}[\mu_{n,m}(l) + \mu_1[-G_{n,m}(u_m(l) - u_n(l)) - \overline{I}_{m,n}]] \tag{5.64}$$

The dual variables also provide information on the congestion in a line through updates of $\mu_{m,n}$ and $\mu_{n,m}$. The updates follow the same mechanism as mentioned in Section 5.1.4.

MODELING FOR DUAL VARIABLES: GENERATOR POWER LIMIT UPDATES

$$\mu_m^{\overline{P}}(l+1) = \mu_m^{\overline{P}}(l) + \mu_P^{high} \frac{\partial L}{\partial \mu_m^{\overline{P}}} \tag{5.65}$$

$$= \mu_m^{\overline{P}}(l) + \mu_P^{high}[i_m^{\mathrm{S}}(l) u_m(l) - \overline{P}_m^{\mathrm{S}}] \tag{5.66}$$

$$\mu_m^{\underline{P}}(l+1) = \mu_m^{\underline{P}}(l) + \mu_P^{low} \frac{\partial L}{\partial \mu_m^{\underline{P}}} \tag{5.67}$$

$$= \mu_m^{\underline{P}}(l) + \mu_P^{low}[-i_m^{\mathrm{S}}(l) u_m(l) + \underline{P}_m^{\mathrm{S}}] \tag{5.68}$$

Since, a projection operator is not implemented for the nodal current update given by Equation (5.57), the dual variables are used and updated to help maintain the constraint limits. $\mu_m^{\overline{P}}$ is the dual variable which keeps a check on the upper bound limit of the power constraint. It attains a positive value for every instant the power from the generator equals its maximum capacity or crosses it. Similarly, $\mu_m^{\underline{P}}$ keeps a check on the lower bound limit of the power constraint. The updates are intuitively added, as they follow similar working mechanism as the update for line congestion multipliers given by Equation (5.61). μ_P^{high} and μ_P^{low} are the tuning parameters which attain only zero or positive values. They are empirically analyzed for a good fit in the update equation. This is done through MATLAB simulations using specific network cases.

MODELING FOR DUAL VARIABLES: NODAL VOLTAGE LIMIT UPDATES

$$\mu_m^{\overline{U}}(l+1) = \mu_m^{\overline{U}}(l) + \mu_U^{high}\frac{\partial L}{\partial \mu_m^{\overline{U}}} \tag{5.69}$$

$$= \mu_m^{\overline{U}}(l) + \mu_U^{high}[u_m(l) - \overline{U}_m] \tag{5.70}$$

$$\mu_m^{\underline{U}}(l+1) = \mu_m^{\underline{U}}(l) + \mu_U^{low}\frac{\partial L}{\partial \mu_m^{\overline{U}}} \tag{5.71}$$

$$= \mu_m^{\underline{U}}(l) + \mu_U^{low}[-u_m(l) + \underline{U}_m] \tag{5.72}$$

The dual variables for nodal voltage limits are also a result of intuition. The updates for these variables are similar to the updates for the power limits. The voltage magnitudes at different nodes in the network are maintained within the desired operational range. For high efficiency DC microgrids, the voltage level generally used is 350 V, see Chapter 1, Section 1.3.4. To achieve such efficiencies during distributed optimization, the voltage magnitudes need to be kept within bounds, for e.g. 325 - 375 V.

The dual variables $\mu_m^{\overline{U}}$ and $\mu_m^{\underline{U}}$ help to conserve the upper and lower voltage constraint limit respectively. For a stabilized output, the differential term given in Equation (5.69) and (5.71) should become either zero or a constant negative value as per the KKT conditions. At this point, convergence is achieved.

5.2.5. SIMPLE THREE NODE CASE

In order for a better understanding of the Exact DC OPF algorithm for a DC distribution system considering congestion and network losses, a simple three node network case is presented below in Figure 5.1.

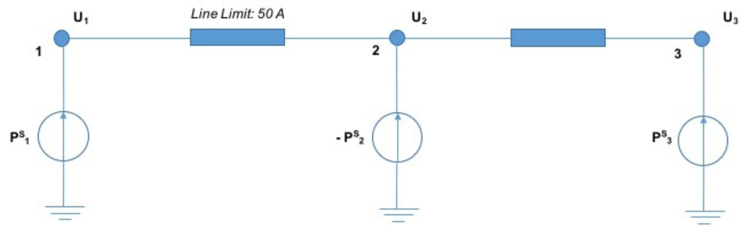

Figure 5.1: Simple three node Exact DC network

Three nodes denoted by 1, 2 and 3 are considered in a DC network. Node 1 consists of a power generator with a maximum capacity of 20 kW (p_1^S) and with a cost function given by $10p_1^S$. Node 3 consists of another power generator with a maximum capacity of 15 kW and with a cost function given by $30p_3^S$. It is evident the generator at node 1 is cheaper to operate. The cost functions considered are linear for all the case studies going ahead. This helps in maintaining a common point of comparison with respect to cost of operation. The cost co-efficient linked to the power produced signifies the operational costs of the generator which, for example is 10 EUR/W for generator at node 1. These cost co-efficients are basically the marginal costs of the generators and are randomly selected for the purpose of explanation of the distributed algorithm. Node 2 consists of a fixed load ($-p_2^S$) with a constant demand of 20 kW. The sign convention followed is positive for power generators and negative for load devices.

The voltage values at the three nodes are denoted by u_1, u_2 and u_3. They are absolute values and given in units of Volt(V). An aluminum cable is considered of 100 meter length with a resistivity value of $2.65 * 10^{-8}\Omega$ m. The cable cross-section is 25 mm^2 [87] [88]. The length of the cable is chosen to be suitable for a DC microgrid. Such a cable length attains a conductance value of 9.43 S.

The cable connecting node 1 and 2 has been assumed to have a current flow limit of 50 A. The cable connecting node 2 and 3 has a current flow limit of 95 A.

SIMULATION SETUP

The Exact DC OPF algorithm is coded in MATLAB. The nodal voltages at the three nodes are initialized to 350 V. The LMP initialization at the nodes is taken as 3000 Euros/A each. Rest of the variables are initialized to 0.

The tuning parameters are tuned according to empirical analysis by running simulations and modifying values for the best fit. These values help in achieving convergence, but are not necessarily the optimal values for fastest convergence rate. That kind of research is out of this thesis scope. The values of tuning parameters used for the simulation are as follows:

Table 5.1: Tuning Parameter Values

Tuning Parameter	**Value**
λ_1	0.008
λ_2	0.1485
U_1	0.01
I_1	0.008
μ_1	0.08
μ_p^{high}	0.000005
μ_p^{low}	0.000005
μ_u^{high}	0.09
μ_u^{low}	0.02

OUTPUT AND ANALYSIS

Figure 5.2 shows the convergence properties of the optimal solution. The convergence of the solution is achieved at an iteration count of around 30000 iterations. The nodal voltage at node 1 reaches a value of 375 V, which signifies the model is trying to reduce distribution losses in the system. Node 2 attains a voltage value of 369.9 V. Due to the line connecting node 1 and node 2 being congested, and the allowable current flow to be 50 A, the current extracted from the cheaper generator is 50 A. The load has a fixed requirement of 20 kW and is at a voltage magnitude of 369.9 V. This makes the current requirement for the load to be 54.1 V. 50 A worth of current is provided by generator at node 1, the rest of the power is extracted from the expensive generator at node 3. Hence, the power produced by generator on node 1 is 18.75 kW. The power extracted from generator at node 3 is 1.52 kW. The total power supplied is therefore, 18.75 + 1.52 = 20.27 kW. The excess 0.27 kW worth of power is lost as distribution losses in the line. The nodal variable values are given in Table 5.2.

Table 5.2: Nodal Variables

Node	**Nodal Current, i_m^S [A]**	**Nodal Voltage, u_m [V]**	**Source Power, p_m^S [kW]**	**Max Source Capacity, P_{max} [kW]**	**Min Source Capacity, P_{min} [kW]**	**LMP, λ_m^I [Euros/A]**	**LMP, λ_m^P [Euros/W]**
1	50	375	18.75	20	0	3750	10
2	-54.1	369.9	20	-20	-20	11124	30.07
3	4.1	370.3	1.52	15	0	11112	30

The LMP values in the table are given in terms of current flow LMP and power LMP. The current flow LMP values are achieved in the simulation result. They are the result of the current flow balance. The power LMP values are calculated by multiplying the nodal voltage to the current LMP at that particular node.

$$\lambda_m^P = \lambda_m^I * u_m \tag{5.73}$$

where, λ_m^P is the power LMP and is denoted in units of EUR/W and λ_m^I is the current LMP with units EUR/A. As expected, the power LMP value at node 1 is equal to the marginal cost of the generator providing maximum power. Since this generator does not reach its full capacity, it can still provide for a unit increase in load at node 1. LMP at Node 2 attains the marginal cost of the expensive generator plus the marginal cost of line losses between node 2 and node 3. This is true due to the presence of congestion and cable losses considered for the network. The load is supplied by a small amount of power from the expensive generator due to congestion in the line. This is reflected in the values given in Figure 5.2. As seen in Table 5.2, the nodal LMP values at node 2 is slightly higher than the nodal LMP at node 3. The difference of 0.07 Euros/W denotes the marginal cost of losses in the connecting line.

The variables are updated according to the Exact DC OPF equations. Every update requires its differential term to either stabilize to zero or attain a constant negative value according to the KKT conditions. This ultimately converges the variable iterations. The graph of the first derivative of the Lagrange function with the system variables is shown in Figure 5.3.

Due to congestion in the line, the value of μ_{12} is seen to be 7224 Euros/A. μ_{21} will attain a value of zero. There is no congestion seen in the line connecting node 2 and 3. The differential of the $\mu_{m,n}$ is seen in Figure 5.3. It stabilizes to give a converged solution of the dual variables.

The generators are capped with a maximum and minimum power capacity output. The dual variables- $\mu_m^{\overline{P}}$ and $\mu_m^{\underline{P}}$ used in the iterative process of the Exact DC OPF help in maintaining these constraints. The converged solution of these variables is given in Figure 5.4. Notice that $\mu_1^{\overline{P}}$ is triggered as power is initially extracted from the cheaper generator which runs at full capacity to fulfill the load requirements. Due to the line flow restriction on the current flow, the power extracted from the first generator gradually reduces to the line flow limit of the cable. As the power extracted reduces, the triggered variable $\mu_1^{\overline{P}}$ goes back to its zero value. This is at around 30000 iteration count. Also at this point, the congestion variable μ_{12} stabilizes to a converged value as seen in Figure 5.2. The lower limit dual variables are not triggered at all as both the generators provide some amount of power. The lower power limit at node 2 is triggered as the load has a fixed demand denoted by a negative sign convention. The stabilized value is 1.1 Euros/W.

Similarly, the voltage limit dual variables $\mu_m^{\overline{U}}$ and $\mu_m^{\underline{U}}$ are shown in Figure 5.4. To reduce overall line losses in the system, the algorithm pushes the nodal voltage value at node 1 to its highest capacity. The dual variable $\mu_1^{\overline{U}}$ helps to keep this quantity within bounds and hence stabilizes to a value of 1000 EUR/V at the same count of iteration value of 30000. This signifies that the social welfare would increase by 1000 euros if the voltage value increased by 1 V. Social welfare is basically the net profit which an ISO would make based on the system dynamics [89]. It is the profit made while selling and buying power.

Figure 5.5 provides the first derivative of the Lagrange function with respect to the dual variables stated above. As per the updates given by Equations (5.65), (5.67), (5.69) and (5.70), the differential value needs to stabilize to a converged solution of the dual variables. As seen in the graphs, this happens at the iteration count of 30000, where the overall system converges to give an optimal solution.

To conclude, the optimal cost of operation for the two node DC system is 233,100 Euros. This is the minimal cost which will be incurred for running the DC system for a single time period. The cost is minimized to encompass least marginal cost of operation, least marginal cost of losses and least marginal cost of congestion.

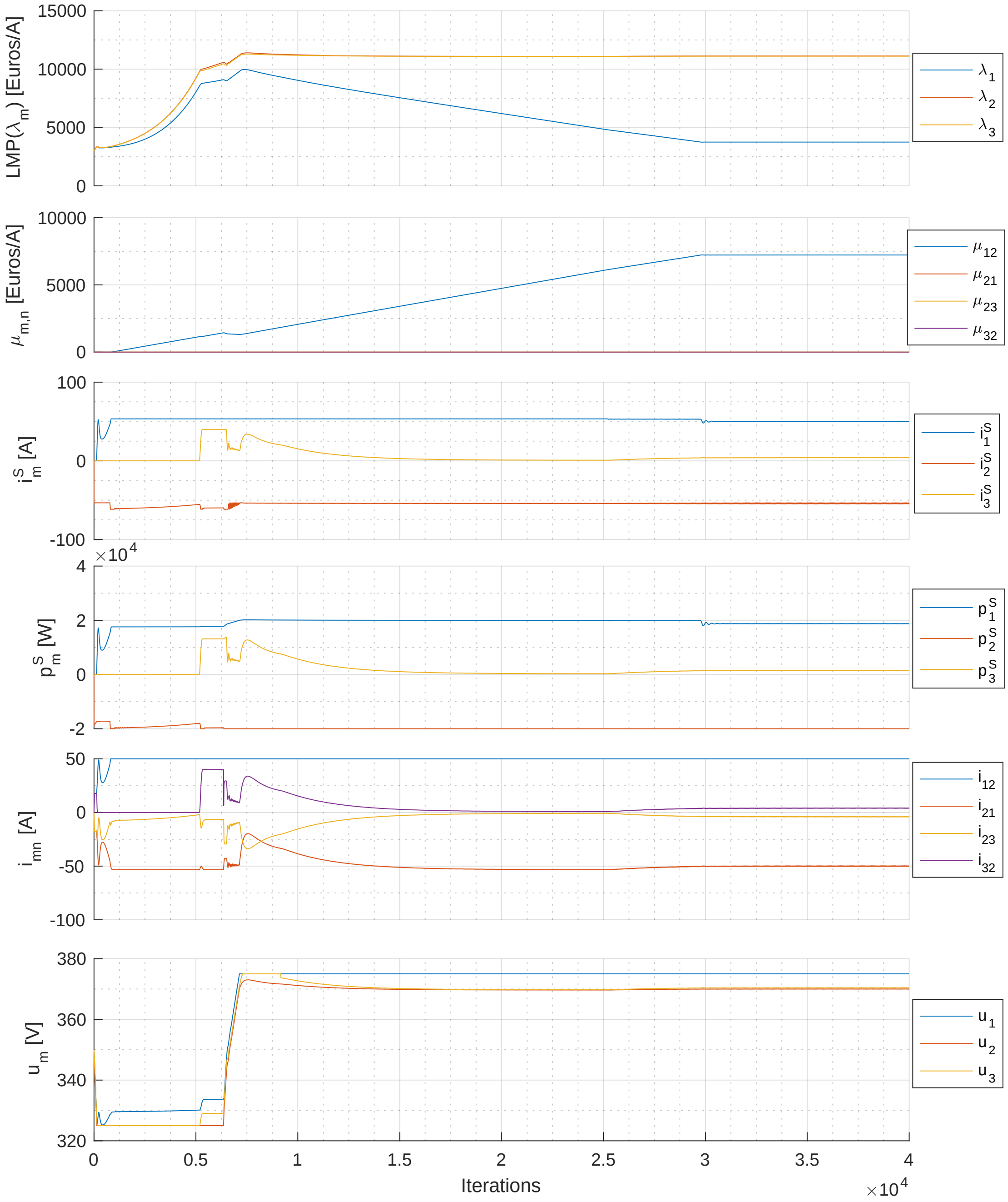

Figure 5.2: Graph 1: LMP(λ_m) vs Iterations, Graph 2: Congestion Dual Variable ($\mu_{m,n}$) vs Iterations, Graph 3: Nodal Current (i_m^S) vs Iterations, Graph 4: Power Generated (p_m^S) vs Iterations, Graph 5: Line Current ($i_{m,n}$) vs Iterations, Graph 6: Nodal Voltage (u_m) vs Iterations.

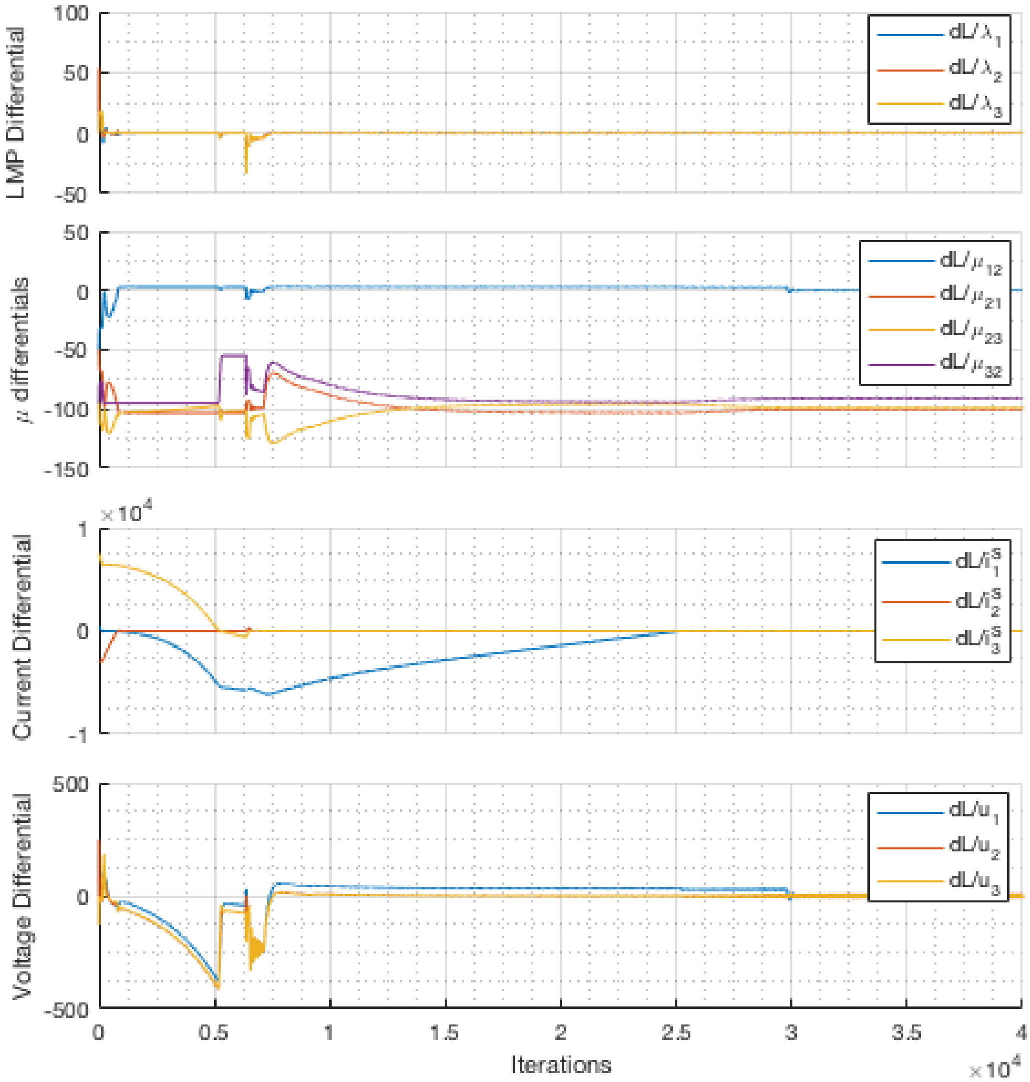

Figure 5.3: Variable Differentials Output

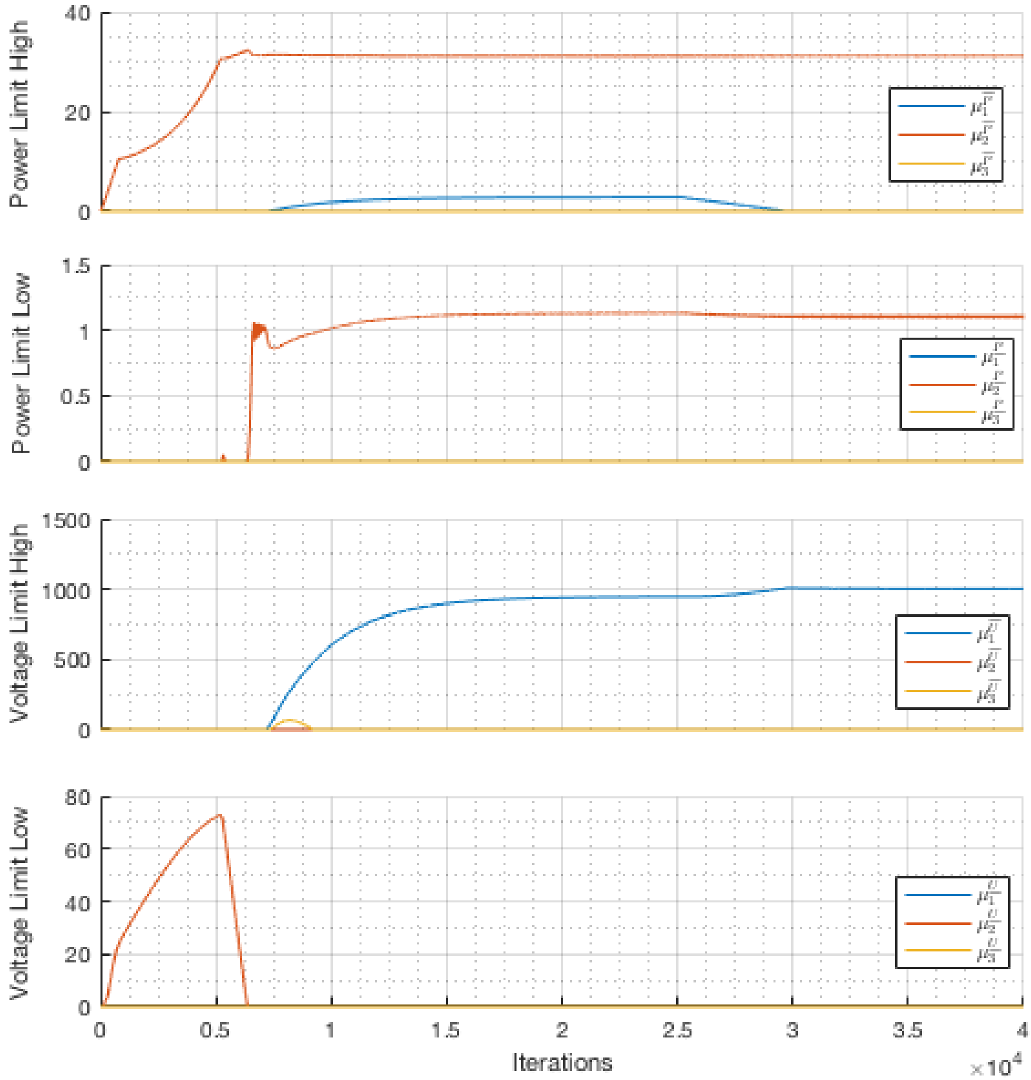

Figure 5.4: Dual Variables Output

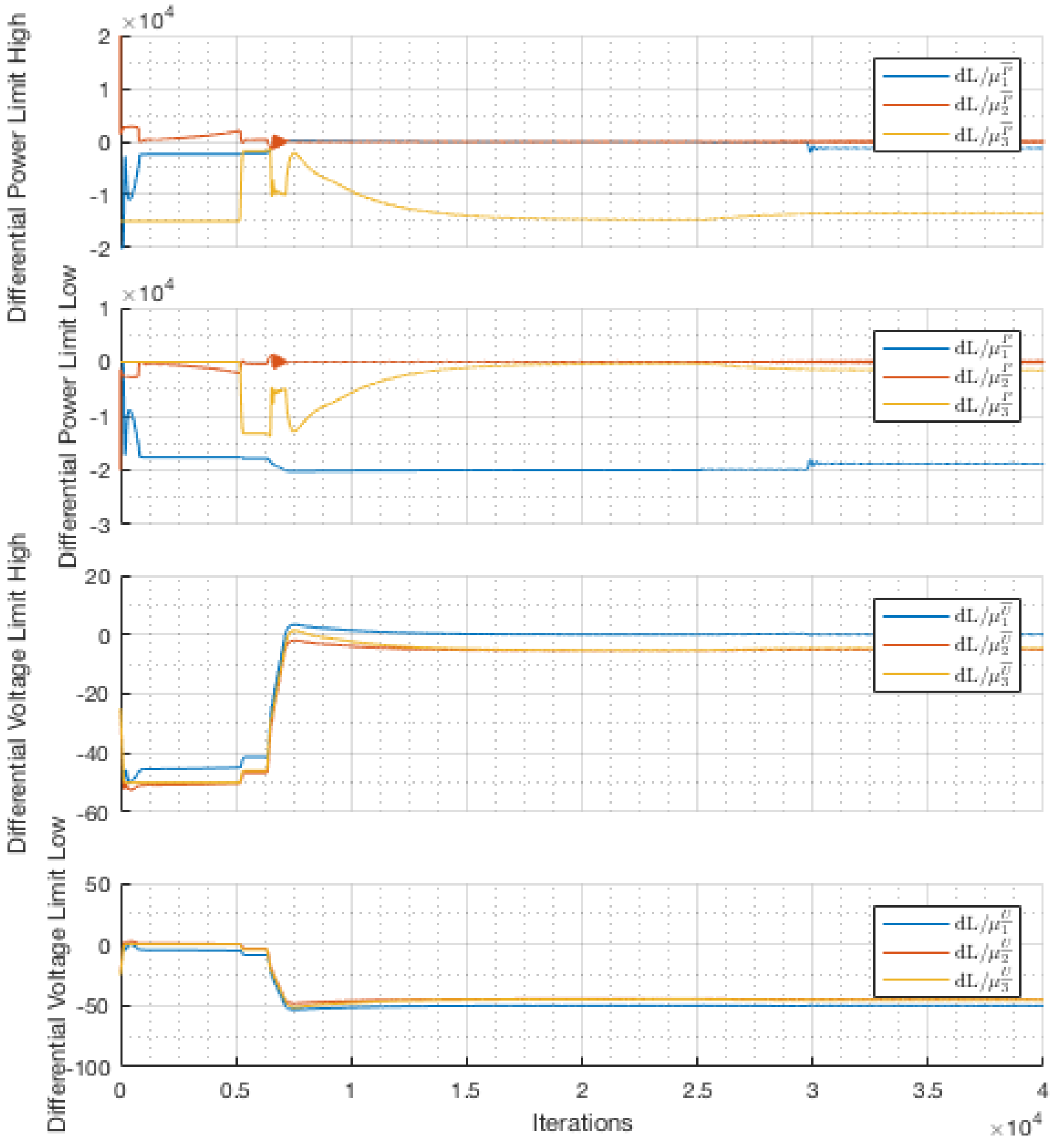

Figure 5.5: Differential of Dual Variables Output

6

EXAMPLES OF DISTRIBUTED OPTIMAL POWER FLOW

This chapter presents different cases that are chosen to show how the exact distributed optimal power flow model functions in specific DC distribution systems which can occur in the practical world. It deals with actual implementation of distributed optimization for scenarios which can be encountered in today's times. For the sake of simplicity and ease of understanding, the DC distribution system is a four bus network.

Case 1 tests the algorithm on a single line DC network with PV generation systems on two separate nodes. An expensive power generator and a fixed load occupy the other two buses. Case 2 presents a meshed DC distribution network. Two nodes consists of an expensive and a zero cost power generator respectively. One of the nodes has no power generation or consumption, while the last node has a fixed load requirement. The aim is to test the effects of the exact DC OPF algorithm on such meshed grids. Case 3 presents a unique T shaped DC network. Node 1, 2 and 4 consists of zero cost, cheap and expensive generators respectively. The remaining node is occupied by a fixed load. Lastly, a scenario involving a long distribution line is considered in a DC network to test the functioning of dual variables for voltage limits. For all the cases, the voltage limits are maintained between 375 and 325 V as maximum and minimum values. The distribution cables used to connect the nodes are assumed to be aluminum cables with a cross-section area of 25 mm^2.

The output of the Exact DC OPF algorithm is a distributed solution. All the cases presented in the below sections are compiled in a distributed as well as centralized fashion. The output of the Exact DC OPF algorithm is compared with the centralized output. The centralized model has been simulated on MATLAB using the *fmincon* solver of MATLAB. The comparison is made to match the exactness of both the solutions. The distributed solution is based on limited information exchange and is heavily dependent on the tuning parameters of the system. The values of the tuning parameters arise based on running multiple simulations to test for the best fit. They are not necessarily the most optimal values for fastest convergence rates.

The algorithm for the Exact DC OPF is a single time period algorithm. The study assumes that for any instant of time while the model runs multiple iterations, the power extracted from renewable energy sources can reach their individual maximum capacities. This means that maximum power can be extracted for e.g. from a PV system at any instant.

6.1. CASE 1: SINGLE LINE DC NETWORK

Figure 6.1 shows the case network considered. Node 1 and node 4 have each a photo-voltaic system with a maximum power capacity of 4 kW and 10 kW respectively. Node 2 comprises of a generator with a marginal cost of 50 EUR/W and a maximum generation capacity of 20 kW. Node 3 comprises of a load with a fixed demand of 15 kW. The lines connecting the nodes are assumed to be approximately 150 m in length. A single line network is considered to test the algorithm for a scenario with two zero-priced marginal generators. It is interesting to observe the functioning of the algorithm for such scenarios which are commonly seen in today's world due to increase in distributed renewable energy sources.

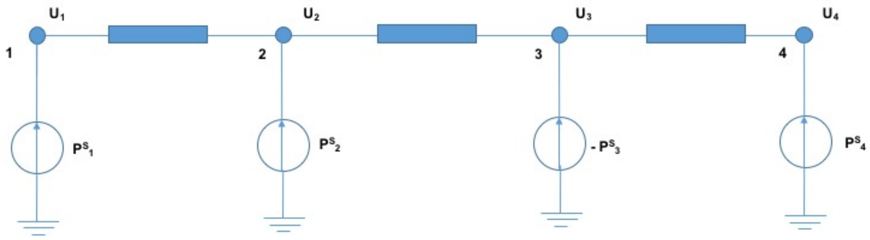

Figure 6.1: Single line DC network of a 4 node system.

6.1.1. OUTPUT AND ANALYSIS

The centralized and distributed algorithms yield very similar results as seen in Table 6.1. Both the PV generators work on full capacity as expected due to the zero marginal cost associated with them. But to satisfy the load completely, power from the source at node 2 is extracted to satisfy the demand as well as the line losses. The power lost in the distribution cables is approximately 220 W. The distributed algorithm is able to work with zero-priced sources and satisfy the demand first with power from these sources. Node 4 works on maximum allowable nodal voltage, thus proving the system works to minimize the line losses in the system. The tuning parameters used for the distributed model are given in Appendix C.

The tuning parameters used for this case result in a converged solution of the decision variables with minimal fluctuations in the stability as seen in the Figure 6.2. The convergence is observed roughly around 170000 iteration count. This is relatively a high iteration count as the dual variables for the upper power limit are triggered due to both the PV generators reaching their maximum capacity. The dual variables eventually get the system to work under the constrained boundary limit. This consumes iterative counts as a low value of tuning parameter associated with the dual variable update is used. Use of higher values will result in instability of the solution and hence non-convergence of the variables. The values of the tuning parameters used in the distributed model are given in Appendix C, Table C.1.

The LMP values at the nodes are a result of the marginal generator which is the source at node 2. As both the PV generators operate on maximum capacity and cannot provide any further power, the LMP is decided based on the marginal cost of the source which still can provide power. As seen in Table 6.1, nodal LMP at node 2 is 50 EUR/W. The LMP at node 1 and node 4 is slightly lower than 50 due to the marginal cost of losses due to current flows in the cables. The LMP at node 3 is slightly higher than 50 due to added cost of marginal losses as this node is the demand center.

Node 4 attains the maximum allowable voltage value of 375 V. To keep this voltage value within bounds the dual variable for high voltage limit is triggered. This is seen in the convergence graph for the dual variables shown in Appendix B, Figure B.2. The dual variable responsible to keep the nodal voltage at node 4 within the maximum range is seen to take a positive value of around 600 EUR/V at an approximate iteration count of $1.8 * 10^5$. This means that if the voltage bound is increased by 1 V to 376 V, the increase in social welfare will be 600 Euros.

The optimal operational value of the system for a single time period is 61,400 Euros.

Table 6.1: Case 1: Nodal Variables

Method	**Node**	**Nodal Current,** i_m^S **[A]**	**Nodal Voltage,** u_m **[V]**	**Source Power,** p_m^S **[kW]**	**Max Source Capacity,** P_{max} **[kW]**	**Min Source Capacity,** P_{min} **[kW]**	**LMP,** $\lambda^I{}_m$ **[Euros/A]**	**LMP,** $\lambda^P{}_m$ **[Euros/W]**
Centralized OPF	1	10.68	374.58	4	4	0	18517	49.43
	2	3.23	372.45	1.204	20	0	18622	50
	3	-40.58	369.67	-15	-15	-15	18760	50.75
	4	26.67	375	10	10	0	18486	49.3
Distributed OPF	1	10.67	374.33	4	4	0	18611	49.7
	2	3.2	372.2	1.228	20	0	18612	50
	3	-41	369.41	-15	-15	-15	18648	50.5
	4	26.67	375	10	10	0	18275	48.73

ZERO COST MARGINAL GENERATOR

The algorithm was also simulated with the same case mentioned above, but with node 1 having 10 kW of maximum PV capacity. The fixed load was hence, satisfied with the PV generation with some amount of surplus PV generated power. Therefore, the nodal LMP at all the nodes in the network would attain a value zero as the marginal generator (PV source in this case) is now having zero cost. But, the Exact DC OPF algorithm fails to attain a converged solution due to the complexity involved. All the dual variables associated with the system updates have to simultaneously attain a zero value. The algorithm does not achieve this due to the fact that one zero valued dual variable triggers another dual variable to take a positive value. This can be attributed to the inefficiency in tuning the tuning parameters of the updates. They need special simulations to take into account the connectedness of the updates. This is not within the scope of this thesis and thus an opportunity for future research.

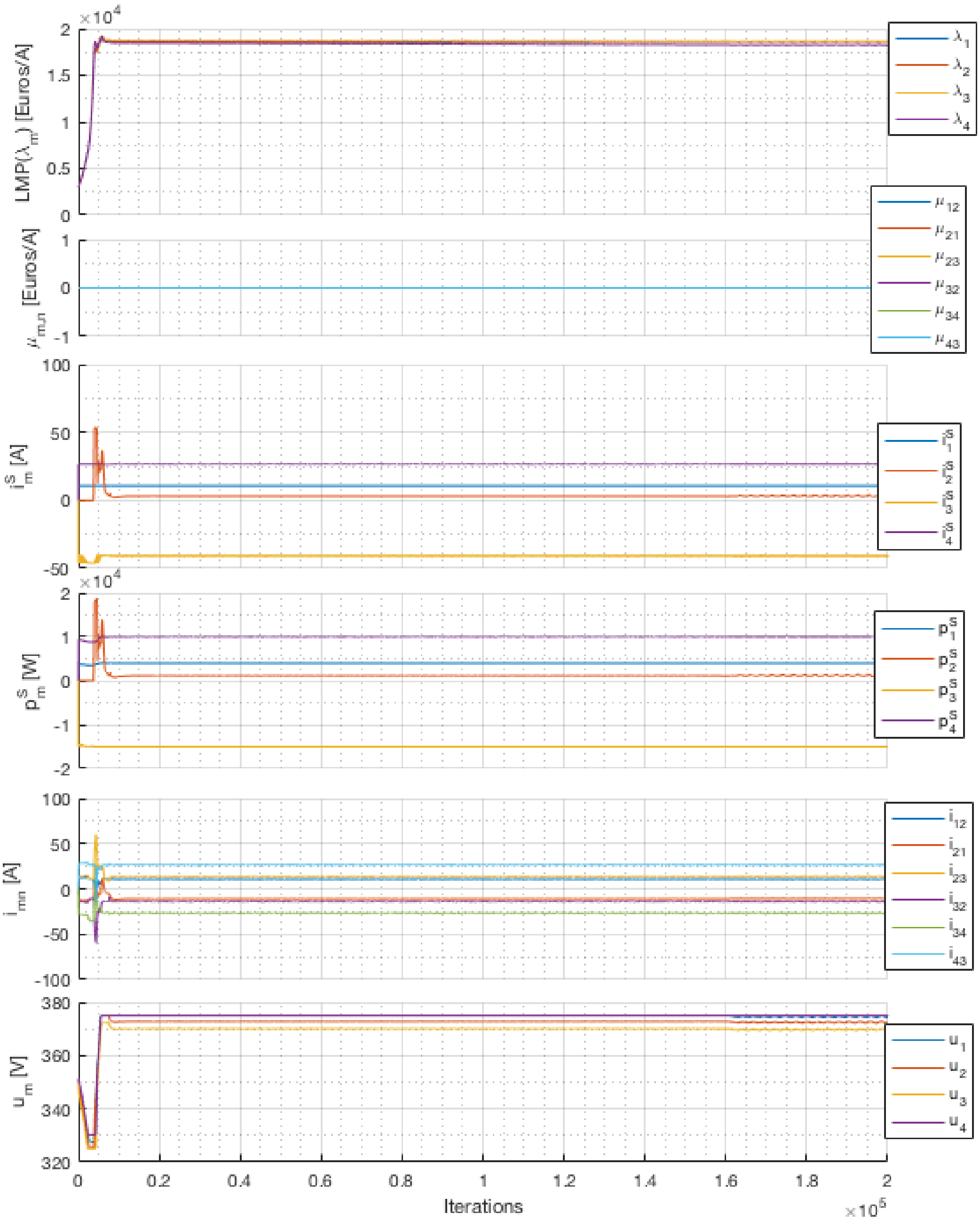

Figure 6.2: **CASE 1** - Graph 1: LMP(λ_m) vs Iterations, Graph 2: Congestion Dual Variable ($\mu_{m,n}$) vs Iterations, Graph 3: Nodal Current (i_m^S) vs Iterations, Graph 4: Power Generated (p_m^S) vs Iterations, Graph 5: Line Current ($i_{m,n}$) vs Iterations, Graph 6: Nodal Voltage (u_m) vs Iterations.

6.2. CASE 2: MESHED DC NETWORK

To test the Exact DC OPF algorithm in a meshed DC network, case 2 is considered. The illustrated network is shown in Figure 6.3. The 4 node meshed network consists of a renewable energy source at node 2 with a maximum capacity of 15 kW. A power generator of 50 kW capacity is present at node 4. The cost function associated with this generator is $25P^S_4$. Node 3 acts like a connecting medium with no source present. A fixed load of 50 kW is considered at node 1. The connecting cables are 150 m in length having constant resistance through out. The objective is to minimize the operational costs while maintaining the meshed network constraints.

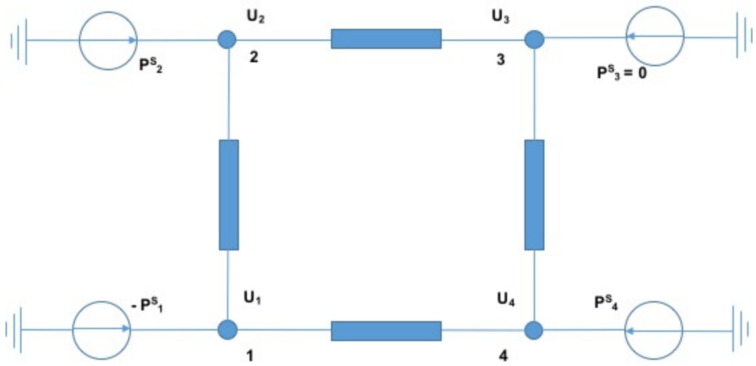

Figure 6.3: Meshed DC network of a 4 node system.

6.2.1. OUTPUT AND ANALYSIS

The distributed algorithm provides a solution providing similar values as compared to the centralized solution. The PV generator is the first to reach it's maximum capacity. To satisfy rest of the load demand, power from source at node 4 is extracted. This value is slightly different for the distributed solution when compared to the centralized solution due to the minor differences in the nodal voltage values. A difference of 0.5 V at node 1 results in a power difference of approximately 70 W, due to the high magnitude of current generation. As seen in Figure 6.5, the minor sporadic nature of the graph is due to the tuning parameters. The high sensitivity of tuning parameters require tuning values to be aligned upto the fifth value after the decimal. This makes it highly complex to arrive at accurate tuning parameter values which can completely eliminate the fluctuations. The values of tuning parameters calculated through empirical analysis is given in Appendix C, Table C.2.

The LMP values at the nodes are based on the marginal generator, which is the source at node 4. Thus, the LMP at node 4 is the marginal cost of the generator. The LMP values at nodes 1, 2 and 3 are accordingly higher than 25 EUR/W based on marginal cost of losses in the connecting cables. For e.g. the LMP at node 3 is 25.57 EUR/W. This means the marginal cost of losses for the line connecting node 3 and node 4 is 0.57 EUR/W.

The power generator at node 4 produces a nodal current of 99.8 A. Due to the meshed nature of the grid, there are back currents observed at this node. The current flowing in the line connecting node 4 and node 1 is 84.82 A and the rest of the current flows in the line connecting node 4 and node 3. This current ultimately reaches the load at node 1 after going through node 2. The branch current flows are shown in Table 6.3. The back currents are caused based on similar reasons for normal current flow. The difference in nodal voltage magnitudes results in current to flow in the cable. This does no harm in terms of optimization within the DC system considered as the network constraints are still maintained.

Table 6.2: Case 2: Nodal Variables

Method	**Node**	**Nodal Current, i_m^S [A]**	**Nodal Voltage, u_m [V]**	**Source Power, p_m^S [kW]**	**Max Source Capacity, P_{max} [kW]**	**Min Source Capacity, P_{min} [kW]**	**LMP, λ_m^I [Euros/A]**	**LMP, λ_m^P [Euros/W]**
Centralized OPF	1	-139.62	358.12	-50	-50	-50	9846	27.49
	2	40.62	369.16	15	15	0	9549	25.9
	3	0	372.08	0	0	0	9462	25.4
	4	99	375	37.12	50	0	9375	25
Distributed OPF	1	-139.8	357.74	-50	-50	-50	9829	27.48
	2	40	368.64	15	15	0	9643	26.16
	3	0	371.63	0	0	0	9504	25.57
	4	99.8	375	37.43	50	0	9365	25

Table 6.3: Case 2: Branch Current Flows

Method	**Branch**	**Branch Current Flow, $i_{m,n}$ [A]**
Centralized OPF	$i_{2,1}$	55.22
	$i_{3,2}$	14.59
	$i_{4,3}$	14.59
	$i_{4,1}$	84.4
Distributed OPF	$i_{2,1}$	54.98
	$i_{3,2}$	14.98
	$i_{4,3}$	14.98
	$i_{4,1}$	84.82

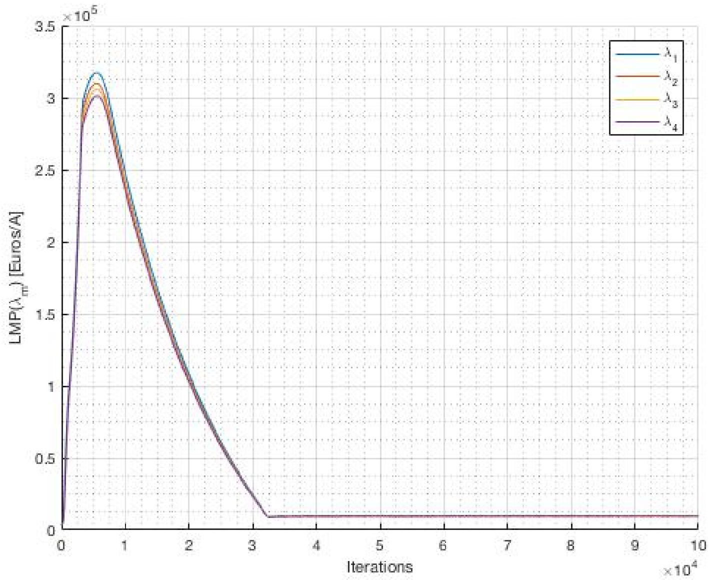

Figure 6.4: **CASE 2**: LMP(λ_m) [Euros/A] vs Iterations

The LMP values shown in Figure 6.5 are not visually clear due to the range of values the iterations calculate. A clearer graph for the convergence of the nodal LMP's is shown in Figure 6.4.

Finally, based on the power generated by the sources present in the system, the optimal operational value of the system for a single time period is 935,625 Euros.

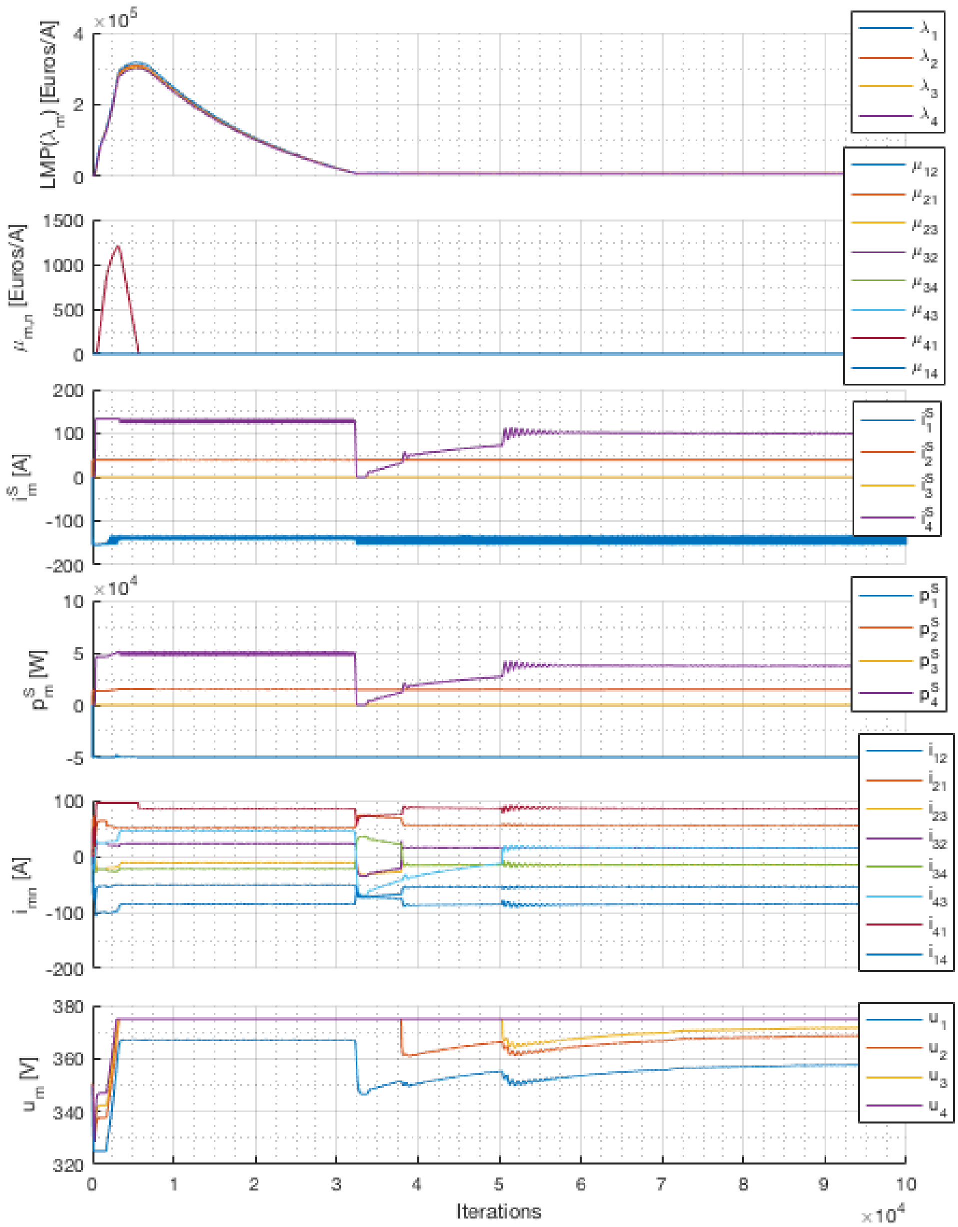

Figure 6.5: **CASE 2** - Graph 1: LMP(λ_m) vs Iterations, Graph 2: Congestion Dual Variable ($\mu_{m,n}$) vs Iterations, Graph 3: Nodal Current (i^S_m) vs Iterations, Graph 4: Power Generated (p^S_m) vs Iterations, Graph 5: Line Current ($i_{m,n}$) vs Iterations, Graph 6: Nodal Voltage (u_m) vs Iterations.

6.3. CASE 3: T SHAPED DC NETWORK

A T-shaped DC network is considered as one of the case studies to present a unique scenario with a single node physically connected to all the other nodes present in the system. The point of power transfer has to be through this particular node. The illustration of such a DC network is shown in Figure 6.6.

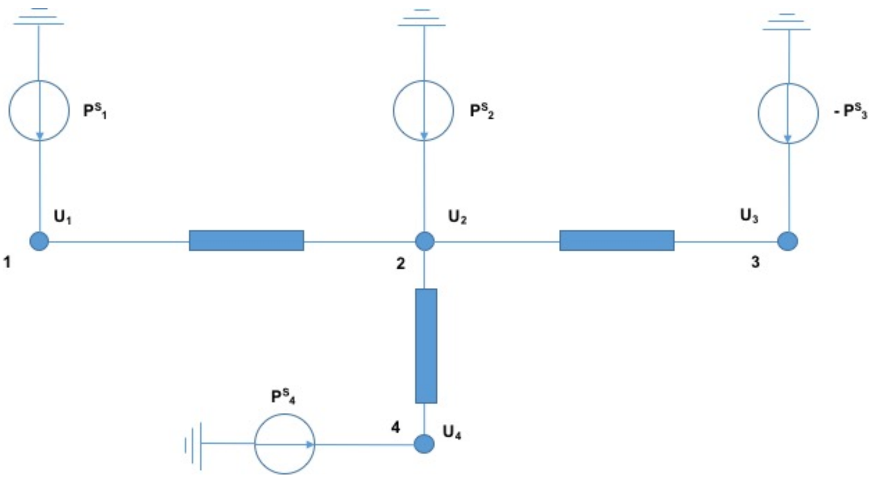

Figure 6.6: T shaped DC network of a 4 node system.

Node 2 is the common link for the nodes 1, 3 and 4. Each node is connected by a 150 m DC distribution cable. A fixed load of 15 kW is present at node 3. There is a PV system of maximum capacity 5 kW present at node 1. It is assumed that at the particular time period of running the algorithm, the PV system can deliver its maximum capacity when needed. Node 2 consists of a power generator of capacity 10 kW. The cost function of this generator is given by $20p_2^S$. Node 4 consists of a cheaper power generator given by a cost function of $10p_4^S$. The maximum generation capacity of this generator is 10 kW as well.

6.3.1. OUTPUT AND ANALYSIS

The output of the variables is shown in Table 6.4. As seen, the centralized solution is solved and compared with the distributed approach. None of the distribution lines are congested due to the current flow in the lines being lower than the allowable cable limit. Node 4 which consists of a cheaper power generator, runs at full capacity along with the zero marginal cost PV system. The total extracted power from node 1 and node 4 is equal to the load demand on node 3. But, due to distribution losses in the cables, the power generator at node 2 is triggered and supplies enough power to compensate the losses. This value is approximately 500 W. Node 4 operates on the maximum nodal voltage value of 375 V, thus minimizing the line losses in the system. When the values of the decision variables for the centralized and distributed approach are compared, the difference is minuscule. The slight difference can be attributed to the preciseness of the tuning parameters in the distributed approach, which decide the convergence of the system. Figure 6.7 shows the graphical output of the distributed approach. If seen closely, the slight fluctuations are due to the non-exactness of the tuning parameters. This non-exactness causes a minor difference in values when compared to the centralized solution.

The LMP values of the distributed approach make complete logical sense. The generators at node 1 and node 4 have been utilized to the full capacity to satisfy the load. The available power is only from the source at node 2 which is associated with a marginal cost of 20 Euros/W. This is reflected at the LMP value at node 2. By the general definition, LMP is the price associated with satisfying one unit of extra power as load at the same location. This extra unit of power for the considered scenario will come only from generator 2. Hence, the other nodes will have the same cost plus or minus the cost for power losses in the connecting lines.

The dual variables for maintaining the power limits of the generators converge to a stable solution as seen in the graph shown in Appendix B, Figure B.8. As it is observed, the dual variable for upper power limit at node 1 is zero due to its zero cost generator (PV). On the other hand, the dual variable value for the upper power limit for node 4 is approximately 92 EUR/W. This signifies that if the generator could supply power of 1 W more, the social welfare would increase by 92 Euros. Similarly, the nodal voltage magnitude at node 4 attains the maximum allowable voltage of 375 V. The upper voltage dual variable is triggered to maintain the nodal voltage within the bounds. The value it converges to is seen to be 344 EUR/W. An increase of voltage bound to 376 V would augment the social welfare by 344 Euros.

Based on the optimal power generation of the power generators to minimize the overall operational costs of the system, both the distributed and the centralized approach yield similar values. The optimal cost of operation is calculated and the values are 109,077 Euros for the distributed algorithm and 110,460 for the centralized approach. The difference is due to slight nodal voltage differences between the two algorithms which result in minor differences in line losses.

Table 6.4: Case 3: Nodal Variables

Method	**Node**	**Nodal Current, i_m^S [A]**	**Nodal Voltage, u_m [V]**	**Source Power, p_m^S [kW]**	**Max Source Capacity, P_{max} [kW]**	**Min Source Capacity, P_{min} [kW]**	**LMP, λ_m^I [Euros/A]**	**LMP, λ_m^P [Euros/W]**
Centralized OPF	1	13.43	372.35	5	5	0	7388	19.84
	2	1.42	369.67	0.53	10	0	7447	20.14
	3	-41.51	361.36	-15	-15	-15	7622	21.1
	4	26.67	375	10	10	0	7331	19.55
Distributed OPF	1	13.33	371.61	5	5	0	7385	19.87
	2	1.23	369	0.46	10	0	7384	20
	3	-42	360.63	-15	-15	-15	7550	21
	4	26.67	375	10	10	0	7217	19.25

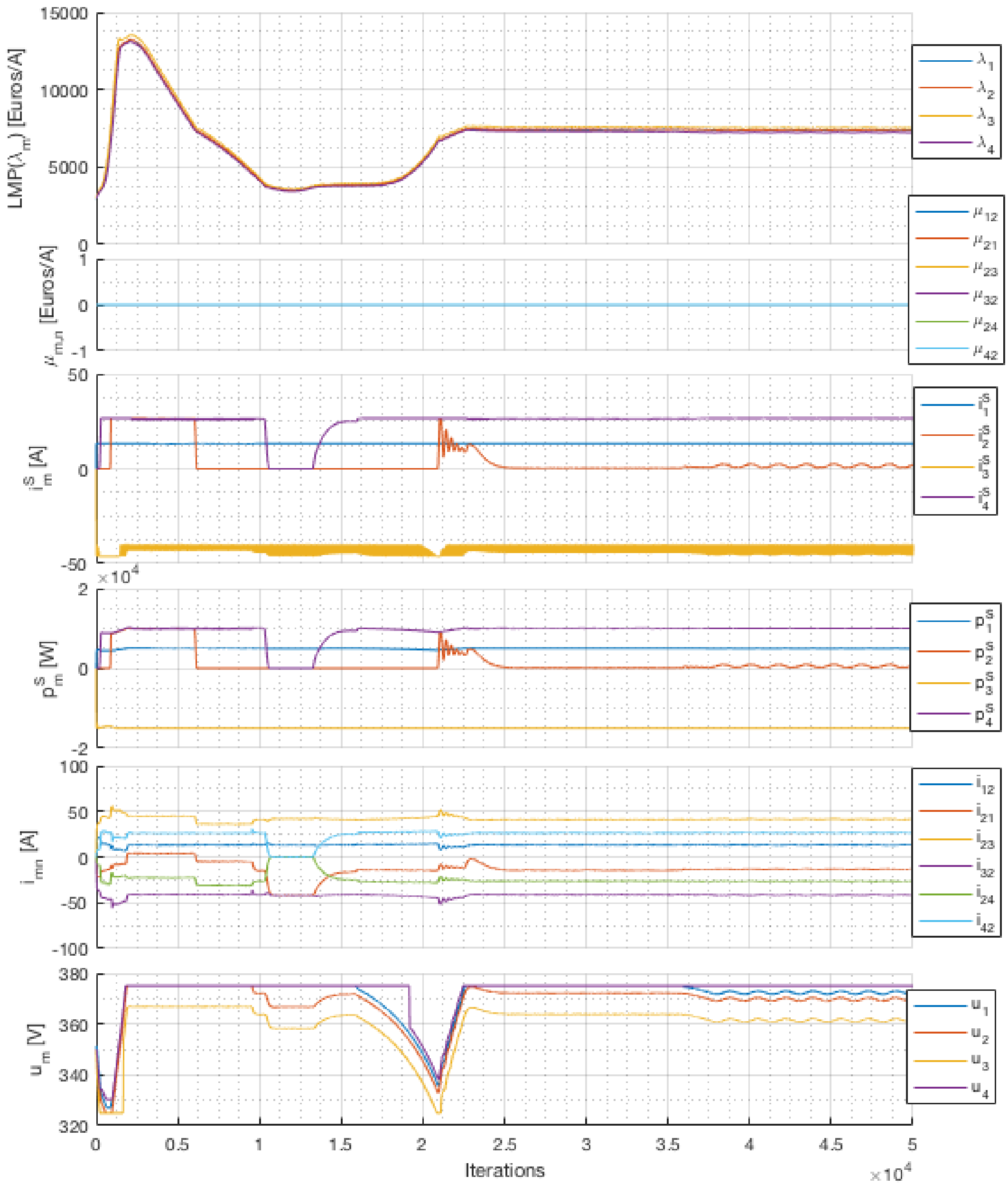

Figure 6.7: **CASE 3** - Graph 1: LMP(λ_m) vs Iterations, Graph 2: Congestion Dual Variable ($\mu_{m,n}$) vs Iterations, Graph 3: Nodal Current (i_m^S) vs Iterations, Graph 4: Power Generated (p_m^S) vs Iterations, Graph 5: Line Current ($i_{m,n}$) vs Iterations, Graph 6: Nodal Voltage (u_m) vs Iterations.

6.4. CASE 4: LONG DISTRIBUTION LINE DC NETWORK

In some cases for a DC microgrid, a power generator source or a load node can be present at a substantial distance from the other nodes of the system. The longer the distribution line, the higher is the resistance offered by the cable. This leads to lowered conductance values. For such scenarios, it is important that the distributed optimization algorithm functions correctly. A similar scenario is illustrated in Figure 6.8. A 4 node DC network is considered with a fixed load of 30 kW at node 3. Node 4 consists of a power source with a maximum capacity of 35 kW and denoted by a marginal cost of 45 EUR/W. Node 1 and 2 consists of other power sources with maximum power capacities of 20 kW and 8 kW respectively. The power generator at node 1 is relatively a cheaper generator as compared to the generator at node 4, and is denoted by a marginal cost of generation of 15 EUR/W. The power source at node 2 is a PV system associated with a zero marginal cost function. Node 2 and node 3 are connected by a long transmission cable, 19 kms in length. The length of distribution cables connecting node 1 and 2 and node 3 and 4 is 150 m each.

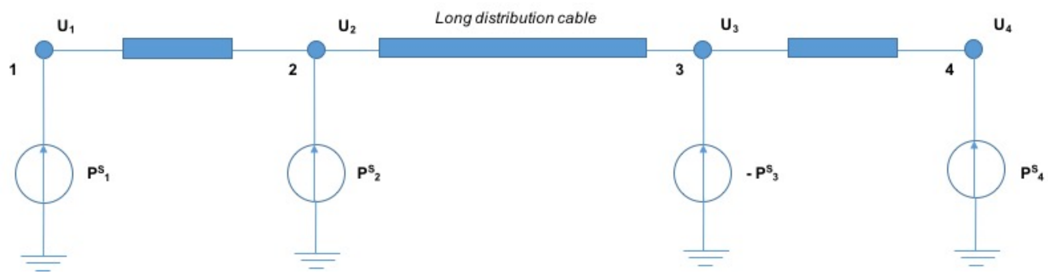

Figure 6.8: Long Distribution Line DC network of a 4 node system.

6.4.1. OUTPUT AND ANALYSIS

The allowable nodal voltage range considered for the DC system is 325 V to 375 V. The dual variables keep this limit in check. Hence, the maximum allowable voltage difference between two connected nodes is 50 V. The network consists of an 8 kW PV system at node 2, and the optimization algorithm will try to extract maximum power from such a zero marginal cost generator. Lets assume for an instance, the nodal voltage at the load attains the least allowable voltage magnitude of 325 V. Now, the current required to fulfill the load requirement would be $30,000/325 = 92.3A$. If this current had to be extracted from the PV source, the cable connecting node 2 and 3 would have a current flow of 92.3 A. Now, here is the limitation. The cable connecting node 2 and 3 is considered to be 19 kms long, which provides a conductance value of 0.05. Also, the allowable voltage difference is 50 V. This leads to a maximum current flow of 2.5 A in the cable. This allowable current flow is much much lower as compared to the required 92.3 A. Hence, the PV system can deliver only 2.5 A which results in a power generation of 937.5 W. Since, the cable connecting node 2 and 3 is the only medium of power transfer for the generator at node 1, the power produced at node 1 is zero. Therefore, the expensive generator at node 4 is summoned to satisfy the load requirements. Node 4 provides 30.72 kW of power. The allowable power production at node 2 is 0.94 kW. This results in a total power production of 31.7 kW. The fixed load requirement is 30 kW. The excess of 1.7 kW is lost as distribution losses in the DC network. This is shown in Table 6.5. The centralized and distributed approach yield nearly similar output values.

The converged values of the nodal variables and congestion dual variable is shown in Figure 6.9. As observed, the algorithm sets the allowable maximum and minimum voltage magnitudes simultaneously. Node 1 and 2 attain maximum voltage magnitude of 375 V, while node 3 attains the minimum allowable voltage value of 325 V. Node 4 attains a voltage value of 342.47 V. This is due to the required current from the source at node 4 to satisfy the load at node 3. Slight bumps of current flow from the source at node 2 is observed in the graph. This is due to the tuning parameters which cause minor fluctuations in the current update function. A solution to the mentioned fluctuations is to have optimal tuning parameters. The congestion dual variable is zero as none of the cables reach there maximum current flow limits.

The LMP values at node 1 and 2 are zero as expected. The PV system is capable to provide load increments at nodes 1 and 2. Due to its zero marginal cost, the LMP at these nodes becomes zero. The LMP at node 4 is the marginal cost of the generator at node 4. Due to the voltage difference restriction between node 2 and 3, any load increment on node 4 needs to be satisfied with the local source. Thus, node 4 attains an LMP value of 45 EUR/W. The nodal LMP at node 3 is observed to be 50 EUR/W. This is slightly higher than the LMP at node 4 due to to the addition of marginal cost of line losses between node 3 and 4. The LMP values are reflected in Table 6.5.

The dual variables responsible to maintain the power and voltage constraints of the system are shown as converged values in Appendix B, Figure B.11. Node 1 and 2 work on maximum allowable voltage magnitude, thus triggering the upper voltage limit dual variables. The associated values for these variables at node 1 and 2 is 580.6 EUR/V and 235 EUR/V respectively. This signifies that a single increment of 1 V at the two nodes would increase the social welfare by 580 EUR and 235 EUR respectively. None of the power generators function on their individual maximum capacities, thus not triggering the upper power limit dual variables. Therefore, these variables for the nodes 1,2 and 4 attain zero values.

Finally, based on the power generated by the sources present in the system, the optimal operational cost of the system for a single time period is 1,382,400 Euros.

Table 6.5: Case 4: Nodal Variables

Method	**Node**	**Nodal Current,** i_m^S **[A]**	**Nodal Voltage,** u_m **[V]**	**Source Power,** p_m^S **[kW]**	**Max Source Capacity,** P_{max} **[kW]**	**Min Source Capacity,** P_{min} **[kW]**	**LMP,** λ_m^I **[Euros/A]**	**LMP,** λ_m^P **[Euros/W]**
Centralized OPF	1	0	375	0	20	0	0	0
	2	2.5	375	0.94	8	0	0	0
	3	-92.3	325	-30	-30	-30	16242	50
	4	89.8	342.96	30.8	35	0	15433	45
Distributed OPF	1	0	375	0	20	0	0	0
	2	2.5	375	0.94	8	0	0	0
	3	-92.21	325	-30	-30	-30	16227	50
	4	89.71	342.47	30.72	35	0	15443	45

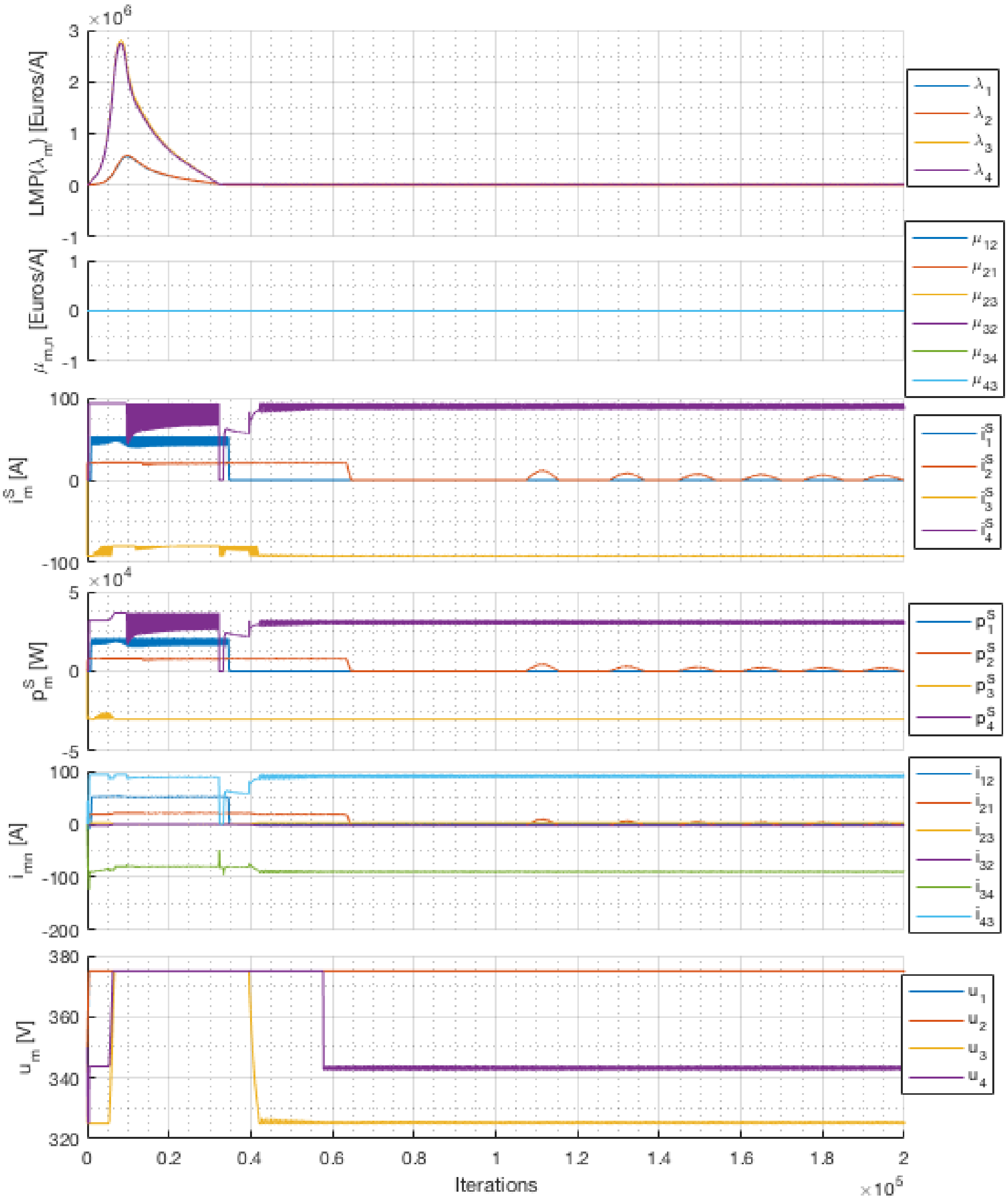

Figure 6.9: **CASE 4** - Graph 1: LMP(λ_m) vs Iterations, Graph 2: Congestion Dual Variable ($\mu_{m,n}$) vs Iterations, Graph 3: Nodal Current (i_m^S) vs Iterations, Graph 4: Power Generated (p_m^S) vs Iterations, Graph 5: Line Current ($i_{m,n}$) vs Iterations, Graph 6: Nodal Voltage (u_m) vs Iterations.

7

Conclusion and Future Scope

7.1. Conclusion

The Exact DC OPF model developed throughout this thesis is an innovative and novel approach to perform distributed optimization within a DC distribution system. The model is built upon the Consensus and Innovations approach and helps to achieve optimal solutions while considering congestion and network line losses. Earlier research available in literature dealt with an approximated DC OPF model for an AC distributed system. Also, the research did not consider losses in the distribution lines. This violates how a practical power grid would function, as transmission and distribution cables in general encounter power losses.

> *How can distributed optimization be implemented in a DC distribution system to account for losses and congestion in the network?*

Considering the limitations of past research, the model developed for this study presented a distributed OPF algorithm which can be implemented in DC distribution systems while taking into consideration network congestion and line losses. The algorithm developed is a non complex procedure of update equations for the various primal and dual variables of the DC system. The only exchange of information between physically connected nodes were the nodal voltage magnitudes and the LMP values. This limited exchange of information between nodes in a DC network justifies the distributed nature of the developed algorithm. Moreover, the developed model considered network practicalities like line losses and thus, was able to obtain a more exact solution as compared to a model which did not consider network losses.

Chapter 5 presented the Exact DC OPF model which was further implemented in a simple three node DC network to study the functioning of the developed model. The model was able to function with the congestion limits provided and also took into account the power lost in distribution cables. Furthermore, the results were compared to the solution obtained from a centralized OPF algorithm. This helped to compare the output and test the effectiveness of the model. Minimal mismatch of output values between the two approaches proved the proper functioning of the distributed OPF algorithm. The minor mismatches in the solution obtained for the distributed approach can be attributed to the tuning of the tuning parameters. Tuning parameters in the update equations play a major role in achieving a fast and stable convergence. This requires efficient tuning of these parameters to curtail any fluctuations in convergence. For this study, the tuning parameters were solely tuned based on empirical analysis by running multiple simulations to check for better fit. They do not reflect the optimal values which can lead to a better convergence rate with high level stability.

> *How can linear cost functions of power generators and zero marginal cost power generators be accounted for?*

The approximated DC OPF model only considered quadratic cost functions of power generators to achieve distributed optimization. This resulted in limitations for using power generators with linear cost functions, for e.g. Fuel Cells [34]. This particular limitation was rectified in the study by modifying the update equation for the current flow from the generators. The rectified update equations were presented in Chapter 5. The simple three node case was then shown for a network consisting of linear cost function power generators. The algorithm managed to obtain a converged solution for the decision variables of the system. The tuning parameter used in the current flow update was calculated using empirical analysis and the value varied for the different network cases considered.

The Exact DC OPF algorithm to achieve distributed optimization in a DC network was implemented on various network scenarios and presented as case studies in Chapter 6. Due to the increase in renewable energy systems like PV and wind, it was imperative to study the functioning of the model with such power sources. As mentioned earlier, such sources have zero marginal costs associated with them as they do not consume any fuel. The only cost applicable is the maintenance cost which can be neglected. In order to test such zero marginal cost generators, Case 1 in Chapter 6 was considered. The algorithm obtained a stable convergence of the nodal variables. The nodal LMP values were decided based on the marginal generator and the algorithm managed to consider marginal losses in the line network.

A vital point of concern for the algorithm while considering zero marginal price generators was when a DC system had surplus renewable energy generation even after supplying power to the load requirement. This would result in zero LMP values at all the nodes, as long as the connecting cables were not congestion. Other dual variables for power and voltage limits would attain zero values as well. The distributed algorithm in this case could not simultaneously achieve zero values for all the dual variables in the system due to the complexities involved. All the dual variables associated with the system updates have to simultaneously attain a zero value. The algorithm does not achieve this due to the fact that one zero valued dual variable triggers another dual variable to take a positive value. This can be attributed to the inefficiency in tuning the tuning parameters of the updates. They need special simulations to take into account the interdependent coupling of the updates.

How can voltage limits be satisfied without the use of a slack bus?

The distributed optimization technique developed for this study used dual variables to maintain the power limits of the generators as well as maintain the allowable voltage limits within boundaries. For the case studies presented in Chapter 6, the nodal voltage was constrained within the range of 325 and 375 V. For general centralized optimization techniques, this constraint limit is maintained by using a hard bound constraint within the optimization problem which simply restricts the nodal voltages to cross the boundary limits. The DC OPF methods presented in past research papers [6] made use of slack buses to oblige to the voltage boundaries. Such slack buses are specified with the upper limit voltage value which in turn keep the system within the bound limit. As for this thesis, the dual variables are solely responsible to maintain the voltage constraints. For minimizing the network losses in the system, the distributed optimization algorithm drives atleast one of the nodal voltage values in the DC system to a maximum (375 V for the cases considered). In the Case 4 shown in Chapter 6, the approach simultaneously yields upper and lower voltage values for nodes separated by a long cable. This demonstrates the proper functioning of the distributed algorithm to retain voltage limits without using a slack bus.

What are the effects of the distributed algorithm on meshed power grids?

Meshed grids can prove to be a tricky scenario for optimization algorithms. To test the effective functioning of the developed distributed OPF in a meshed DC grid, Case 2 in Chapter 6 was considered. The optimal solution of the decision variables converged to a stable solution. The results were compared with the output from the centralized solution. The current flow deviations were within 1 percent, while the voltage deviations were within 0.5 percent. Nodal LMP deviations were observed to be well within 1 percent. Such minor deviations prove the effectiveness of the developed distributed model.

Due to the meshed nature of the power grid, back current flows were observed at certain node points. This was simply due to nodal voltage differences between connected lines which caused current to flow. These back currents did not harm the final optimal solution. A potential solution to back currents could be the use of a slack bus. The slack bus can be specified with a similar voltage value as the node of the source current. This would help to mitigate current flows and prevent back currents.

A paramount conclusion from the distributed algorithm using the Consensus and Innovations approach is the high sensitivity of the tuning parameters used in the variable updates. Every case requires specific tuned values of tuning parameters. To arrive at an optimal tuning value can prove difficult while using empirical analysis. Also, high conductance values of cables affect the convergence properties of the decision variables. This is due to the manner in which the iterative updates take place. A high conductance value could cause high jumps in an iterative value, therefore leading to fluctuations and instability.

7.2. FUTURE SCOPE

Based on some of the flaws mentioned in the earlier section, the distributed algorithm requires further research and opens opportunities for fostering more innovative findings. The most critical aspect is the set optimal values for the tuning parameters. The tuning parameters can be tuned in a better fashion to achieve better convergence properties. Regression analysis, by using the Least Square method for goodness of fit could be a potential solution to tune the parameters.

Consideration of asynchronous updates for the C+I algorithm could prove beneficial. Using intra as well as inter-area communications in the optimization framework could be a start. The intra-area communication exchange represents the exchange of information between buses in the same area (within a micorgrid) which takes place after each iteration of variable update. The inter-area communication can be used for neighbouring microgrids where exchange of information occurs every few iterations. This will augment the convergence rate and reduce computation time for the OPF solution. Mohammadi et al. presents a solution in his paper [75] for such a modification, but it deals with an approximated DC OPF problem. The solution is valid for a lossless power network which in practicality never exists.

The Exact DC OPF approach presented in this thesis is a single time period (E.g. 15 minutes or one hour) scheduling problem. However, a day-ahead unit commitment can be incorporated using integer variables. This is usually used in electricity markets to schedule the system. This is a natural extension to the presented code and will help in the planning processes of energy markets. Adding other functions such as demand response to specify a cost function for loads could help in demand side management.

A

Appendix A

A.1. Exact DC OPF

A.1.1. Problem Formulation

Objective

$$\min \sum_{m\in\mathcal{N}} \sum_{s\in\mathscr{S}} A_m (p_m^{\mathrm{S}})^2 + B_m p_m^{\mathrm{S}} + C_m \tag{A.1}$$

$$\min \sum_{m\in\mathcal{N}} \sum_{s\in\mathscr{S}} A_m (i_m^{\mathrm{S}})^2 u_m^2 + B_m i_m^{\mathrm{S}} u_m + C_m \tag{A.2}$$

Subject to

$$\sum i_m^{\mathrm{S}} = \sum G_{m,n}(u_m - u_n) \qquad \forall (m,n) \in \mathcal{N} \tag{A.3}$$

$$-\overline{I}_{m,n} \leq G_{m,n}(u_m - u_n) \leq \overline{I}_{m,n} \qquad \forall (m,n) \in \mathcal{N} \tag{A.4}$$

$$\underline{P}_m^{\mathrm{S}} \leq p_m^{\mathrm{S}} \leq \overline{P}_m^{\mathrm{S}} \qquad \forall s \in \mathscr{S} \tag{A.5}$$

$$\underline{P}_m^{\mathrm{S}} \leq i_m^{\mathrm{S}} u_m \leq \overline{P}_m^{\mathrm{S}} \qquad \forall s \in \mathscr{S} \tag{A.6}$$

$$\underline{U}_m \leq u_m \leq \overline{U}_m \qquad \forall m \in \mathcal{N} \tag{A.7}$$

A.1.2. Lagrangian Function

$$\begin{aligned}
\mathscr{L} = &\Big(\sum_{m\in\mathcal{N}} \sum_{s\in\mathscr{S}} A_m (i_m^{\mathrm{S}})^2 u_m^2 + B_m i_m^{\mathrm{S}} u_m + C_m\Big) \\
&+ \Big(\sum \lambda_m \big(\sum G_{m,n}(u_m - u_n) - \sum i_m^{\mathrm{S}}\big)\Big) \\
&+ \Big(\sum \mu_{m,n}\big(G_{m,n}(u_m - u_n) - \overline{I}_{m,n}\big)\Big) \\
&+ \Big(\sum \mu_{n,m}\big(-G_{m,n}(u_m - u_n) - \overline{I}_{m,n}\big)\Big) \\
&+ \Big(\sum \mu_m^{\overline{P}}\big(i_m^{\mathrm{S}} u_m - \overline{P}_m^{\mathrm{S}}\big) \\
&+ \sum \mu_m^{\underline{P}}\big(-i_m^{\mathrm{S}} u_m + \underline{P}_m^{\mathrm{S}}\big)\Big) \\
&+ \Big(\sum \mu_m^{\overline{U}}\big(u_m - \overline{U}_m\big) \\
&+ \Big(\sum \mu_m^{\underline{U}}\big(-u_m + \underline{U}_m\big)
\end{aligned} \tag{A.8}$$

First order optimality conditions

$$\frac{\partial L}{\partial i^{\mathrm{S}}_m} = \sum_{s\in\mathscr{S}} 2A_m u_m^2 i^{\mathrm{S}}_m + B_m u_m - \lambda_m + u_m(\mu^{\overline{P}}_m - \mu^{\underline{P}}_m) = 0 \tag{A.9}$$

$$\frac{\partial L}{\partial u_m} = \sum_{s\in\mathscr{S}} 2A_m (i^{\mathrm{S}}_m)^2 u_m + B_m i^{\mathrm{S}}_m + \lambda_m \sum G_{m,n} - \sum \lambda_n G_{m,n} + \sum G_{m,n}(\mu_{m,n} - \mu_{n,m}) + i^{\mathrm{S}}_m(\mu^{\overline{P}}_m - \mu^{\underline{P}}_m) + \mu^{\overline{U}}_m - \mu^{\underline{U}}_m = 0 \tag{A.10}$$

$$\frac{\partial L}{\partial \lambda_m} = -\sum i^{\mathrm{S}}_m + \sum G_{m,n}(u_m - u_n) = 0 \tag{A.11}$$

$$\frac{\partial L}{\partial \mu_{m,n}} = \sum G_{m,n}(u_m - u_n) - \overline{I}_{m,n} \le 0 \tag{A.12}$$

$$\frac{\partial L}{\partial \mu_{n,m}} = -\sum G_{m,n}(u_m - u_n) - \overline{I}_{m,n} \le 0 \tag{A.13}$$

$$\frac{\partial L}{\partial \mu^{\overline{P}}_m} = i^{\mathrm{S}}_m u_m - \overline{P}^{\mathrm{S}}_m \le 0 \tag{A.14}$$

$$\frac{\partial L}{\partial \mu^{\underline{P}}_m} = -i^{\mathrm{S}}_m u_m + \underline{P}^{\mathrm{S}}_m \le 0 \tag{A.15}$$

$$\frac{\partial L}{\partial \mu^{\overline{U}}_m} = u_m - \overline{U}_m \le 0 \tag{A.16}$$

$$\frac{\partial L}{\partial \mu^{\underline{U}}_m} = -u_m + \underline{U}_m \le 0 \tag{A.17}$$

Complementary Slackness Conditions

$$\mu_{m,n}(\overline{I}_{m,n} - \sum G_{m,n}(u_m - u_n)) = 0 \tag{A.18}$$

$$\mu_{n,m}(-\overline{I}_{m,n} + \sum G_{m,n}(u_m - u_n)) = 0 \tag{A.19}$$

$$\mu^{\overline{P}}_m(\overline{P}^{\mathrm{S}}_m - i^{\mathrm{S}}_m u_m) = 0 \tag{A.20}$$

$$\mu^{\underline{P}}_m(i^{\mathrm{S}}_m u_m - \underline{P}^{\mathrm{S}}_m) = 0 \tag{A.21}$$

$$\mu^{\overline{U}}_m(\overline{U}_m - u_m) = 0 \tag{A.22}$$

$$\mu^{\underline{U}}_m(u_m - \underline{U}_m) = 0 \tag{A.23}$$

Positivity Conditions

$$\mu_{m,n}, \mu_{n,m}, \mu^{\overline{P}}_m, \mu^{\underline{P}}_m, \mu^{\overline{U}}_m, \mu^{\underline{U}}_m \ge 0 \tag{A.24}$$

A.1.3. VARIABLE ITERATIVE UPDATES

Locational Marginal Price Update

$$
\begin{aligned}
\lambda_m(l+1) &= \lambda_m(l) - \lambda_1(\frac{\partial L}{\partial u_m}) + \lambda_2(\frac{\partial L}{\partial \lambda_m}) && \text{(A.25)}\\
&= \lambda_m(l) - \lambda_1[\sum_{s\in\mathcal{S}} 2A_m(i^{\mathrm{S}}_m(l))^2 u_m(l) + B_m i^{\mathrm{S}}_m(l) && \text{(A.26)}\\
&+ \lambda_m(l)\sum G_{m,n} - \sum \lambda_n(l) G_{m,n}\\
&+ \sum G_{m,n}(\mu_{m,n}(l) - \mu_{n,m}(l))\\
&+ i^{\mathrm{S}}_m(l)(\mu^{\overline{P}}_m(l) - \mu^{\underline{P}}_m(l))\\
&+ \mu^{\overline{U}}_m(l) - \mu^{\underline{U}}_m(l)]\\
&+ \lambda_2[-\sum i^{\mathrm{S}}_m(l) + \sum G_{m,n}(u_m(l) - u_n(l))]
\end{aligned}
$$

Generator Current Update

$$
\begin{aligned}
i^{\mathrm{S}}_m(l+1) &= i^{\mathrm{S}}_m(l) - I_1\frac{\partial L}{\partial i^{\mathrm{S}}_m} && \text{(A.27)}\\
&= i^{\mathrm{S}}_m(l) - I_1[\sum_{s\in\mathcal{S}} 2A_m u^2_m(l) i^{\mathrm{S}}_m(l) && \text{(A.28)}\\
&+ B_m u_m(l) - \lambda_m(l) + u_m(l)(\mu^{\overline{P}}_m(l) - \mu^{\underline{P}}_m(l))]
\end{aligned}
$$

Nodal Voltage Update

$$
\begin{aligned}
u_m(l+1) &= u_m(l) - U_1\frac{\partial L}{\partial \lambda_m} && \text{(A.29)}\\
&= u_m(l) - U_1[-\sum i^{\mathrm{S}}_m(l) + \sum G_{m,n}(u_m(l) - u_n(l))] && \text{(A.30)}
\end{aligned}
$$

Line Congestion Update

$$
\begin{aligned}
\mu_{m,n}(l+1) &= \mathbb{P}[\mu_{m,n}(l) + \mu_1\frac{\partial L}{\partial \mu_{m,n}}] && \text{(A.31)}\\
&= \mathbb{P}[\mu_{m,n}(l) + \mu_1[G_{m,n}(u_m(l) - u_n(l)) - \overline{I}_{m,n}]] && \text{(A.32)}
\end{aligned}
$$

$$
\begin{aligned}
\mu_{n,m}(l+1) &= \mathbb{P}[\mu_{n,m}(l) + \mu_1\frac{\partial L}{\partial \mu_{n,m}}] && \text{(A.33)}\\
&= \mathbb{P}[\mu_{n,m}(l) + \mu_1[-G_{n,m}(u_m(l) - u_n(l)) - \overline{I}_{m,n}]] && \text{(A.34)}
\end{aligned}
$$

Power Limit Update

$$
\begin{aligned}
\mu^{\overline{P}}_m(l+1) &= \mu^{\overline{P}}_m(l) + \mu^{high}_P\frac{\partial L}{\partial \mu^{\overline{P}}_m} && \text{(A.35)}\\
&= \mu^{\overline{P}}_m(l) + \mu^{high}_P[i^{\mathrm{S}}_m(l) u_m(l) - \overline{P}^{\mathrm{S}}_m] && \text{(A.36)}
\end{aligned}
$$

$$
\begin{aligned}
\mu^{\underline{P}}_m(l+1) &= \mu^{\underline{P}}_m(l) + \mu^{low}_P\frac{\partial L}{\partial \mu^{\underline{P}}_m} && \text{(A.37)}\\
&= \mu^{\underline{P}}_m(l) + \mu^{low}_P[-i^{\mathrm{S}}_m(l) u_m(l) + \underline{P}^{\mathrm{S}}_m] && \text{(A.38)}
\end{aligned}
$$

Voltage Limit Update

$$\mu_m^{\overline{U}}(l+1) = \mu_m^{\overline{U}}(l) + \mu_U^{high} \frac{\partial L}{\partial \mu_m^{\overline{U}}} \tag{A.39}$$

$$= \mu_m^{\overline{U}}(l) + \mu_U^{high} [u_m(l) - \overline{U}_m] \tag{A.40}$$

$$\mu_m^{\underline{U}}(l+1) = \mu_m^{\underline{U}}(l) + \mu_U^{low} \frac{\partial L}{\partial \mu_m^{\overline{U}}} \tag{A.41}$$

$$= \mu_m^{\underline{U}}(l) + \mu_U^{low} [-u_m(l) + \underline{U}_m] \tag{A.42}$$

B

APPENDIX B

B.1. SUPPORTING GRAPHS FOR CASES: IMPLEMENTING THE EXACT DC OPF ALGORITHM

B.1.1. CASE 1: SINGLE LINE DC NETWORK

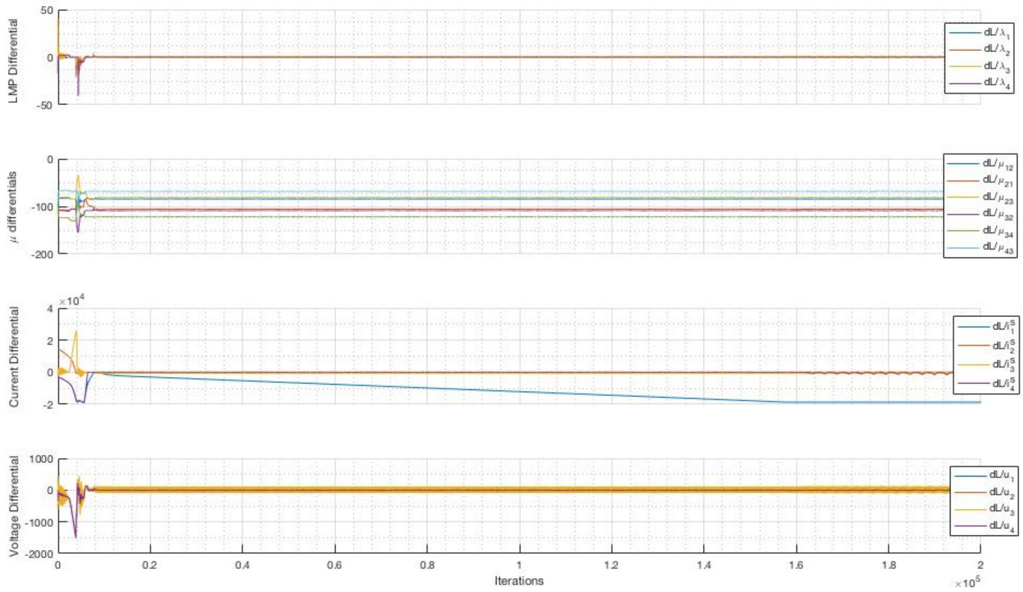

Figure B.1: Case 1: Variable Differentials Output

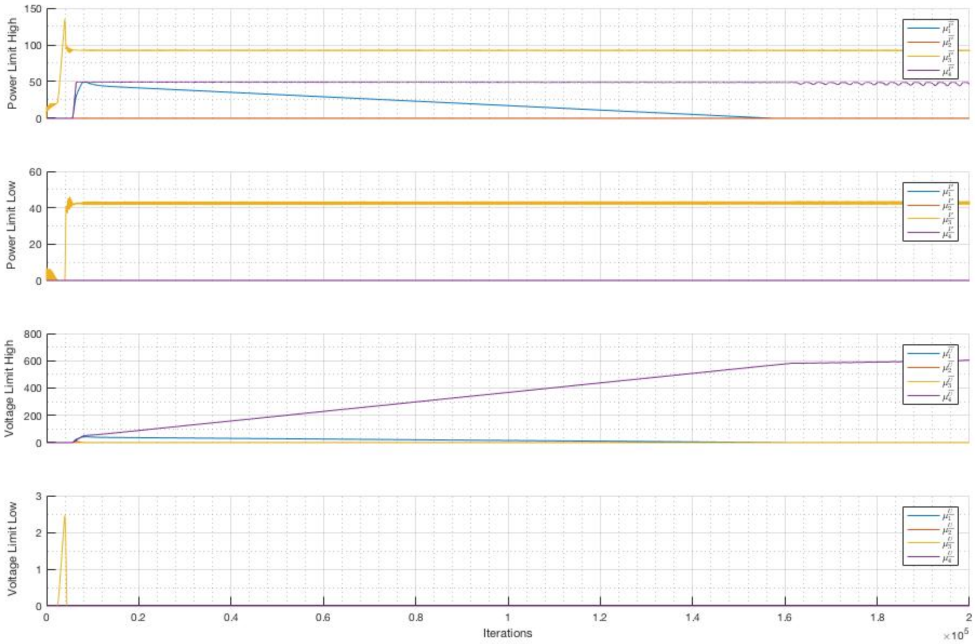

Figure B.2: Case 1: Dual Variables Output

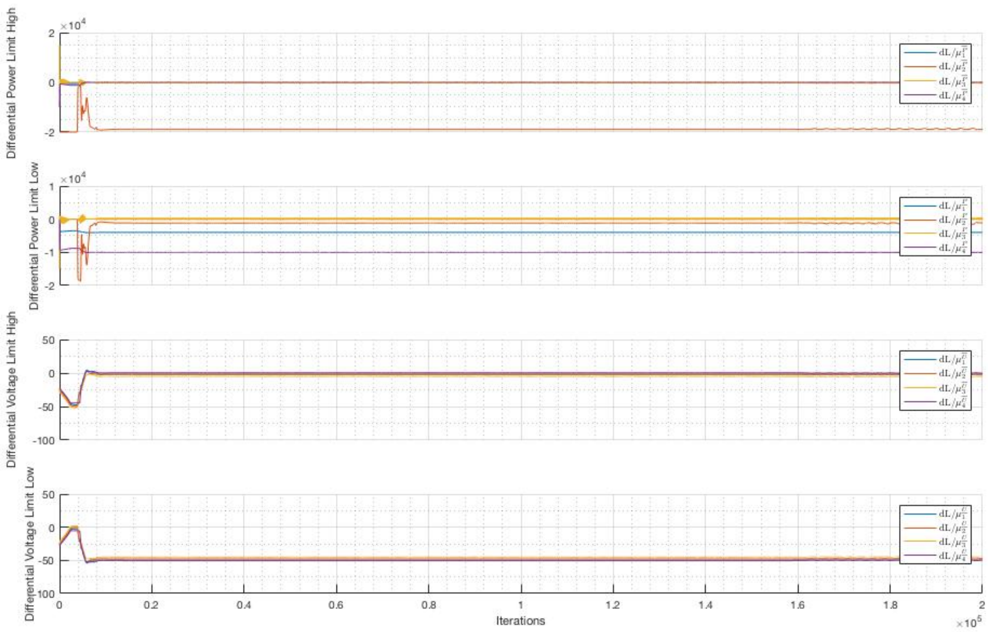

Figure B.3: Case 1: Differential of Dual Variables Output

B.1.2. CASE 2: MESHED DC NETWORK

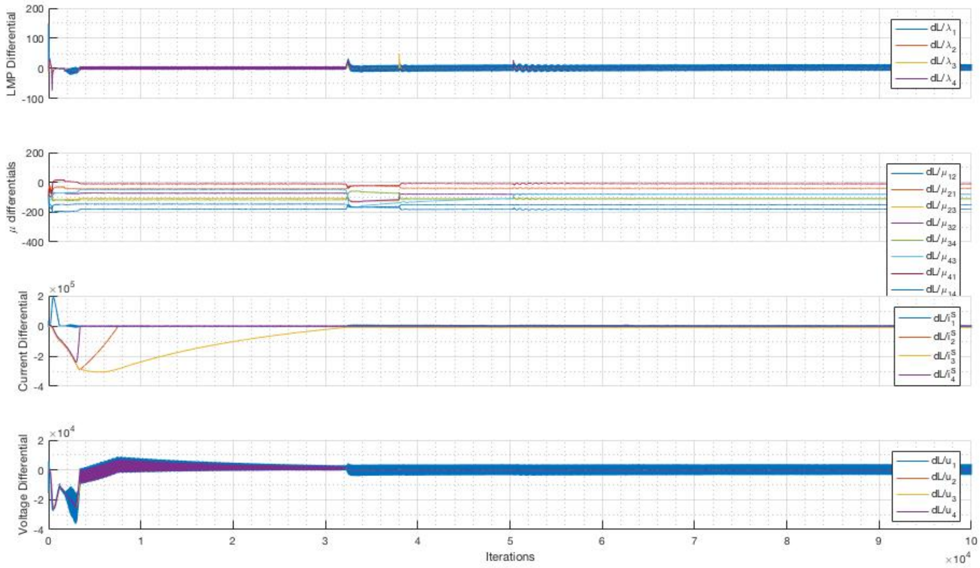

Figure B.4: Case 2: Variable Differentials Output

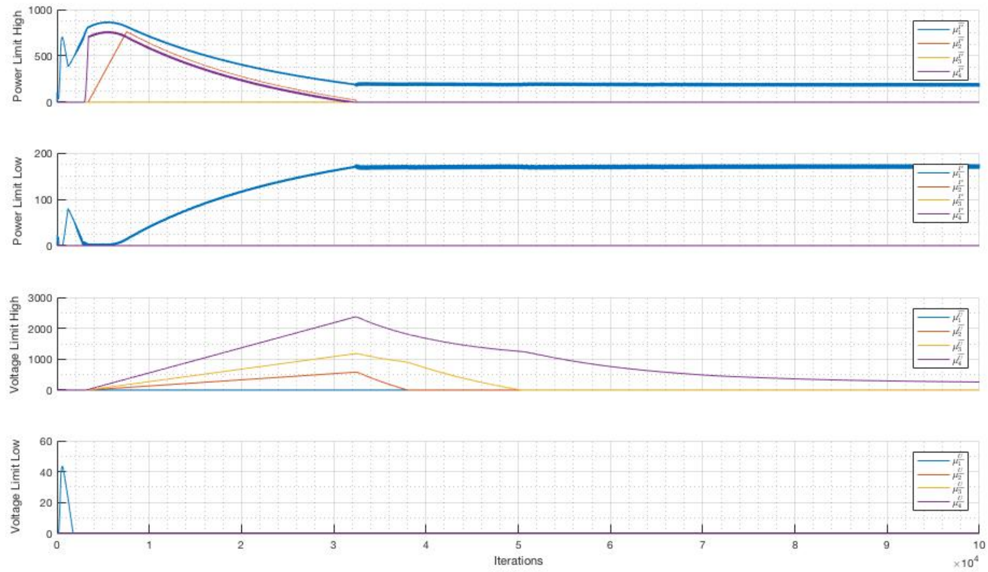

Figure B.5: Case 2: Dual Variables Output

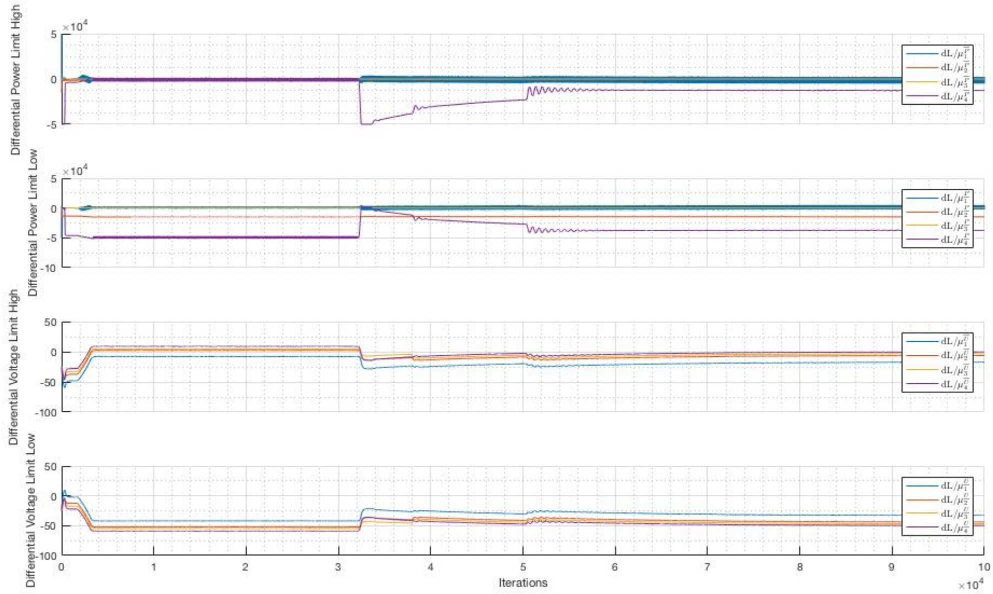

Figure B.6: Case 2: Differential of Dual Variables Output

B.1.3. CASE 3: T SHAPED DC NETWORK

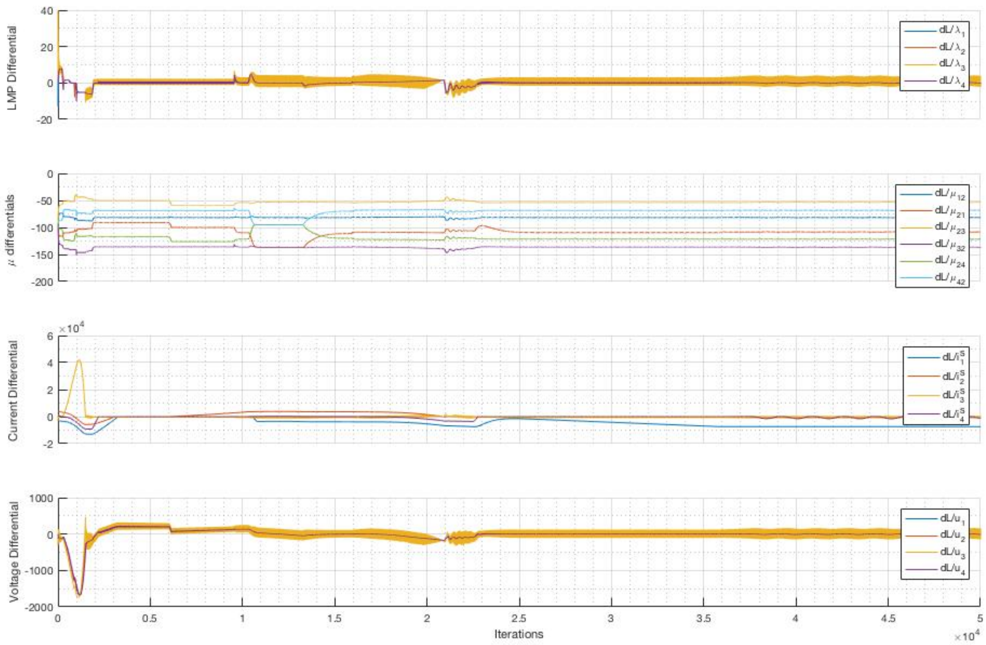

Figure B.7: Case 3: Variable Differentials Output

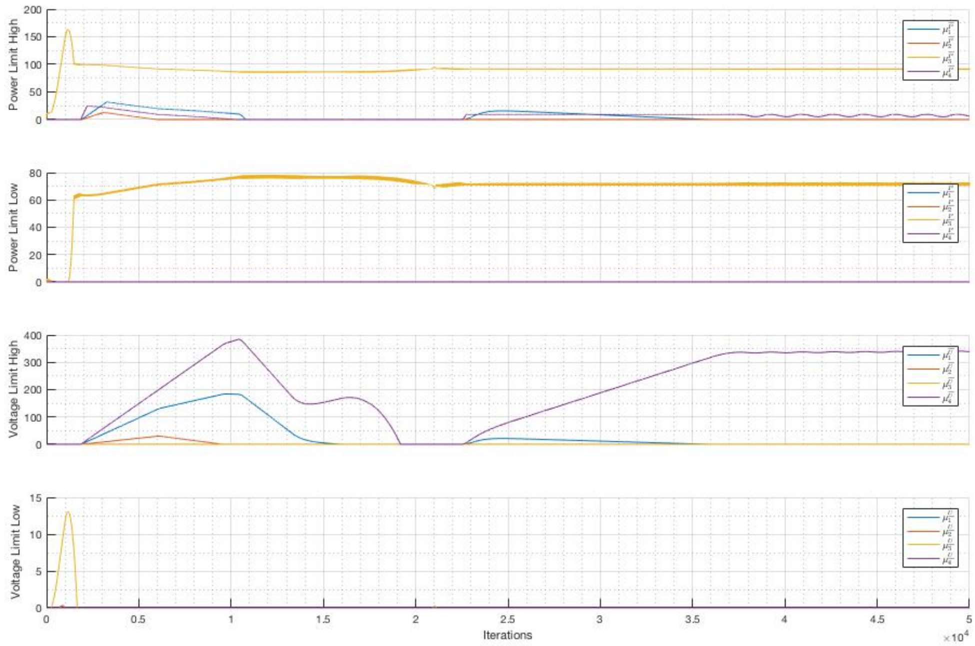

Figure B.8: Case 3: Dual Variables Output

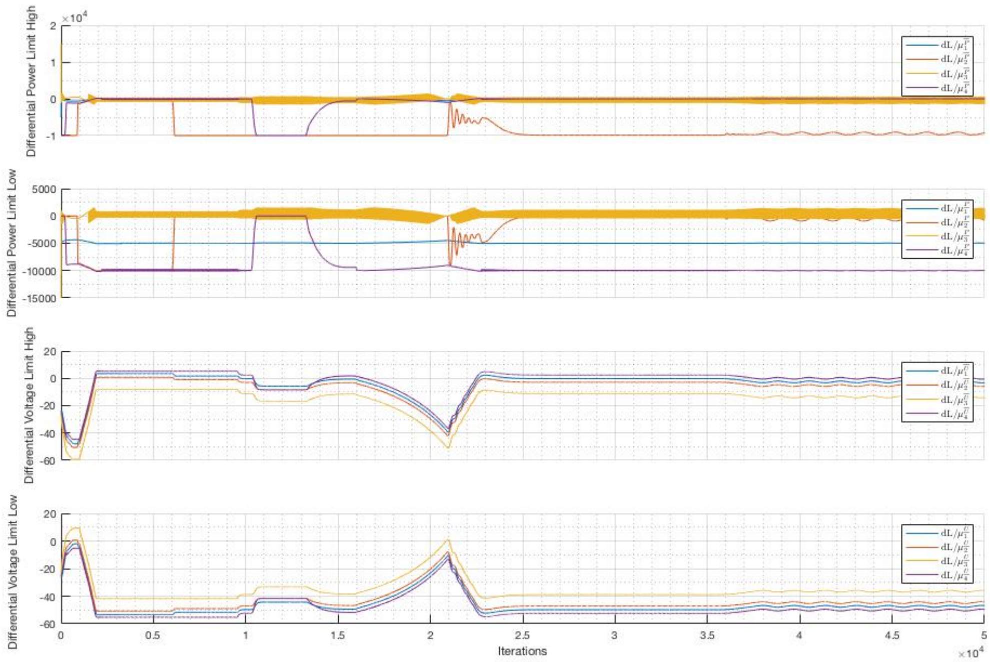

Figure B.9: Case 3: Differential of Dual Variables Output

B.1.4. CASE 4: LONG DISTRIBUTION LINE DC NETWORK

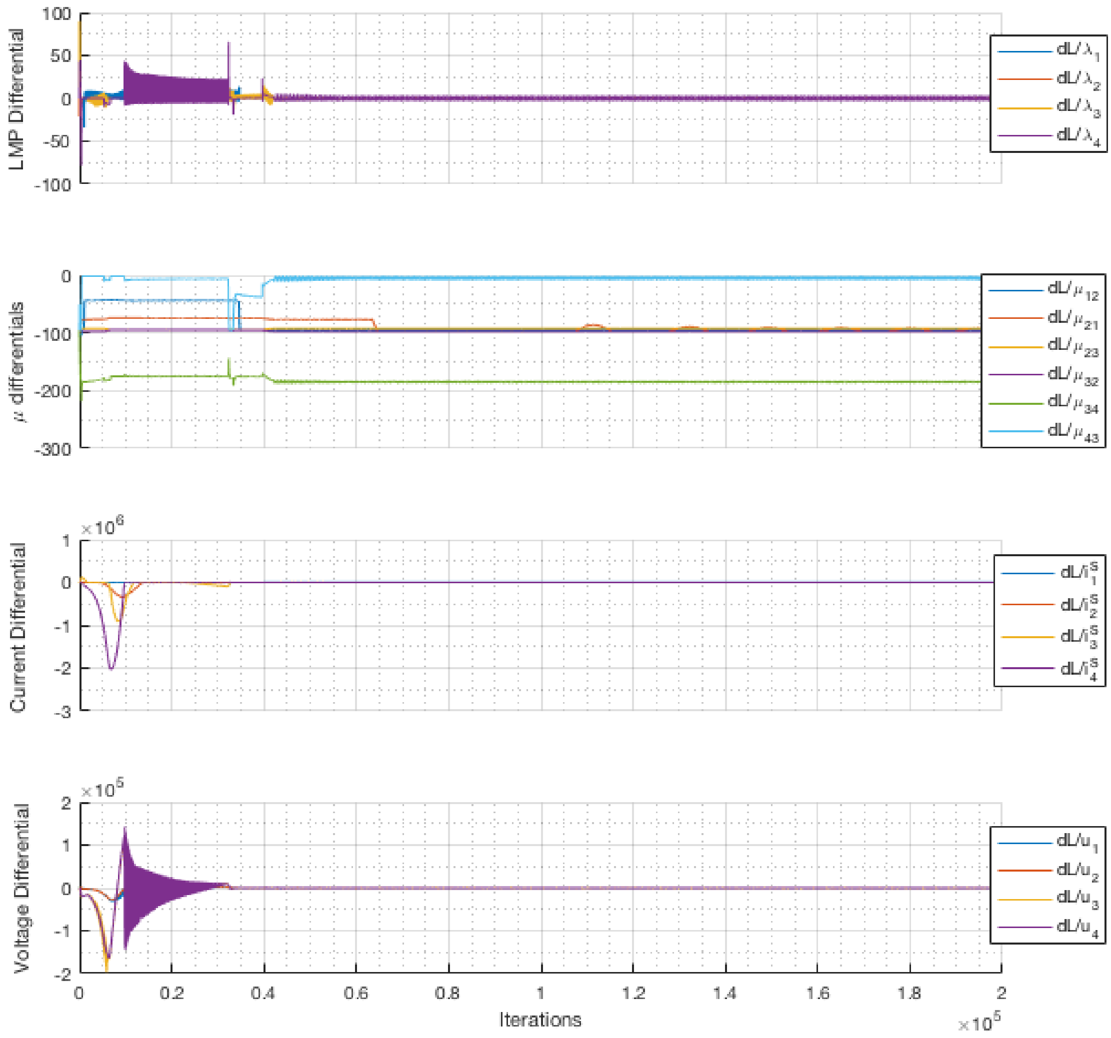

Figure B.10: Case 4: Variable Differentials Output

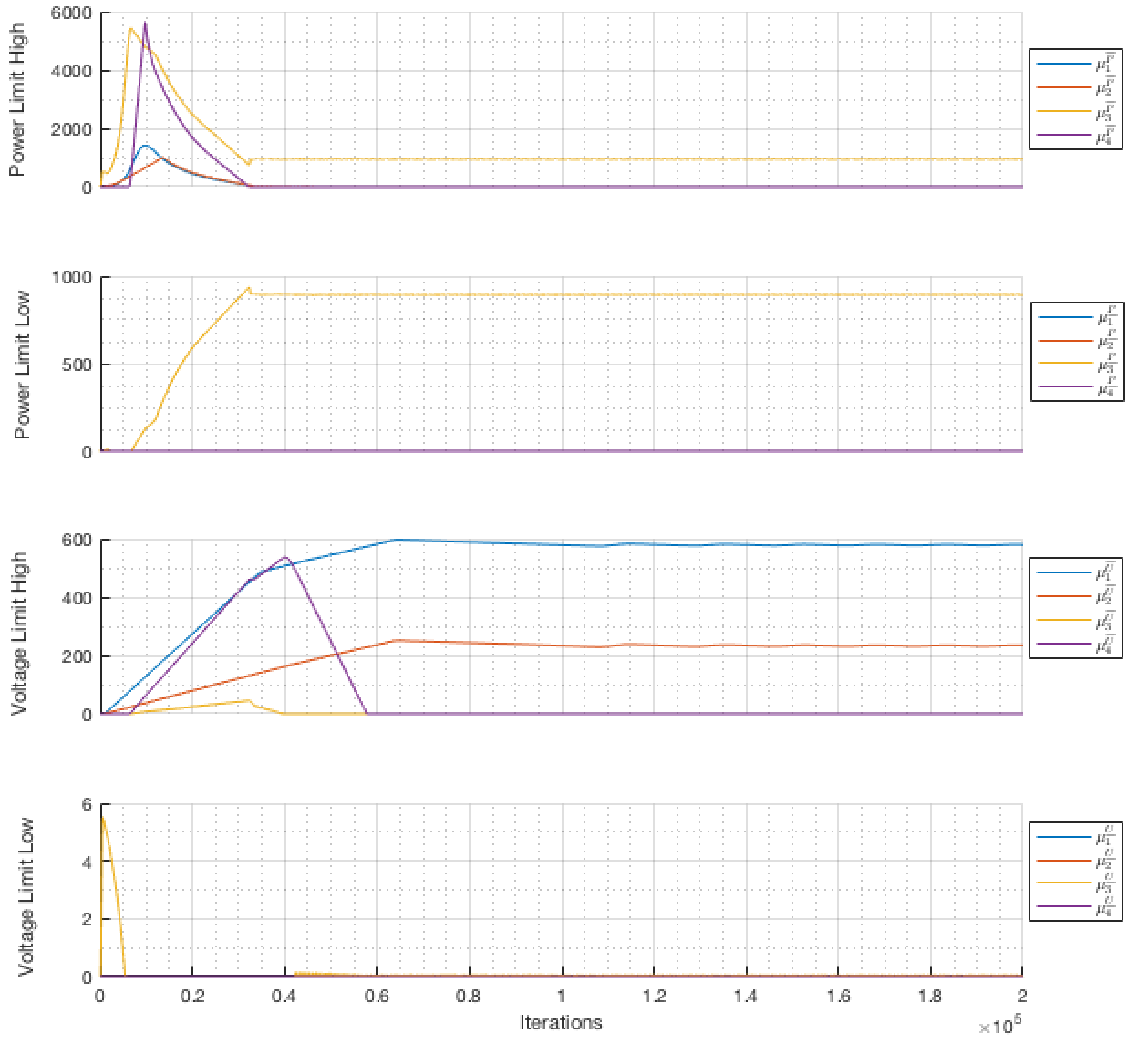

Figure B.11: Case 4: Dual Variables Output

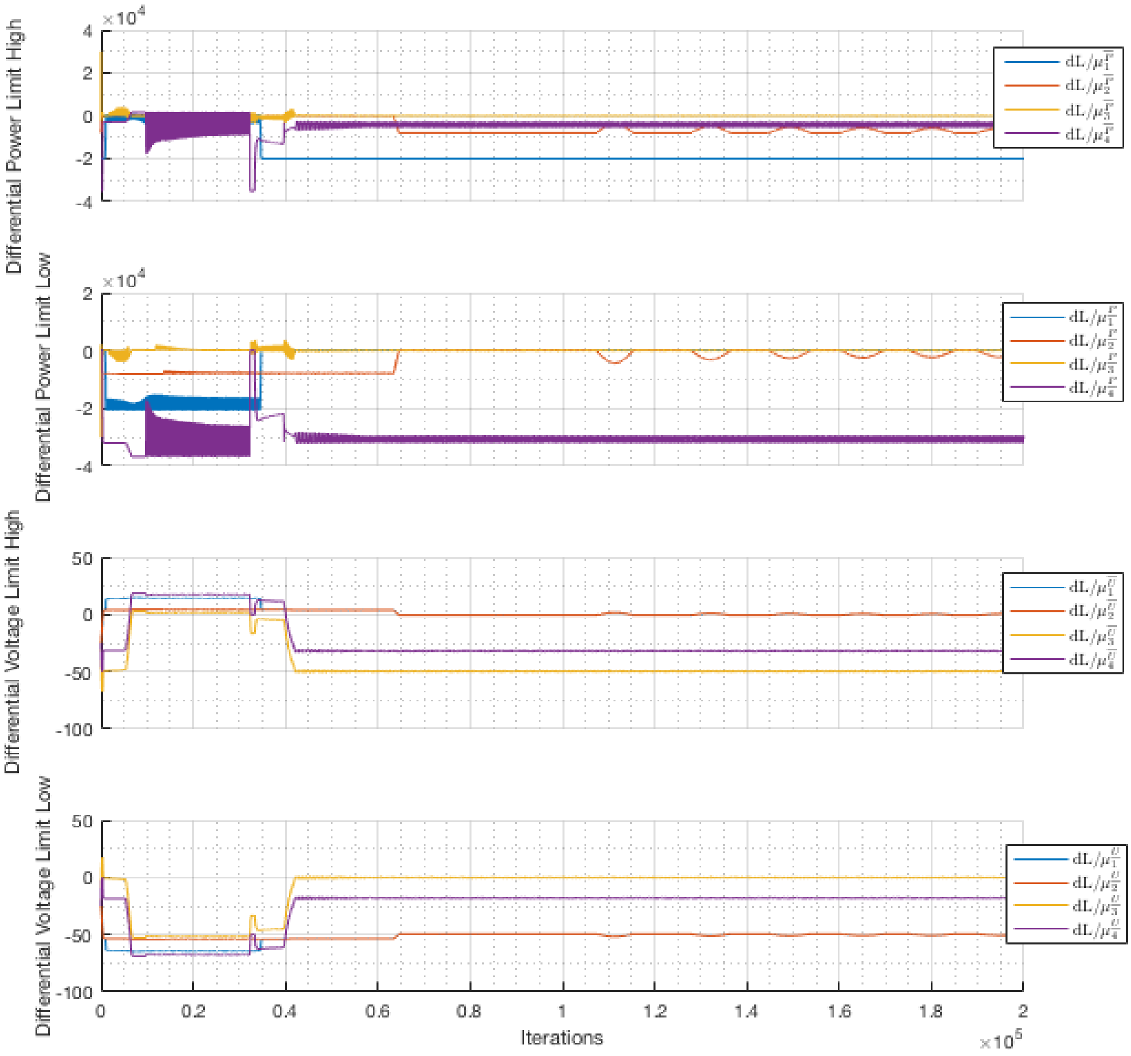

Figure B.12: Case 4: Differential of Dual Variables Output

C

Appendix C

C.1. Tuning Parameter Values used in Cases

C.1.1. Case 1: Single Line DC Network

Table C.1: Tuning Parameter Values for Case 1

Tuning Parameter	Empirical Value
λ_1	0.008
λ_2	0.1485
U_1	0.005
I_1	0.001
μ_1	0.05
μ_p^{high}	0.001
μ_p^{low}	0.001
μ_u^{high}	0.009
μ_u^{low}	0.001

C.1.2. Case 2: Meshed DC Network

Table C.2: Tuning Parameter Values for Case 2

Tuning Parameter	Empirical Value
λ_1	0.005
λ_2	0.1485
U_1	0.0035
I_1	0.001
μ_1	0.05
μ_p^{high}	0.002
μ_p^{low}	0.0005
μ_u^{high}	0.009
μ_u^{low}	0.02

C.1.3. CASE 3: T SHAPED DC NETWORK

Table C.3: Tuning Parameter Values for Case 3

Tuning Parameter	Empirical Value
λ_1	0.008
λ_2	0.1485
U_1	0.01
I_1	0.003
μ_1	0.01
μ_p^{high}	0.0005
μ_p^{low}	0.0005
μ_u^{high}	0.009
μ_u^{low}	0.002

C.1.4. CASE 4: LONG DISTRIBUTION LINE DC NETWORK

Table C.4: Tuning Parameter Values for Case 4

Tuning Parameter	Empirical Value
λ_1	0.0052
λ_2	0.1485
U_1	0.006
I_1	0.008
μ_1	0.03
μ_p^{high}	0.001
μ_p^{low}	0.0002
μ_u^{high}	0.001
μ_u^{low}	0.001

Bibliography

[1] J. J. Justo, F. Mwasilu, J. Lee, and J.-W. Jung, *Ac-microgrids versus dc-microgrids with distributed energy resources: A review,* Renewable and Sustainable Energy Reviews **24**, 387 (2013).

[2] R. Chauhan, B. Rajpurohit, S. Singh, and F. Gonzalez-Longatt, *Dc grid interconnection for conversion losses and cost optimization,* in *Renewable Energy Integration* (Springer, 2014) pp. 327–345.

[3] S. Tosserams, L. Etman, P. Papalambros, and J. Rooda, *An augmented lagrangian relaxation for analytical target cascading using the alternating direction method of multipliers,* Structural and multidisciplinary optimization **31**, 176 (2006).

[4] D. Hur, J.-K. Park, and B. H. Kim, *Evaluation of convergence rate in the auxiliary problem principle for distributed optimal power flow,* IEE Proceedings-Generation, Transmission and Distribution **149**, 525 (2002).

[5] A. Kargarian, J. Mohammadi, J. Guo, S. Chakrabarti, M. Barati, G. Hug, S. Kar, and R. Baldick, *Toward distributed/decentralized dc optimal power flow implementation in future electric power systems,* IEEE Transactions on Smart Grid (2016).

[6] J. Mohammadi, S. Kar, and G. Hug, *Distributed approach for dc optimal power flow calculations,* arXiv preprint arXiv:1410.4236 (2014).

[7] E. T. Commission, *Shaping energy transitions,* (2016).

[8] P. Droege, *Urban energy transition: from fossil fuels to renewable power* (Elsevier, 2011).

[9] D. Pudjianto, C. Ramsay, and G. Strbac, *Virtual power plant and system integration of distributed energy resources,* IET Renewable Power Generation **1**, 10 (2007).

[10] G. Allan, I. Eromenko, M. Gilmartin, I. Kockar, and P. McGregor, *The economics of distributed energy generation: A literature review,* Renewable and Sustainable Energy Reviews **42**, 543 (2015).

[11] K. Alanne and A. Saari, *Distributed energy generation and sustainable development,* Renewable and sustainable energy reviews **10**, 539 (2006).

[12] H. Jiayi, J. Chuanwen, and X. Rong, *A review on distributed energy resources and microgrid,* Renewable and Sustainable Energy Reviews **12**, 2472 (2008).

[13] R. Lasseter, A. Akhil, C. Marnay, J. Stevens, J. Dagle, R. Guttromson, S. A. Meliopoulous, R. Yinger, and J. Eto, *The certs microgrid concept, white paper on integration of distributed energy resources,* California Energy Commission, Office of Power Technologies-US Department of Energy, LBNL-50829, http://certs. lbl. gov (2002).

[14] S. Dubey, *Load generation balance report 2016-17,* (2016).

[15] K. Sun, L. Zhang, Y. Xing, and J. M. Guerrero, *A distributed control strategy based on dc bus signaling for modular photovoltaic generation systems with battery energy storage,* IEEE Transactions on Power Electronics **26**, 3032 (2011).

[16] J. Lago and M. L. Heldwein, *Operation and control-oriented modeling of a power converter for current balancing and stability improvement of dc active distribution networks,* IEEE Transactions on Power Electronics **26**, 877 (2011).

[17] R. Noroozian, M. Abedi, G. Gharehpetian, and S. Hosseini, *Combined operation of dc isolated distribution and pv systems for supplying unbalanced ac loads,* Renewable Energy **34**, 899 (2009).

[18] M. H. Rashid, *Power electronics handbook: devices, circuits and applications* (Academic press, 2010).

[19] A. Chakraborty, *Advancements in power electronics and drives in interface with growing renewable energy resources,* Renewable and Sustainable Energy Reviews **15**, 1816 (2011).

[20] L. Mackay, N. H. v. d. Blij, L. Ramirez-Elizondo, and P. Bauer, *Toward the universal dc distribution system,* Electric Power Components and Systems **45**, 1032 (2017).

[21] U. P. Group, *Universal serial bus revision 3.1 specification@ONLINE,* (2014).

[22] L. Mackay, L. Ramirez-Elizondo, and P. Bauer, *Dc ready devices-is redimensioning of the rectification components necessary?* in *Mechatronics-Mechatronika (ME), 2014 16th International Conference on* (IEEE, 2014) pp. 1–5.

[23] D. J. Becker and B. Sonnenberg, *Dc microgrids in buildings and data centers,* in *Telecommunications Energy Conference (INTELEC), 2011 IEEE 33rd International* (IEEE, 2011) pp. 1–7.

[24] A. A. Bazmi and G. Zahedi, *Sustainable energy systems: Role of optimization modeling techniques in power generation and supply—a review,* Renewable and sustainable energy reviews **15**, 3480 (2011).

[25] R. Banos, F. Manzano-Agugliaro, F. Montoya, C. Gil, A. Alcayde, and J. Gómez, *Optimization methods applied to renewable and sustainable energy: A review,* Renewable and Sustainable Energy Reviews **15**, 1753 (2011).

[26] Y. Cai, G. Huang, Z. Yang, Q. Lin, and Q. Tan, *Community-scale renewable energy systems planning under uncertainty—an interval chance-constrained programming approach,* Renewable and Sustainable Energy Reviews **13**, 721 (2009).

[27] J. Moreno, M. E. Ortúzar, and J. W. Dixon, *Energy-management system for a hybrid electric vehicle, using ultracapacitors and neural networks,* IEEE transactions on Industrial Electronics **53**, 614 (2006).

[28] F. J, *Locational marginal pricing,* In Power Engineering Society Winter Meeting **1**, 377 (2001).

[29] C. Unsihuay, J. M. Lima, and A. Z. De Souza, *Modeling the integrated natural gas and electricity optimal power flow,* in *Power Engineering Society General Meeting, 2007. IEEE* (IEEE, 2007) pp. 1–7.

[30] S. K. Mishra and S. K. Mishra, *A comparative study of solution of economic load dispatch problem in power systems in the environmental perspective,* Procedia Computer Science **48**, 96 (2015).

[31] H. W. Dommel and W. F. Tinney, *Optimal power flow solutions,* IEEE Transactions on power apparatus and systems , 1866 (1968).

[32] J. A. Momoh, R. Adapa, and M. El-Hawary, *A review of selected optimal power flow literature to 1993. i. nonlinear and quadratic programming approaches,* IEEE transactions on power systems **14**, 96 (1999).

[33] W.-T. Huang, K.-C. Yao, and C.-C. Wu, *Using the direct search method for optimal dispatch of distributed generation in a medium-voltage microgrid,* Energies **7**, 8355 (2014).

[34] M. G. Simoes, C. S. Uriarte, S. Chakraborty, and F. A. Farret, *Cost considerations on fuel cell renewable energy systems,* in *Industry Applications Conference, 2006. 41st IAS Annual Meeting. Conference Record of the 2006 IEEE,* Vol. 5 (IEEE, 2006) pp. 2169–2176.

[35] Z. Lukszo, *Lecture notes in engineering optimization and integrating renewables in electricity markets,* (2016).

[36] M. B. Nappu, A. Arief, and R. C. Bansal, *Transmission management for congested power system: A review of concepts, technical challenges and development of a new methodology,* Renewable and Sustainable Energy Reviews **38**, 572 (2014).

[37] R. E. Bohn, M. C. Caramanis, and F. C. Schweppe, *Optimal pricing in electrical networks over space and time,* The Rand Journal of Economics , 360 (1984).

[38] T. Orfanogianni and G. Gross, *A general formulation for lmp evaluation,* IEEE Transactions on Power Systems **22**, 1163 (2007).

[39] F. C. Schweppe, M. C. Caramanis, R. D. Tabors, and R. E. Bohn, *Spot pricing of electricity* (Springer Science & Business Media, 2013).

[40] E. Litvinov, *Design and operation of the locational marginal prices-based electricity markets,* IET generation, transmission & distribution **4**, 315 (2010).

[41] D. K. Molzahn, F. Dörfler, H. Sandberg, S. H. Low, S. Chakrabarti, R. Baldick, and J. Lavaei, *A survey of distributed optimization and control algorithms for electric power systems,* IEEE Transactions on Smart Grid (2017).

[42] F. M. Cleveland, *Cyber security issues for advanced metering infrasttructure (ami),* in *Power and Energy Society General Meeting-Conversion and Delivery of Electrical Energy in the 21st Century, 2008 IEEE* (IEEE, 2008) pp. 1–5.

[43] P. P. Varaiya, F. F. Wu, and J. W. Bialek, *Smart operation of smart grid: Risk-limiting dispatch,* Proceedings of the IEEE **99**, 40 (2011).

[44] C. Cecati, G. Mokryani, A. Piccolo, and P. Siano, *An overview on the smart grid concept,* in *IECON 2010-36th Annual Conference on IEEE Industrial Electronics Society* (IEEE, 2010) pp. 3322–3327.

[45] B. H. Kim and R. Baldick, *A comparison of distributed optimal power flow algorithms,* IEEE Transactions on Power Systems **15**, 599 (2000).

[46] J. Mohammadi, G. Hug, and S. Kar, *Fully distributed dc-opf approach for power flow control,* in *Power & Energy Society General Meeting, 2015 IEEE* (IEEE, 2015) pp. 1–5.

[47] S. Kar, G. Hug, J. Mohammadi, and J. M. Moura, *Distributed state estimation and energy management in smart grids: A consensus + innovations approach,* IEEE Journal of Selected Topics in Signal Processing **8**, 1022 (2014).

[48] A. J. Conejo, E. Castillo, R. Minguez, and R. Garcia-Bertrand, *Decomposition techniques in mathematical programming: engineering and science applications* (Springer Science & Business Media, 2006).

[49] S. Boyd, N. Parikh, E. Chu, B. Peleato, and J. Eckstein, *Distributed optimization and statistical learning via the alternating direction method of multipliers,* Foundations and Trends® in Machine Learning **3**, 1 (2011).

[50] T. Erseghe, *Distributed optimal power flow using admm,* IEEE transactions on power systems **29**, 2370 (2014).

[51] M. Ma, L. Fan, and Z. Miao, *Consensus admm and proximal admm for economic dispatch and ac opf with socp relaxation,* in *North American Power Symposium (NAPS), 2016* (IEEE, 2016) pp. 1–6.

[52] M. Kraning, E. Chu, J. Lavaei, S. Boyd, *et al.*, *Dynamic network energy management via proximal message passing,* Foundations and Trends® in Optimization **1**, 73 (2014).

[53] S. Chakrabarti, M. Kraning, E. Chu, R. Baldick, and S. Boyd, *Security constrained optimal power flow via proximal message passing,* in *Power Systems Conference (PSC), 2014 Clemson University* (IEEE, 2014) pp. 1–8.

[54] H. M. Kim, N. F. Michelena, P. Y. Papalambros, and T. Jiang, *Target cascading in optimal system design,* Journal of mechanical design **125**, 474 (2003).

[55] H. M. Kim, M. Kokkolaras, L. S. Louca, G. J. Delagrammatikas, N. F. Michelena, Z. S. Filipi, P. Y. Papalambros, J. L. Stein, and D. N. Assanis, *Target cascading in vehicle redesign: a class vi truck study,* International journal of vehicle design **29**, 199 (2002).

[56] S. Tosserams, *Analytical target cascading: convergence improvement by sub-problem post-optimality sensitivities*, Ph.D. thesis, MS thesis, Eindhoven University of Technology, Eindhoven, The Netherlands (2004).

[57] N. Tzevelekos, M. Kokkolaras, P. Y. Papalambros, M. F. Hulshof, L. Etman, and J. Rooda, *An empirical local convergence study of alternative coordination schemes in analytical target cascading,* in *World Congress of Structural and Multidisziplinary Optimization: 19/05/2003-23/05/2003* (Schönenfeld & Ziegler, 2003).

[58] J. J. Michalek and P. Y. Papalambros, *An efficient weighting update method to achieve acceptable consistency deviation in analytical target cascading,* Transactions of the ASME-R-Journal of Mechanical Design **127**, 206 (2005).

[59] D. P. Bertsekas, A. Nedi, A. E. Ozdaglar, *et al.*, *Convex analysis and optimization,* (2003).

[60] J. B. Lassiter, M. M. Wiecek, and K. R. Andrighetti, *Lagrangian coordination and analytical target cascading: solving atc-decomposed problems with lagrangian duality,* Optimization and Engineering **6**, 361 (2005).

[61] B. H. Kim and R. Baldick, *Coarse-grained distributed optimal power flow,* IEEE Transactions on Power Systems **12**, 932 (1997).

[62] R. Baldick, B. H. Kim, C. Chase, and Y. Luo, *A fast distributed implementation of optimal power flow,* IEEE Transactions on Power Systems **14**, 858 (1999).

[63] A. Ahmadi-Khatir, A. J. Conejo, and R. Cherkaoui, *Multi-area unit scheduling and reserve allocation under wind power uncertainty,* IEEE Transactions on Power Systems **29**, 1701 (2014).

[64] G. Cohen, *Auxiliary problem principle and decomposition of optimization problems,* Journal of optimization Theory and Applications **32**, 277 (1980).

[65] A. J. Conejo, F. J. Nogales, and F. J. Prieto, *A decomposition procedure based on approximate newton directions,* Mathematical programming **93**, 495 (2002).

[66] G. Hug-Glanzmann and G. Andersson, *Decentralized optimal power flow control for overlapping areas in power systems,* IEEE Transactions on Power Systems **24**, 327 (2009).

[67] F. J. Nogales, F. J. Prieto, and A. J. Conejo, *A decomposition methodology applied to the multi-area optimal power flow problem,* Annals of operations research **120**, 99 (2003).

[68] X. Lai, L. Xie, Q. Xia, H. Zhong, and C. Kang, *Decentralized multi-area economic dispatch via dynamic multiplier-based lagrangian relaxation,* IEEE Transactions on Power Systems **30**, 3225 (2015).

[69] K. Gokbayrak and C. G. Cassandras, *A hierarchical decomposition method for optimal control of hybrid systems,* in *Decision and Control, 2000. Proceedings of the 39th IEEE Conference on,* Vol. 2 (IEEE, 2000) pp. 1816–1821.

[70] G. Binetti, A. Davoudi, D. Naso, B. Turchiano, and F. L. Lewis, *A distributed auction-based algorithm for the nonconvex economic dispatch problem,* IEEE Transactions on Industrial Informatics **10**, 1124 (2014).

[71] Z. Zhang and M.-Y. Chow, *Convergence analysis of the incremental cost consensus algorithm under different communication network topologies in a smart grid,* IEEE Transactions on Power Systems **27**, 1761 (2012).

[72] S. Kar and G. Hug, *Distributed robust economic dispatch in power systems: A consensus+ innovations approach,* in *Power and Energy Society General Meeting, 2012 IEEE* (IEEE, 2012) pp. 1–8.

[73] S. Yang, S. Tan, and J.-X. Xu, *Consensus based approach for economic dispatch problem in a smart grid,* IEEE Transactions on Power Systems **28**, 4416 (2013).

[74] J. Mohammadi, G. Hug, and S. Kar, *Role of communication on the convergence rate of fully distributed dc optimal power flow,* in *Smart Grid Communications (SmartGridComm), 2014 IEEE International Conference on* (IEEE, 2014) pp. 43–48.

[75] J. Mohammadi, G. Hug, and S. Kar, *Asynchronous distributed approach for dc optimal power flow,* in *PowerTech, 2015 IEEE Eindhoven* (IEEE, 2015) pp. 1–6.

[76] K. J. Arrow, L. Hurwicz, H. Uzawa, and H. B. Chenery, *Studies in linear and non-linear programming,* (1958).

[77] D. Feijer and F. Paganini, *Stability of primal–dual gradient dynamics and applications to network optimization,* Automatica **46**, 1974 (2010).

[78] J. Wang and N. Elia, *A control perspective for centralized and distributed convex optimization,* in *Decision and Control and European Control Conference (CDC-ECC), 2011 50th IEEE Conference on* (IEEE, 2011) pp. 3800–3805.

[79] X. Ma and N. Elia, *A distributed continuous-time gradient dynamics approach for the active power loss minimizations,* in *Communication, Control, and Computing (Allerton), 2013 51st Annual Allerton Conference on* (IEEE, 2013) pp. 100–106.

[80] X. Ma and N. Elia, *Convergence analysis for the primal-dual gradient dynamics associated with optimal power flow problems,* in *Control Conference (ECC), 2015 European* (IEEE, 2015) pp. 1261–1266.

[81] L. Mackay, A. Dimou, R. Guarnotta, G. Morales-Espania, L. Ramirez-Elizondo, and P. Bauer, *Optimal power flow in bipolar dc distribution grids with asymmetric loading,* in *Energy Conference (ENERGYCON), 2016 IEEE International* (IEEE, 2016) pp. 1–6.

[82] D. P. Chassin and S. E. Widergren, *Simulating demand participation in market operations,* in *Power & Energy Society General Meeting, 2009. PES'09. IEEE* (IEEE, 2009) pp. 1–5.

[83] Y. Fu and Z. Li, *Different models and properties on lmp calculations,* in *Power Engineering Society General Meeting, 2006. IEEE* (IEEE, 2006) pp. 11–pp.

[84] D. Gautam and M. Nadarajah, *Influence of distributed generation on congestion and lmp in competitive electricity market,* Int. Jour. Electr. Power Eng **3**, 228 (2010).

[85] N. Kaur, K. Singh, and S. Kansal, *Optimal placement of distributed generator in transmission system using an algorithmic approach,* in *Power Electronics (IICPE), 2014 IEEE 6th India International Conference on* (IEEE, 2014) pp. 1–6.

[86] S. M. H. Nabavi, S. Hajforoosh, and M. A. Masoum, *Placement and sizing of distributed generation units for congestion management and improvement of voltage profile using particle swarm optimization,* in *Innovative Smart Grid Technologies Asia (ISGT), 2011 IEEE PES* (IEEE, 2011) pp. 1–6.

[87] P. Karlsson and J. Svensson, *Dc bus voltage control for a distributed power system,* IEEE Transactions on Power Electronics **18**, 1405 (2003).

[88] D. Salomonsson and A. Sannino, *Low-voltage dc distribution system for commercial power systems with sensitive electronic loads,* IEEE Transactions on Power Delivery **22**, 1620 (2007).

[89] T. T. Nguyen, M. Roos, and J. Rothe, *A survey of approximability and inapproximability results for social welfare optimization in multiagent resource allocation.* Ann. Math. Artif. Intell. **68**, 65 (2013).